RADIATIVE HEAT TRANSFER IN THE GASEOUS CORE NUCLEAR ROCKET

A THESIS

Presented to

The Faculty of the Graduate Division

by

James Richard Williams

In Partial Fulfillment

of the Requirements for the Degree

Doctor of Philosophy

in the School of Nuclear Engineering

Georgia Institute of Technology

May, 1967

In presenting the dissertation as a partial fulfillment of the requirements for an advanced degree from the Georgia Institute of Technology, I agree that the Library of the Institute shall make it available for inspection and circulation in accordance with its regulations governing materials of this type. I agree that permission to copy from, or to publish from, this dissertation may be granted by the professor under whose direction it was written, or, in his absence, by the Dean of the Graduate Division when such copying or publication is solely for scholarly purposes and does not involve potential financial gain. It is understood that any copying from, or publication of, this dissertation which involves potential financial gain will not be allowed without written permission.

3/17/65
b

RADIATIVE HEAT TRANSFER IN THE GASEOUS CORE NUCLEAR ROCKET

Approved:

Chairman

Date approved by Chairman: 5-17-67

ACKNOWLEDGMENTS

TABLE OF CONTENTS

Chapter

        Background
        Purpose of the Research

        General Arrangement
        Spectrometer
        Detector System
        Furnace
        Thermocouple
        Heater Power Supply
        Aerosol Generator
        Sampling Apparatus

        Data Aquisition
        Data Reduction

        Data
        Sample Calculation
        Error Analysis
        Destructive Test

TABLE OF CONTENTS (Continued)

LIST OF TABLES

LIST OF ILLUSTRATIONS

LIST OF ILLUSTRATIONS (Continued)

LIST OF ILLUSTRATIONS (Continued)

SUMMARY

The gaseous core nuclear rocket is generally considered to be the most promising approach to achieve both high thrust and high specific impulse for a space vehicle propulsion system. In this system a very hot core of gaseous fissioning fuel radiates energy to the propellant containing very small particles which render the propellant opaque to the radiation.

This thesis measured the absorption parameters as a function of temperature and wavelength for a carbon particle seed in hot nitrogen. This information is required in order to evaluate the absorptive properties of seeded propellant for various core temperatures, propellant temperatures, seed concentrations and pressures.

Nitrogen, first unseeded, and then seeded, was heated to the desired temperature by a furnace employing an electrically heated tungsten strip. A beam of monochromatic light from a vacuum ultraviolet spectrometer was passed through unseeded and then seeded nitrogen at a given temperature. Measurements of the transmission for the two cases yielded the linear attenuation coefficient for the particle seed. The density of seed material in the gas was simultaneously measured by withdrawing a known volume of seeded gas through a filter, and dividing the weight of carbon deposited on the filter by the volume of gas that passed through. The mass absorption coefficient, which is independent of particle concentration, was the measured linear attenuation coefficient divided by the measured seed density.

The resulting data showed that at room temperature the mass absorp-

tion coefficient of the carbon seed used was essentially independent of wavelength from 1100 Å to 8000 Å. Observations at higher temperatures up to 1525°F indicated no change in either the magnitude (about 20,000 cm^2/gm) or the wavelength independence of the mass absorption coefficient of the particle cloud.

CHAPTER I

INTRODUCTION

Background

The basic purpose of a rocket engine is to produce thrust by
accelerating gases from rest with respect to the rocket to an exhaust
velocity v_e with respect to the rocket. This acceleration is usually
achieved by heating the gases to a high temperature inside the engine and
then allowing them to escape through a nozzle. In chemical rockets this
heating is accomplished by burning the fuel in the combustion chamber and
then the combustion products become the ejected gases. The nuclear rocket
heats the gases with a nuclear reactor instead of by combustion.

The performance of a rocket engine is measured by two criteria: the
specific impulse, defined by Equation (2), and the thrust-to-weight ratio,
which is the thrust of the propulsion system divided by the total vehicle
weight. The thrust-to-weight ratio for a space propulsion system should
be as large as possible so that the mission can be accomplished with a
minimum fuel expenditure and in a minimum time period. The specific im-
pulse, which is a measure of the effective exhaust velocity of the pro-
pellant, is the primary factor determining the mission capability of a
propulsion system.

Letting M_i and M_f be the initial and final masses of a rocket which
has executed a mission equivalent to a velocity change Δv in free space,
the mass ratio M_i/M_f is then related to Δv by

$$\frac{M_i}{M_f} = e^{\frac{\Delta v}{v_e}} \tag{1}$$

where v_e is the effective exhaust velocity. The specific impulse, I_{sp}, may be defined by

$$I_{sp} = \frac{Thurst}{\dot{m} \, g} \tag{2}$$

where $\dot{m}$ is the mass flow rate of the propellant, and g is a constant equal to the acceleration of gravity at sea level. Since the thrust is given by $\dot{m} \, v_e$, I_{sp} may also be written

$$I_{sp} = \frac{v_e}{g} \tag{3}$$

so I_{sp} is actually a measure of the effective exhaust velocity. Equation (1) may now be written

$$\frac{M_i}{M_f} = e^{\frac{\Delta v}{g \, I_{sp}}} \tag{4}$$

Since the relationship between the mass ratio and I_{sp} is exponential, a small change in I_{sp} may produce a very large change in the corresponding mass ratio. This means that for a given payload and mission requirement, the size of the rocket vehicle decreases considerably when the specific impulse of the propulsion system is increased.

Economical space travel will require a rocket propulsion system that has both high specific impulse and a high thrust-to-weight ratio (unity or greater). Today's chemical boosters have an adequate thrust-to-weight ratio

but their specific impulse is limited to about 500 seconds[1]. The solid
core nuclear rocket, which utilizes a graphite-fuel reactor to heat the
propellant, is expected eventually to develop a specific impulse of about
1000 seconds[2]. But for practical, economical space transportation a
rocket engine capable of a specific impulse of several thousand seconds,
which also produces a thrust-to-weight ratio of unity or greater, is needed.

Nuclear electric rockets (ion propulsion) have the required specific
impulse, but they have extremely low thrust-to-weight ratios[1] and there-
fore would not be suitable for many space missions.

In order to increase the specific impulse of a propulsion system one
must increase the effective exhaust velocity, v_e. For propulsion systems
which obtain thrust by exhausting a hot gas through a nozzle, v_e is in-
creased by increasing the average velocity of the gas molecules inside the
engine.

The root mean square velocity of the gas molecules may be found from

$$E = \tfrac{1}{2} mv^2 = \tfrac{3}{2} kT \tag{5}$$

where m is the molecular weight, T is the absolute temperature of the gas,
and k is the Boltzmann constant. Thus,

$$v^2 = \frac{3\ kT}{m} \tag{6}$$

and

$$v = \frac{\sqrt{3\ kT}}{\sqrt{m}} = \text{const.}\ \sqrt{\frac{T}{m}} \tag{7}$$

Hence the exhaust velocity, v_e, which is proportional to v, is given by

$$v_e = \text{const.} \sqrt{\frac{T}{m}} \qquad (8)$$

so one may write

$$I_{sp} \; \alpha \; \sqrt{\frac{T}{m}} \qquad (9)$$

where α means "is proportional to."

The greater specific impulse of graphite core nuclear rockets results not from an increase in the propellant temperature (actually T is lower than in the LOX-hydrogen system), but from a considerable decrease in m. In the LOX-hydrogen rocket the exhaust gas is water with a molecular mass nine times that of molecular hydrogen, the exhaust gas of the nuclear rocket; so the specific impulse of the nuclear rocket is considerably greater, even at a slightly lower propellant temperature.

Further increases in the specific impulse can be obtained by increasing T. The solid core nuclear rocket is limited to a specific impulse of about 1000 seconds because raising the temperature further would cause the core to melt. In order to circumvent this temperature limitation, considerable attention has been given in recent years to the gaseous core reactor propulsion concept because of the very high temperatures that might be achieved[3]. A specific impulse of several thousand seconds might be attainable with such a system.

Three approaches have been proposed which, in principle, might lead to an engine with the desired thrust-to-weight ratio and a specific impulse

of several thousand seconds or greater. These are the Orion concept (in which thrust would be obtained from nuclear explosions behind the space-craft), the gaseous core nuclear rocket, and the thermonuclear fusion rocket.

The Orion concept, or the nuclear pulse rocket, originated at Los Alamos shortly after the Second World War, and the first report on the project was written in 1955[4]. General Atomics developed a design weighing 2,500 tons which would have a specific impulse of the order of 4000 seconds. However, the cost of actually building such a vehicle would be about a billion dollars[4]. Nuclear pulse rockets presently are not considered practical because of their size and cost.

Fusion propulsion may eventually be developed after fusion becomes practical as an energy source. At the present, however, of the three approaches to achieving high thrust and high specific impulse, the gaseous reactor concept, in which the propellant is heated by fission energy produced in a cavity reactor having its nuclear fuel in gaseous form, appears closest to becoming a reality[1].

Most of the earlier ideas for using gaseous fission cavity reactors to propel rockets involved diffusion of the propellant through the gaseous fuel so that heating occurred by direct conduction and convection[1]. The separation ratio (ratio of propellant mass flow rate to fuel mass flow rate) must be kept as high as possible because of the high cost of nuclear fuel and the undesirable effect of the fuel nuclei on the specific impulse. To date, the possibilities of achieving high separations with these diffusion systems have appeared remote.

The prospects for a practical gaseous fission rocket have brightened,

however, with the recent introduction of a new family of systems that operate on a basically different principle[1]. In these systems the propellant is heated by radiation from the fission plasma, rather than by direct intermixing. The containment problem is then not so difficult because the gases are never mixed. Two concepts that are being investigated are the coaxial flow reactor, in which a slow moving central stream of fissioning fuel heats a fast moving annular stream of hydrogen solely by radiation, and the nuclear light bulb concept, in which the fissioning fuel is contained in a transparent partition and the propellant is heated by radiation through the partition[5].
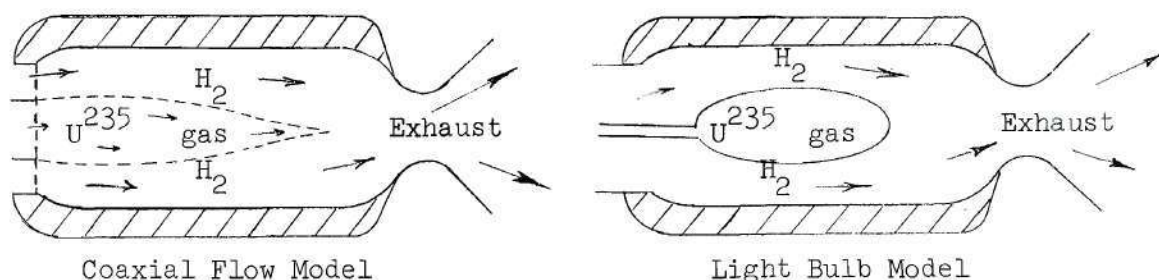
Figure 1.

In both of these concepts, the propellant (hydrogen containing very small particles) is heated by thermal radiation from the very hot gaseous core. The particles are necessary to make the propellant opaque to the radiation from the core in order to insure maximum heat transfer to the propellant and minimum heating of the containment vessel.

Some investigations with seeded gases and liquids have been carried out by several groups. Lanzo and Ragsdale[6,7] investigated experimentally

the absorption of suspended particles as a function of material, size and concentration; and investigated heat transfer from an arc to a flowing seeded gas. Masser[8] made an analytical study of radiant heating of a seeded gas for a particular reactor configuration. McAlister et al.[9,10], have reported theoretical and experimental studies of radiant heat transfer from a heated tungsten cylindrical enclosure to a cloud within it. Experimentally they endeavored to avoid conduction and convection and measured the heat gained by the cloud. Results were in good agreement with theory.

Marteney[11] studied techniques of producing dispersions of submicron-radius solid particles in a carrier gas and investigated the optical parameters of these particles for several wavelengths. Tests were conducted with carbon and tungsten particles having nominal radii of 0.0045 and 0.01 microns, respectively, dispersed in helium and nitrogen. These studies showed that the application of aerodynamic shear forces on a carbon aerosol resulted in an increase in the extinction parameter for carbon particles from approximately 10,000 cm^2/gm to 58,000 cm^2/gm. These increases are believed to be caused by a reduction in the size of particle agglomerates since theoretically a decrease in the average agglomerate size should result in an increase in the value of the extinction parameter[12].

The first experimental work involving seeded gases at elevated temperatures was reported this year by Valerie Burkig[13]. In this experiment a cloud of particles in a gas was injected into a transparent quartz tube and exposed to the two millisecond flash of a xenon flashtube. The temperature rise of the gas was inferred from the pressure rise measured with a fast response pressure transducer. The bulk of the work was with carbon, iron, and tantalum carbide particles of about one micron diameter. Helium

and hydrogen were used as carrier gases.

During the flash, the temperature of the carbon aerosol rose to about 2000°K for about one millisecond. After the flash gaseous and solid residues were examined for chemical products and evidence of vaporization; no evidence of chemical changes was found.

To date no work has been reported on the optical properties of equilibrium carbon aerosols at elevated temperatures. The residence time of the propellant in the gaseous core rocket engine would be of the order of 100 milliseconds, and Burkig[13] demonstrated that the aerosol required only about a millisecond to come into equilibrium. Also, the work reported thus far primarily involves the attenuation of energy from broad spectrum radiation sources. Few measurements have been made on the optical properties of seeded gases as a function of wavelength over a broad range of wavelengths, and nothing has been reported regarding the optical properties of aerosols in the vacuum ultraviolet between 1000 and 2000 Å. In the gaseous core rocket, most of the energy reaching the particles would probably lie in this wavelength range (Figures 2 and 3).

One problem with experiments involving the transfer of heat from hot plates or arcs to a gas containing small particles, is that the maximum temperature of the plate (about 3000°K)[9] or the arc (about 8000°K)[14] is much lower than the expected temperature for the gaseous core (about 40,000°K)[15]. This means that the emission of the radiation from the gaseous core will be almost entirely in the ultraviolet, whereas for the arc and tungsten plates the emission is primarily in the visible or in-frared (Figure 2). The ultraviolet region down to about 1000 Å is the region most applicable to the gaseous core. Below about 1000 Å hydrogen
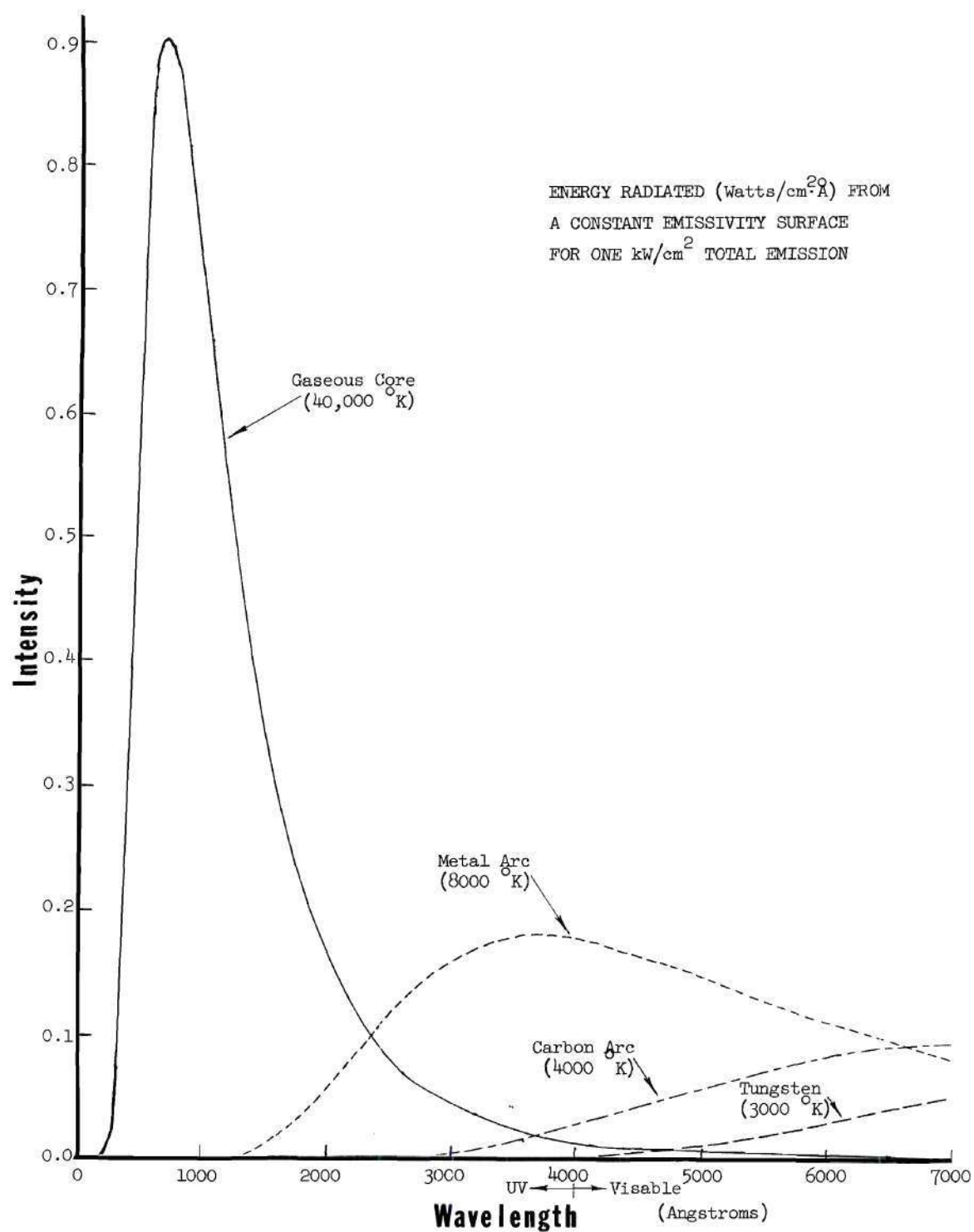
Figure 2. Emission Spectra from a Constant Emissivity Surface
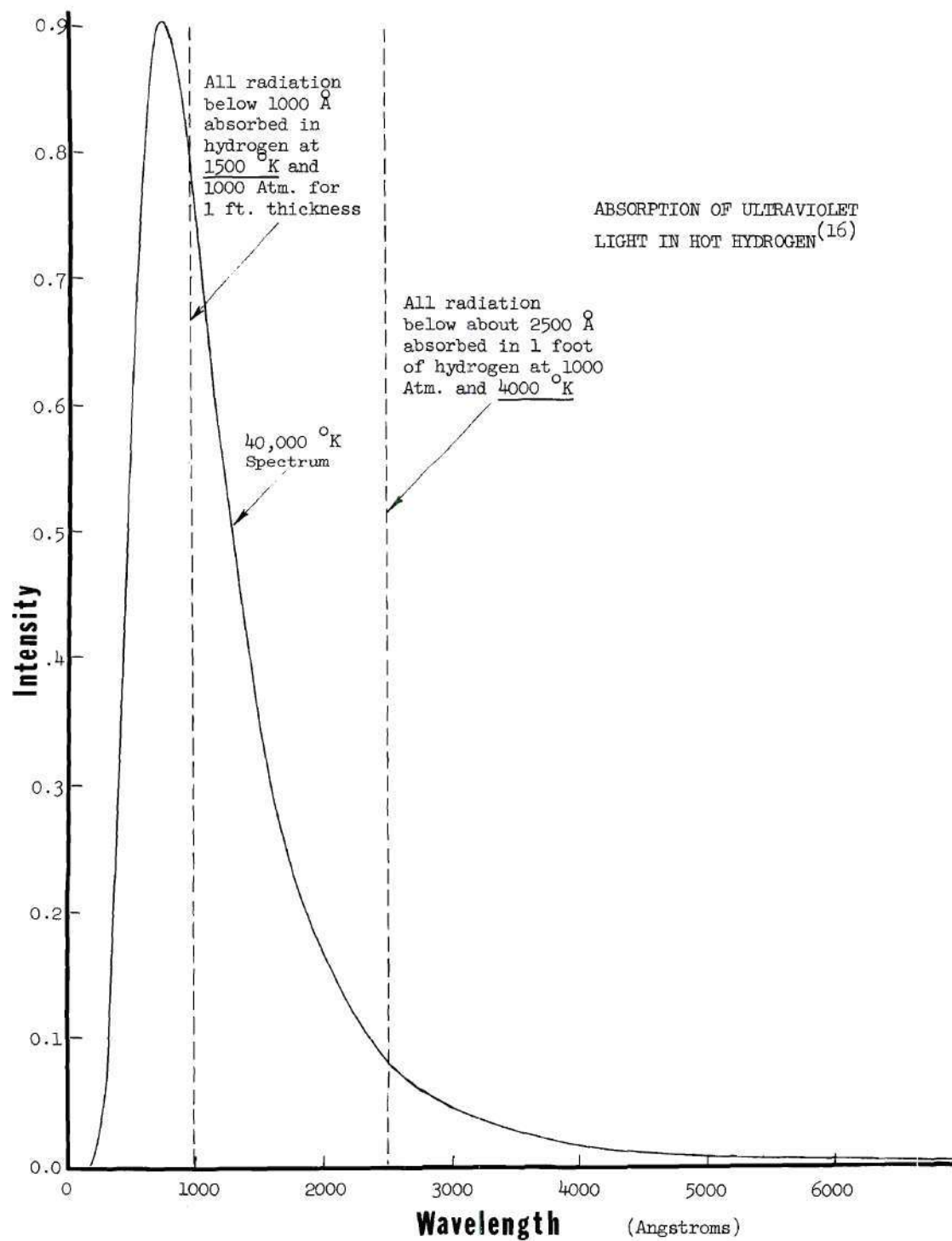
Figure 3.   Absorption of Radiant Energy in Hydrogen

becomes essentially opaque to the radiation (Figure 3).

The absorption of a beam of radiation in a purely absorbing medium is governed by the simple expression

$$I(\lambda, x) = I(\lambda, o) \ e^{-k_T(\lambda)x} \tag{10}$$

where $k_T(\lambda)$ is the total linear attenuation coefficient at wavelength λ and x is the distance into the medium. This equation holds as long as $k_T(\lambda)$ is independent of wavelength. $k_T(\lambda)$ has dimensions of reciprocal length. For light of multiple wavelengths, one can write

$$I(x) = \int_o^\infty I(\lambda, x) \ d\lambda = \int_o^\infty I(\lambda, o) \ e^{-k_T(\lambda)x} \ d\lambda \ . \tag{11}$$

Thus, if one is given the attenuation coefficient $k(\lambda)$ and the spectrum of the light source $I(\lambda, 0)$, the intensity of the radiation $I(x)$ at any distance x in the absorber can be calculated.

If the absorption takes place by more than one process, say two processes, called 1 and 2, then $k_T(\lambda)$ is the sum of the attenuation coefficients for each process separately, i.e.,

$$k_T(\lambda) = k_1(\lambda) + k_2(\lambda) \ . \tag{12}$$

In a gas containing particles, the absorption takes place by absorption in the gas and absorption by the particles. Letting $k_g(\lambda)$ be the absorption coefficient due to absorption in the gas alone, and $k_p(\lambda)$ be absorption coefficient for the particles in the gas, then the total absorption coefficient

is given by

$$k_T(\lambda) = k_g(\lambda) + K_p(\lambda) \quad .$$

(13)

For the case of hydrogen, $k_g(\lambda)$ has been evaluated by Krascella[16] from the extreme ultraviolet to the far infrared (Figure 4). Thus, if $k_p(\lambda)$ can be measured for a given type of particle seed, then $k_T(\lambda)$ can be calculated from Equation (13) for hydrogen containing that type of particle seed, assuming no chemical interactions between seed and hydrogen. Knowing $k_T(\lambda)$ for that propellant mixture, then $I(x)$ can be found for any core emission spectrum $I(\lambda,0)$.

If a beam of light is passed through a transparent gas containing very small particles, the attenuation of the beam takes place almost entirely by absorption. The Mie theory of light scattering by particles, which is discussed in Appendix A, and numerous experiments using particle suspensions have verified that scattering is negligible for particles of interest[11,17-19].

Thus, $k_p(\lambda)$ can be obtained by passing a beam of light of wavelength λ through a transparent gas containing very small particles and measuring the attenuation of the light. The value of $k_p(\lambda)$ for all particle concentrations of interest can be obtained by measuring it for a known particle concentration and assuming that it is proportional to particle concentration.* Once $k_p(\lambda)$ is known, the absorptive properties of the seeded pro-

---

* The proportionality holds as long as the particle volume fraction in the gas is small (that is, the average distance between particles is much greater than the average effective particle radius) and the particles are randomly oriented. These conditions hold for all concentrations of interest to nuclear propulsion.
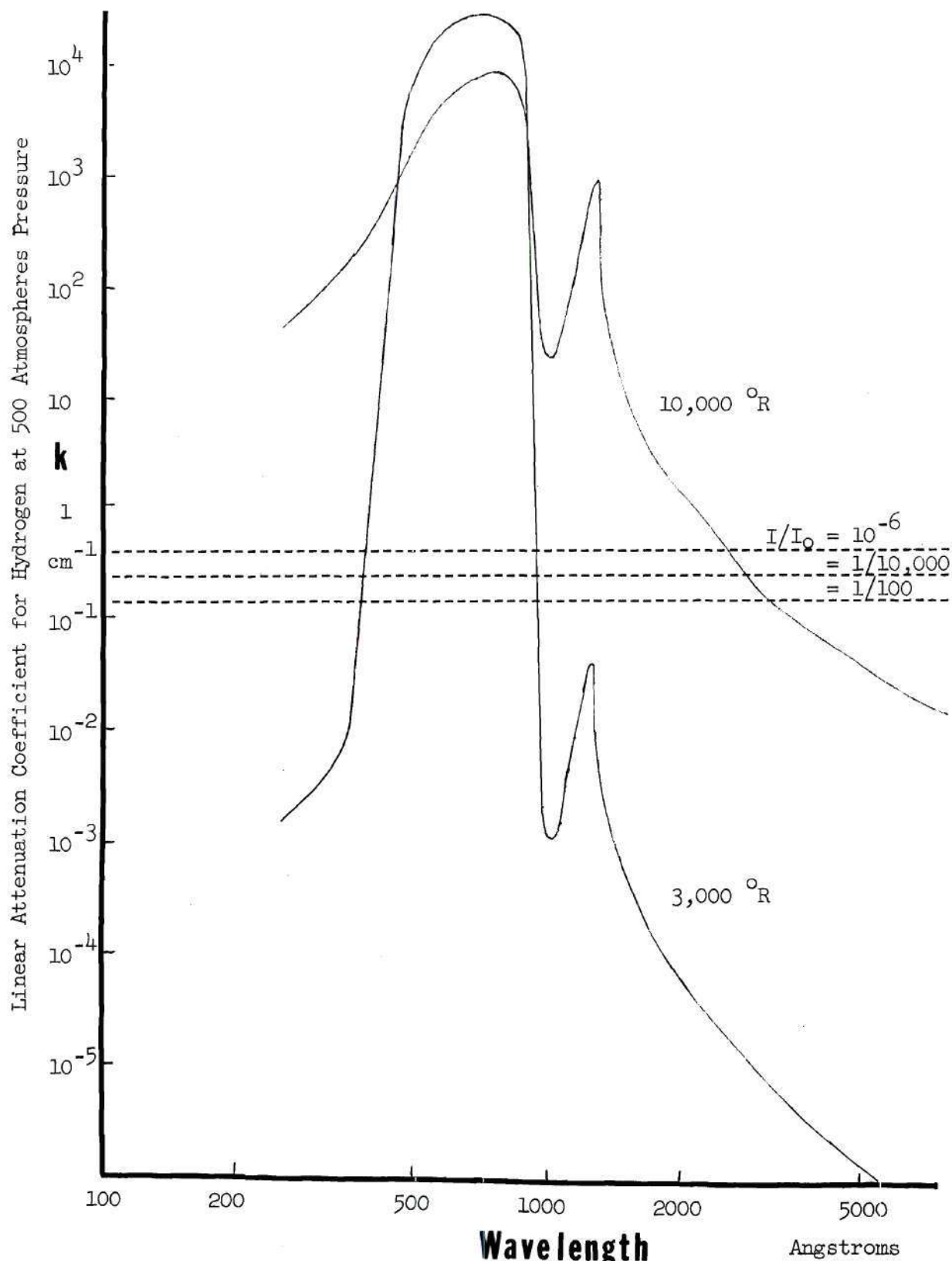
Figure 4.   Theoretical Values of the Linear Attenuation Coefficient of Hydrogen at a Pressure of 500 atmospheres

pellant can be calculated.

Purpose of the Research

The purpose of the research described in this thesis was to:

1. Measure the mass absorption coefficient of a transparent gas (nitrogen) seeded with carbon particles as a function of incident radiation wavelength in the range from 1100 Å to 8000 Å at room temperature and at elevated temperatures. The mass absorption coefficient is defined as the linear attenuation coefficient, k_p, divided by the density of the seed material in mass of seed material per unit volume of aerosol.

2. Relate the measured mass absorption coefficient to the radiative heat transfer problem in the gaseous core nuclear rocket by calculating the total energy attenuation as a function of distance through the propellant for various seed concentrations.

CHAPTER II

INSTRUMENTATION AND EQUIPMENT

General Arrangement

An objective of this project was to obtain measurements of the attenuation of monochromatic light in hot nitrogen seeded with very small carbon particles. The experimental system (Figure 5) consisted basically of the following components. A vacuum ultraviolet spectrometer which utilized a capillary discharge tube served as a monochromatic light source of variable wavelength. A photomultiplier detector observed the light which passed through the observation chamber, and the resulting signal was recorded by a micro-microammeter. The furnace consisted of three parts: a heating chamber which raised the aerosol temperature, an observation chamber through which a beam of light was passed, and an exhaust chimney. A shielded chromel-alumel thermocouple in the observation chamber connected to a millivolt meter indicated the gas temperature. An aerosol generator seeded nitrogen with carbon particles. A sampling system allowed the carbon density in the gas to be measured. Three power supplies provided power for the tungsten heater, the photomultiplier, and the capillary discharge tube, respectively.

In general, the system operated as follows. The aerosol generator was first filled with carbon black. Nitrogen passed through this aerosol generator and carbon particles were injected into it which remained suspended in the gas. The resulting aerosol entered the heating chamber of
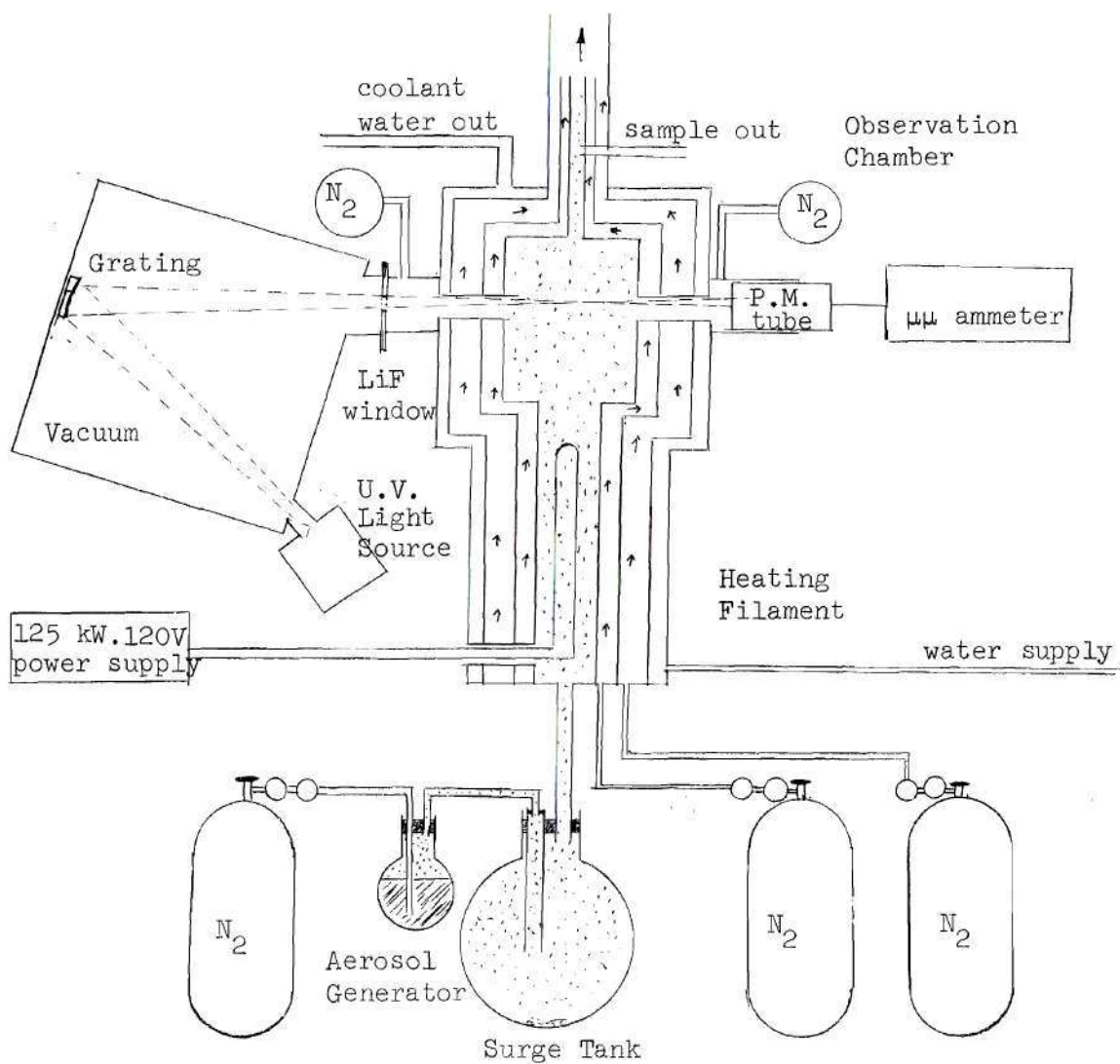
Figure 5. General Arrangement of Apparatus

the furnace and was heated to the desired temperature. When the aerosol emerged from the heating chamber into the observation chamber, it intersected a beam of light passing through the chamber. The hot aerosol then passed out of the exhaust chimney, became mixed with air to bring down the temperature, and was drawn through a filtering system to clean the exhaust gas.

The aerosol in the observation chamber attenuated the beam of light from the spectrometer. This attenuation was measured by the photomultiplier detector, and the linear attenuation coefficient of the aerosol could then be calculated. The aerosol density was measured by drawing a known volume of aerosol through a millipore filter and finding the weight of the deposited carbon.

Spectrometer

A vacuum ultraviolet spectrometer was utilized to provide a beam of monochromatic light of a wavelength which could be varied from 1100 Å to 8000 Å. The light source was a capillary discharge tube filled with hydrogen or helium. A concave reflection type diffraction grating located at the opposite end of the spectrometer focused a spectrum on the plate containing the exit aperture. The wavelength of the light passing through the exit hole and through the furnace could be selected by slightly rotating the grating. This was accomplished by turning a wavelength dial on the outside of the spectrometer, which turned the grating through a gear mechanism.

Since the grating was used at nearly normal incidence, the wavelength dial could be calibrated by taking two readings at the beginning of a run; the first at the "white point" with the grating at normal incidence which

corresponded to zero wavelength (Figure 34), and the second at a known line in the spectrum. The dial reading, D, was related to the wavelength λ by a first-order equation[*].

$$\lambda = C_1 D + C_2 \quad . \tag{14}$$

These two calibrations established the values of the constants C_1 and C_2.

A mechanical pump maintained a pressure of about five microns of mercury inside the spectrometer whenever the spectrometer was not in operation. Since the gas flowing through the capillary discharge tube passed into the spectrometer before being pumped out, the pressure rose to several hundred microns when the spectrometer was operating. Both hydrogen and helium were used in the discharge tube.

The only solid material between the discharge tube and photomultiplier was a lithium fluoride window covering the exit aperture. This window transmitted only those wavelengths above 1100 $\overset{\circ}{A}$[(29)].

Detector System

An EMI 95145 photomultiplier tube operating at 1200 volts attached to the furnace opposite the spectrometer detected the light emerging from the observation chamber. The face of the photomultiplier was covered with a thin coating of sodium salicylate which fluoresced when irradiated by ultraviolet light. With this arrangement the photomultiplier responded to both visible and ultraviolet light. Without the phosphor coating, a large portion of the ultraviolet spectrum would have been undetected because

---

[*] Actually there is a sine relationship, but the angle involved is so small the correspondence appears to be linear.

of absorption in the front face of the photomultiplier tube.

The photomultiplier output was recorded by a Keithley model 415 micro-microammeter, which in turn operated a chart recorder. The micro-microammeter was located at the end of the spectrometer with the wavelength dial so that the photomultiplier signal could be observed as the wavelength was changed. Data were taken directly from the micro-micro-ammeter. The chart recorder was used primarily when the aerosol concentration was being adjusted.

Furnace

Figure 6 illustrates the furnace design. The furnace consisted basically of two stainless steel cylinders inside a water jacket. The inner cylinder contained the aerosol, while nitrogen coolant flowed in the annular regions outside of the inner cylinder and inside the water jacket. About twenty liters per minute of water flowed through the water jacket to keep the outside of the furnace cool at all times.

One-eighth inch hot pressed boron nitride was used as an insulating and structural material surrounding and supporting the tungsten heating element in the heating chamber. The heating element was a two-foot long by one-half inch wide strip of five mil thick tungsten. The ends of the strip were connected to the copper power leads.

The copper water jacket was made in two parts so that the furnace could be disassembled and reassembled easily. By lifting off the top half of the water jacket, the inner stainless steel components were exposed, and these could be taken apart easily. The furance was designed so that the filament could be easily replaced should it burn out.
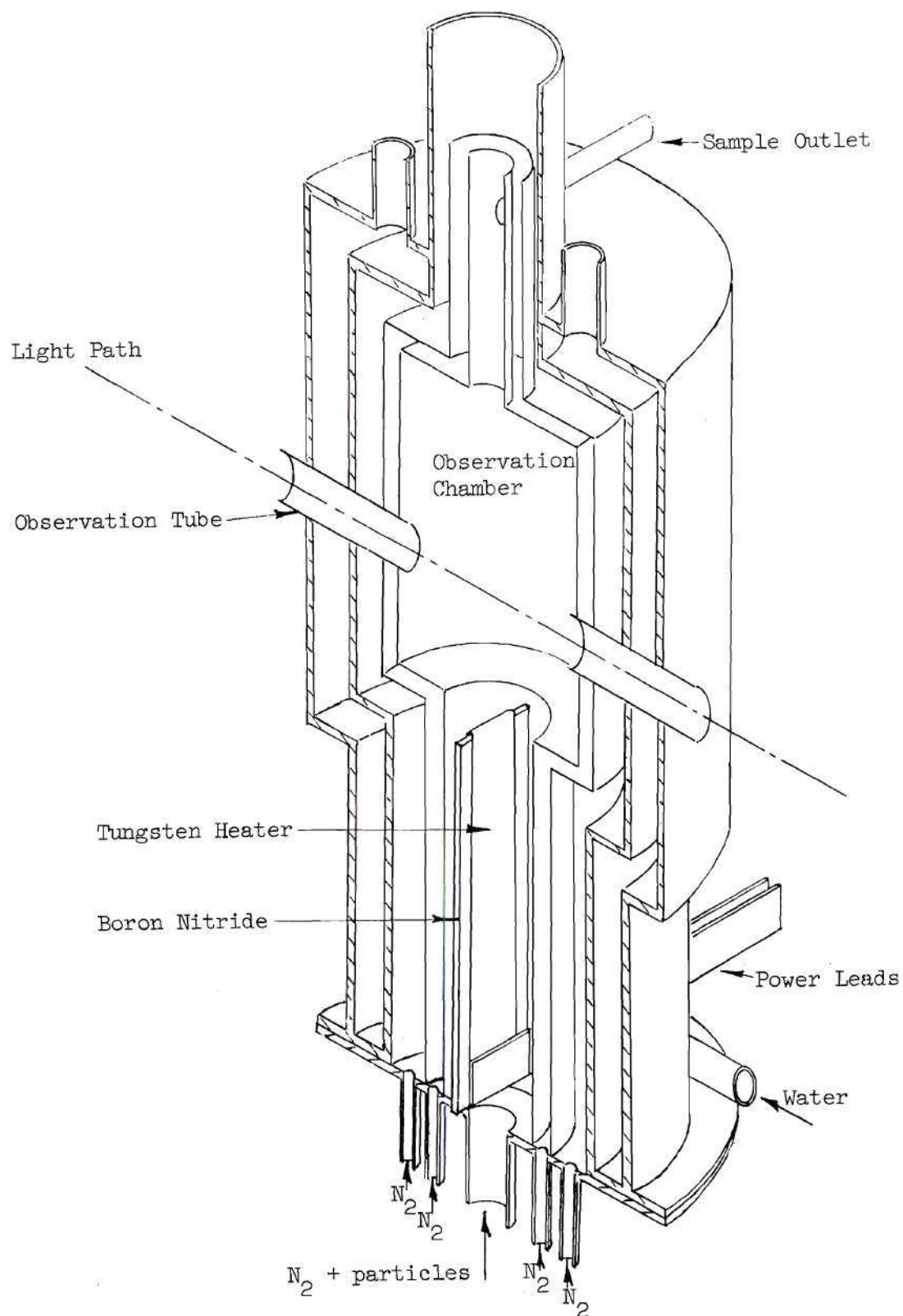
Figure 6. Furnace Sketch

The aerosol was prevented from backing up in the tubes and depositing carbon on the lithium fluoride window or the photomultiplier by a very small flow of nitrogen into the observation chamber through the observation tubes. This window flow had to be adjusted carefully for a given aerosol-coolant flow, and usually amounted to less than one percent of the total flow.
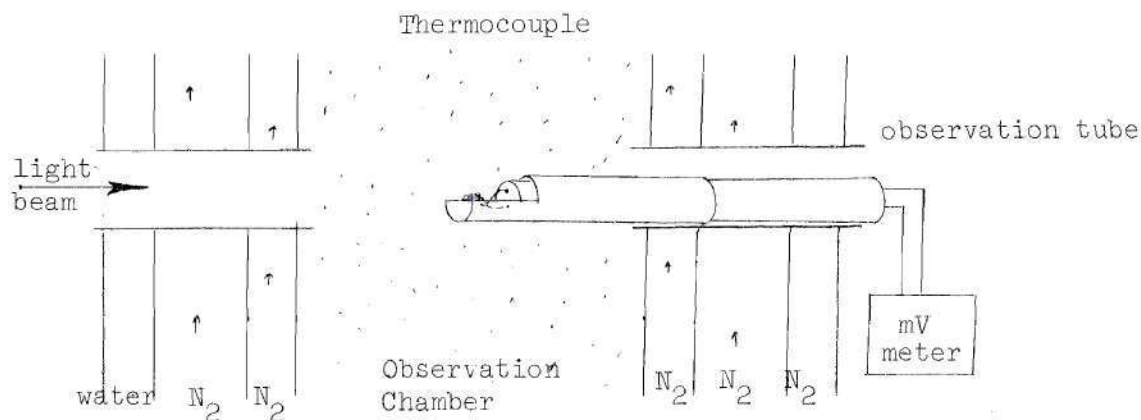
Figure 7.   Thermocouple Configuration

The temperature of the heated gas was measured with a chromel-alumel thermocouple. An alumel wire and a chromel wire were inserted through a ceramic sleeve and twisted together for one quarter inch at the end. The end was shielded from the filament by stainless steel. A Keithley millivolt meter indicated the thermocouple voltage.

Heater Power Supply

The power supply used for the heater is located in the Unit Operations Lab of the Chemical Engineering Building at the Georgia Institute of Technology. A saturable core reactor was employed to allow the heater power to be varied from zero to 125 kilowatts of single phase power.

Since another project was using the power supply concurrently with this thesis work, a switch was made and installed to allow the power to be easily transferred from one set of equipment to the other. Three 4/0 cables, capable of carrying 600 amps, carried the power from the switch to the hot copper lead, and three more 4/0 cables grounded the other lead. The copper leads from the cables to the tungsten heater had a cross section of 7/8 inch by 1/8 inch.

Aerosol Generator

The aerosol generator consisted of a two-liter round bottom flask and a twelve-liter flask mounted on a ringstand with assorted tubing and rubber stoppers. The arrangement is illustrated below. Nitrogen under five to ten psi pressure flowed through a small oriface in the end of the tube in the generator flask, agitating the carbon black and producing the aerosol. A twelve-liter flask acted as a trap for the large particles and as a surge tank to smoothe out the fluctuations in the aerosol concentration from the generator flask.

about 10 psi

aerosol output

N₂

Generator
Flask

Surge Tank
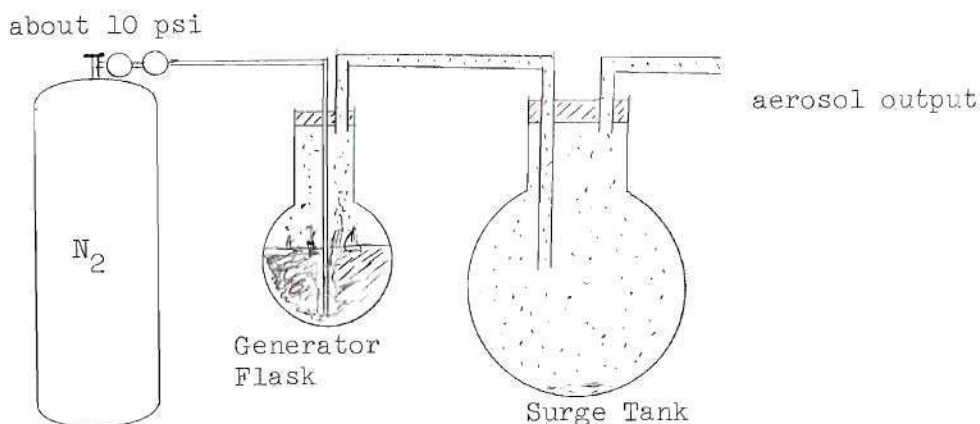
Figure 8. Aerosol Generator

This arrangement produced a uniform aerosol for the flow rates used. A total of twenty-eight cylinders (224 ft.^{3} each) of extra dry grade nitrogen were used.

Sampling Apparatus

In order to measure the density of the aerosol, in grams of carbon per cubic centimeter of aerosol, a known volume of gas was drawn through a filter and the weight of the deposited carbon measured. The sampling apparatus consisted of a vacuum pump, two one-gallon jugs, a filter holder, a filter, a stopcock, and assorted tubing and stoppers. The arrangement is indicated by the following drawings.
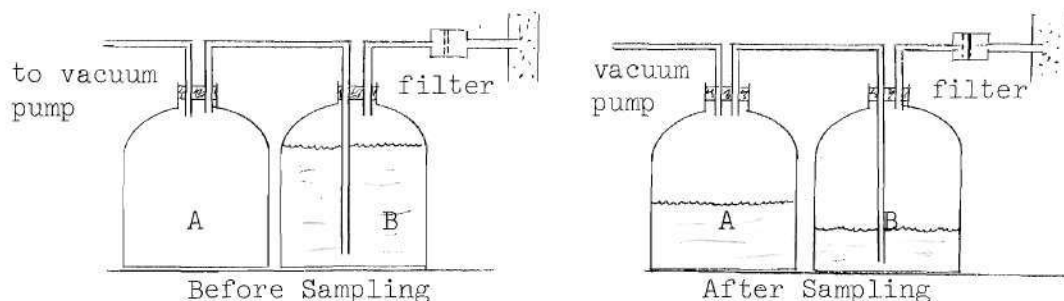
Figure 9.   Sampling Apparatus

To take a sample, the vacuum pump was turned on and the stopcock opened. This reduced the pressure in jug A so that water flowed from B into A. Then the stopcock was closed and the pump turned off. When pressure equilibrium was again established the volume of water in A equaled the volume of water which left B, which in turn was equal to the volume of gas entering B. This was the gas that passed through the filter at one atmosphere pressure. The aerosol concentration was the weight of carbon deposited on the filter divided by the volume of water in A.

The weight of the deposited carbon was found by weighing the filter before and after the sample was taken. The volume of the water was measured with a graduated cylinder. The volume of the filter holder was subtracted from the water volume to get the volume of gas passing through the filter.

About a minute was required to pull a sample. The sample was pulled slowly to avoid significantly perturbing the aerosol concentration. The attenuation of a reference line was carefully watched while a sample was taken to insure that the particle concentration did not change significantly while the sample was collected.

CHAPTER III

PROCEDURES

Data Acquisition

The experimental procedure for taking data is outlined in detail in Appendix B. The resulting data were the values of the photomultiplier output for a number of spectrometer wavelength dial settings with seeded nitrogen and with unseeded nitrogen in the observation chamber. Since the photomultiplier output was taken to be proportional to the intensity of the light emerging from the observation chamber, for a single wavelength, the desired light intensity ratio (intensity with particles to intensity without particles) was simply the ratio of the signals for the two cases. The wavelength dial was calibrated (Equation (14)) so that the wavelength corresponding to each dial setting was known.

Two factors that had to be considered when taking data were the variation of the aerosol concentration during a run and the background signal which was a function of the temperature of the observation chamber. The aerosol concentration was monitored by quickly turning the wavelength dial back to a reference wavelength each time a data point was taken with particles in the nitrogen. Thus, each time the signal corresponding to the light of a given wavelength, which passed through the aerosol, was recorded, the signal for the reference wavelength was also recorded. Signal variations at the reference wavelength were related quantitatively to variations in the aerosol concentration.

The density of the aerosol was measured by withdrawing a known volume of aerosol through a filter. The aerosol density in weight of carbon per unit volume of aerosol was the weight of carbon deposited on the filter divided by the volume of gas passing through. When the sample was withdrawn, the signal corresponding to the reference wavelength was recorded so that changes in the reference signal could be related to changes in the measured particle concentration.

At elevated gas temperatures the walls of the observation chamber and the inner ends of the observation tubes became hot enough to emit visible light. Even though the photomultiplier was less sensitive to red light than to visible light of shorter wavelengths, the intensity of thermal radiation from the observation chamber which reached the photomultiplier was great enough to produce a significant background signal. This background was taken into account by observing a "black" part of the spectrum (any wavelength below 1100 Å) occasionally during a run and recording the value of the background signal. The background was observed as often as required to ensure that it was known accurately throughout a run. The background dropped considerably when particles were introduced into the gas.

The thermocouple voltage was recorded periodically. This voltage was related to the temperature by using a table giving the thermal EMF of a chromel-alumel junction as a function of temperature. Tank pressures were recorded before and after a run so that the nitrogen flow rates could be estimated.

Data Reduction

The first step in reducing the data was establishing the value of I_o/I, the attenuation of the signal in the aerosol, for each wavelength λ for which data was taken. I_o is the signal without the particles, minus the background. Since the signal without particles was taken twice during each run (before and after the data are taken with the particles), I_o was taken to be the average of the two signal minus background measurements. I is the signal with particles in the gas, minus the background. Then the linear attenuation coefficient k could be evaluated from

$$k(\lambda) = \frac{1}{x} \, |N \, \frac{I_o(\lambda)}{I(\lambda)} \tag{15}$$

for each wavelength λ, where x, the path length between the two inner ends of the observation tubes, was five centimeters.

The signal $I'(\lambda_r)$ at the reference wavelength λ_r, which was recorded each time a value of $I(\lambda)$ was obtained, was used to evaluate the linear attenuation coefficient at the reference wavelength λ_r for the aerosol concentration at the time $I(\lambda)$ was measured. $k'(\lambda_r)$ is given by

$$k'(\lambda_r) = \frac{1}{x} \, |N \, \frac{I_o(\lambda_r)}{I'(\lambda_r)} \tag{16}$$

This data required for the calculation of $k(\lambda)$ and $k'(\lambda_r)$ were taken together for the same aerosol concentration. $k(\lambda)$ and $k'(\lambda_r)$ are both proportional to the aerosol concentration, so $k(\lambda)/k'(\lambda_r)$ is independent of the concentration. Thus, values of $k(\lambda)/k'(\lambda_r)$ may be calculated which give relative

values of the linear attenuation coefficient that are independent of changes in the aerosol concentration. $k(\lambda)/k'(\lambda_r)$ is evaluated from

$$\frac{k(\lambda)}{k'(\lambda_r)} = \frac{\left| \ln \dfrac{I_o(\lambda)}{I(\lambda)} \right.}{\left| \ln \dfrac{I_o(\lambda_r)}{I'(\lambda_r)} \right.} \quad . \tag{17}$$

At some time during the run, a sample of the aerosol was taken while the signal at the reference wavelength was recorded. Thus, the density ρ' which produced the recorded signal $I'(\lambda_r)$ was found, and $k'(\lambda_r)$ corresponding to the measured density ρ' was calculated. This fixed the value of the mass absorption coefficient k/ρ at wavelength λ_r as $k'(\lambda_r)/\rho'$. The mass absorption coefficient corresponding to the other wavelengths is then

$$\frac{k(\lambda)}{\rho} = \frac{k(\lambda)}{k'(\lambda_r)} \cdot \frac{k'(\lambda_r)}{\rho'} \quad . \tag{18}$$

The mass absorption coefficient is independent of the particle mass density ρ_p.

CHAPTER IV

RESULTS

Experimental Data

Attenuation data were obtained from 1100 Å to 8000 Å at room temperature, and over a more limited wavelength range at higher temperatures because of the increasing background signal. These data are presented in Appendix C. The calculated values of k/ρ_p, based on measurements, are presented in Figures 10 through 15 for $63^\circ F$, $500^\circ F$, $750^\circ F$, $900^\circ F$, $1400^\circ F$, and $1525^\circ F$. The data indicated the mass absorption coefficient of the carbon aerosol to be essentially independent of wavelength over the range of wavelengths and temperatures investigated.

The first runs (Tables 2 through 4) indicated a peak in k/ρ_p values in the vacuum ultraviolet region, however, when more care was taken to keep oxygen out of the observation chamber, this peak disappeared. The largest k/ρ_p values were at wavelengths at which oxygen absorbs the strongest. The data in Tables 2 through 4 which were affected by oxygen absorption were not plotted in Figure 10.

The carbon mass density in the aerosol, ρ_p, varied from about 6 $\mu gm/cm^3$ to about 20 $\mu gm/cm^3$ for different runs. The accuracy with which ρ_p was estimated is expected to be about fifty percent (Appendix C). Since the mass absorption coefficient, k/ρ_p, depends on the particle size distribution, which in turn depends on how the aerosol is produced and the type of powder used, the data obtained in this experiment apply to a parti-
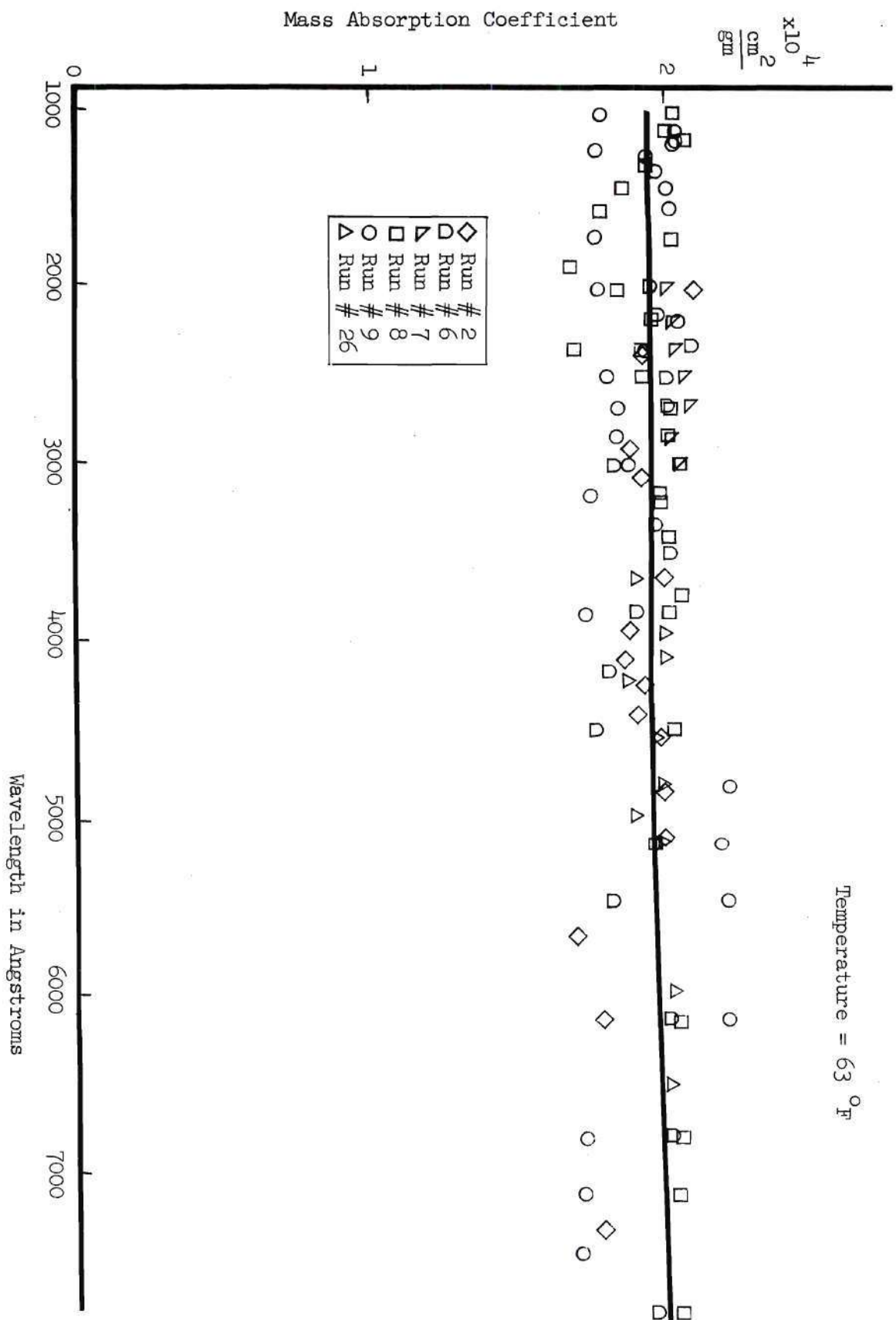
Figure 10. Mass Absorption Coefficient vs. Wavelength at 63 °F
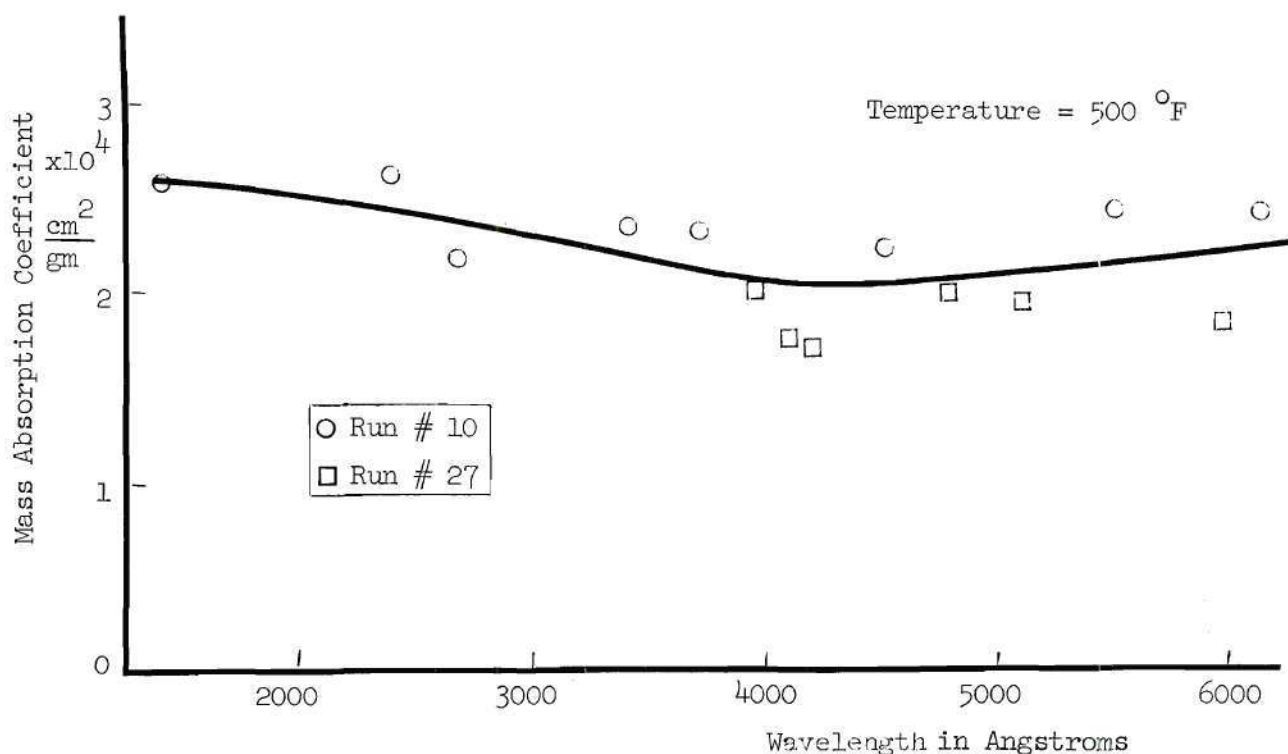
Figure 11.   Mass Absorption Coefficient of a Carbon Particle Cloud
Function of Wavelength at 500°F - Experimental Results
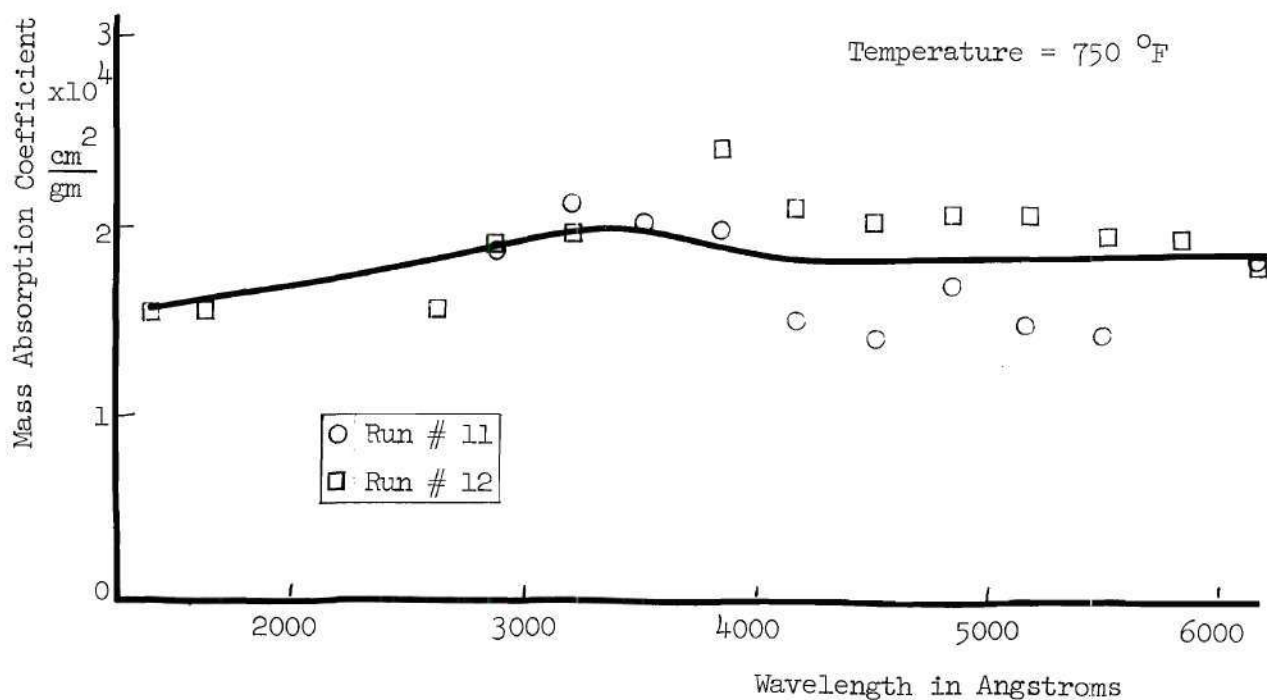
Figure 12.   Mass Absorption Coefficient of a Carbon Particle Cloud as a
Function of Wavelength at 750°F - Experimental Results
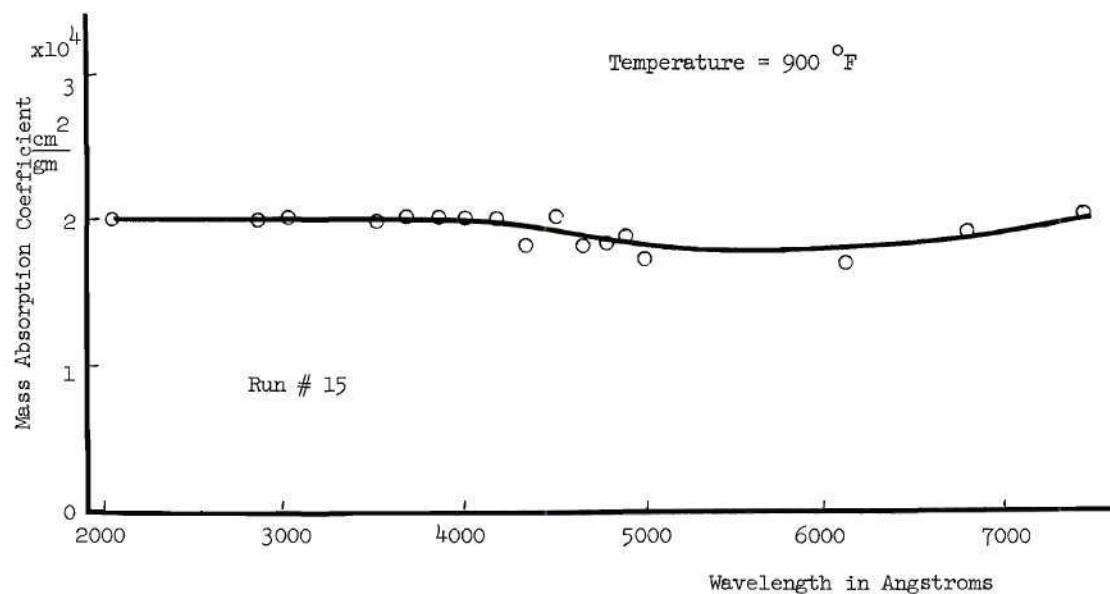
Figure 13.   Mass Absorption Coefficient of a Carbon Particle Cloud as a
Function of Wavelength at 900°F - Experimental Results
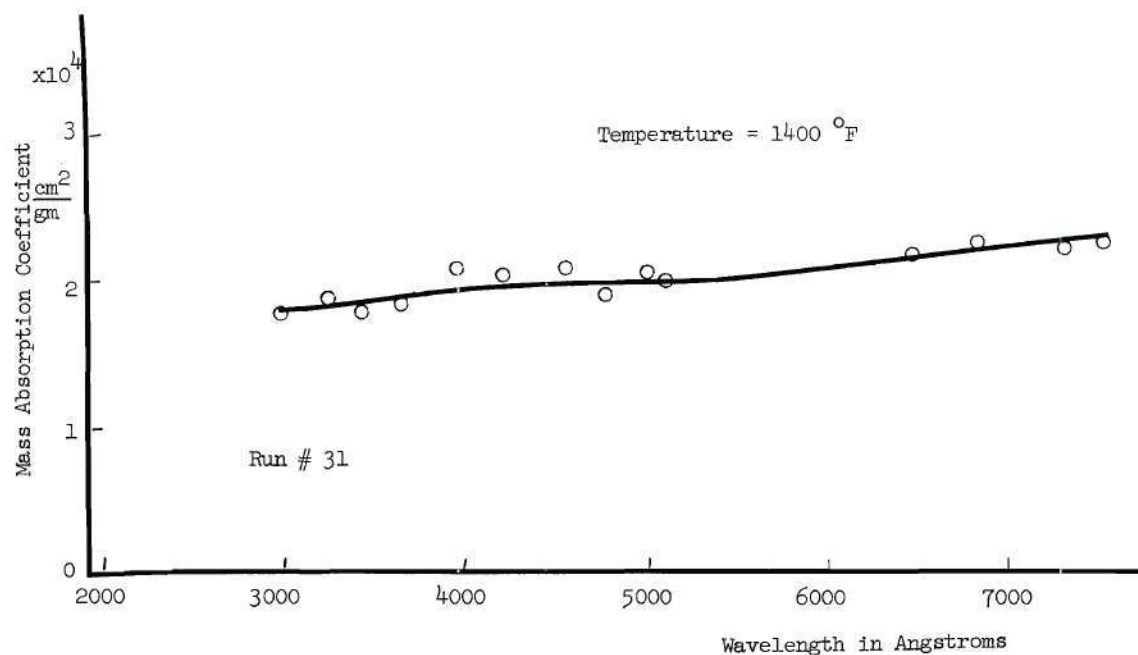
Figure 14.   Mass Absorption Coefficient of a Carbon Particle Cloud as a
Function of Wavelength at 1400°F - Experimental Results
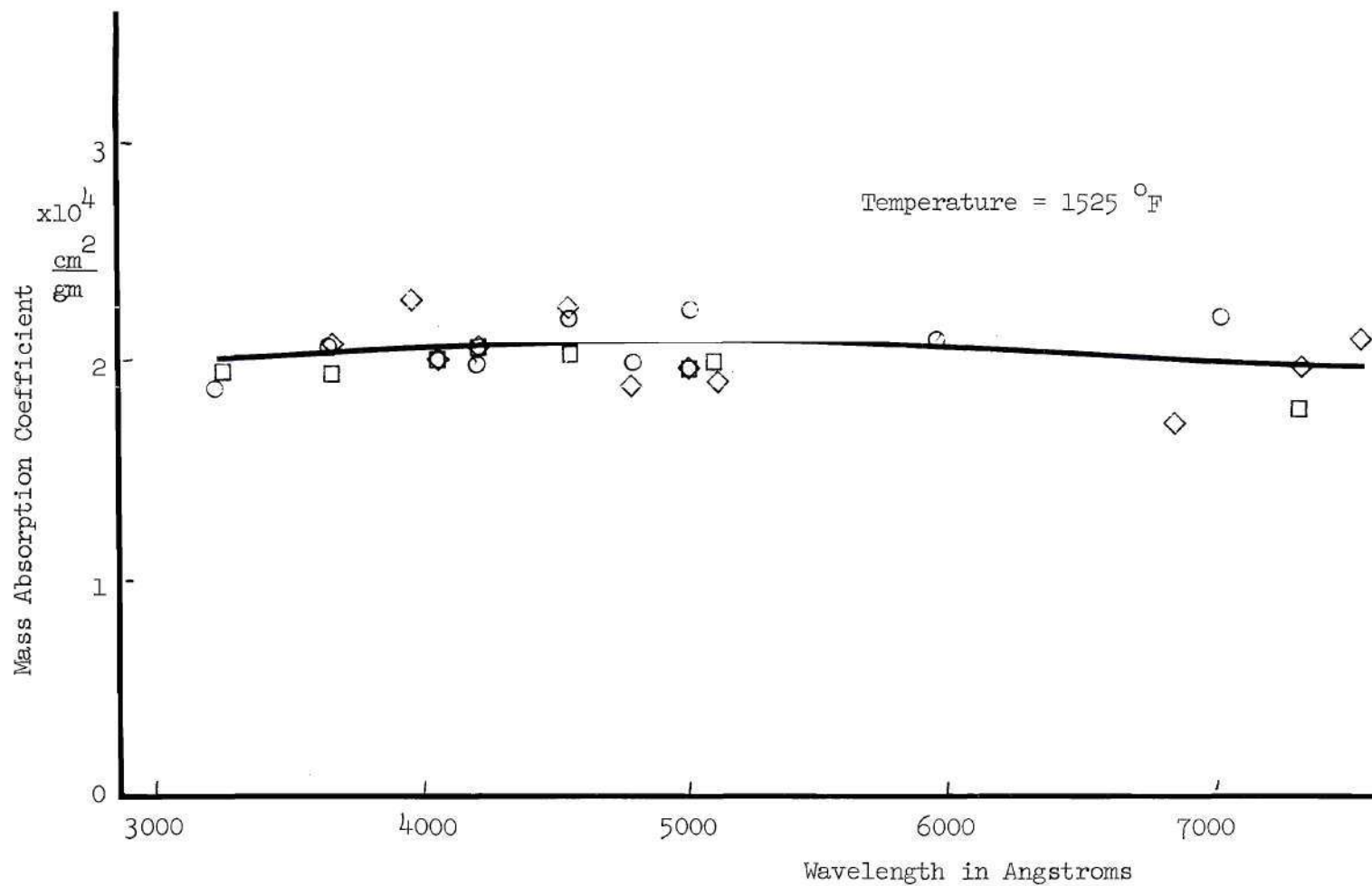
Figure 15. Mass Absorption Coefficient of a Carbon Particle Cloud as a
Function of Wavelength at 1525°F - Experimental Results

33

cular carbon aerosol rather than to all carbon aerosols. However, this work has shown that a carbon aerosol can be easily produced for which k/ρ_p is essentially wavelength independent over the entire wavelength range of interest. Similar work using the same type of carbolac powder and generating the aerosol with a high velocity gas stream demonstrated the nominal particle size to be about 0.01 microns (Reference No. 11, page 32).

The seed material used was Cabot carbolac powdered carbon. Extra dry grade nitrogen was used as the carrier gas.

Sample Calculation

The value of k/ρ_p for each scale setting was calculated from the measured values of I_o, I, I', and ρ_p using the procedure described in Chapter III. A sample calculation of the first k/ρ_p value in run number 35 follows.

The measured value of I_o (signal minus background for the gas without particles) with the wavelength dial set on 1084 was 21 microamps. The value of I (signal minus background for the gas with particles) was 3.6 microamps. Immediately after I was measured, the value of I' (signal minus background at a scale setting of 611, the reference setting) was measured to be 14.5 microamps.

$$\frac{I_o}{I} = \frac{21}{3.6} = 5.84 \tag{19}$$

The value of I_o at a wavelength setting of 611 had been 91 microamps, so I'_o = 91 microamps.

$$\frac{I_o}{I} = \frac{91}{14.5} = 6.28 \tag{20}$$

so

$$\frac{k}{k'} = \frac{\ln \frac{I_o}{I}}{\ln \frac{I_o'}{I'}} = \frac{1.76}{1.83} = 0.972 \quad . \tag{21}$$

The value of k'/ρ_p had been evaluated from several density measurements with a gas temperature of about 1500^oF which were taken while k' was measured with the wavelength dial at 611. k'/ρ_p was found to be 2×10^4 cm^2/gm with a probable error of about fifty percent. Using this value of k'/ρ_p, one obtains

$$k/\rho_p = k/k' \cdot k'/\rho_p = (0.9725)(2 \times 10^4) = 1.95 \times 10^4 \text{ cm}^2/\text{gm} \tag{22}$$

Error Analysis

Some of the factors that introduced errors into the data are enumerated below.

Errors in k/k'

1. Fluctuations in the aerosol concentration between the measurements of the signal and the background, or between the measurement of I and I'. These fluctuations were minimized by taking the respective measurements as quickly as possible, but could not be eliminated entirely because of the finite amount of time required to turn from one dial setting to the other.

2. Fluctuations in X, the distance the light passed through the

aerosol. With the window gas flow and aerosol generator adjusted properly, the intensity of a monochromatic beam of light which was significantly attenuated by the aerosol did not change noticeably with time. Under these circumstances, X was not fluctuating measureably, and these conditions were always established before data were taken. However, it is possible that fluctuations in X due to changes in the flow pattern in the observation chamber could occur during the run and affect the results.

3. The voltage to the capillary discharge tube, the voltage to the photomultiplier, the amplitifcation of the micro-microammeter, all could be affected by a change in line voltage, which could occur during a run if there was a significant change in the power used in the rest of the building. The electronics equipment and spectrometer were allowed at least an hour to warm up before data were taken, and since all of the data were taken in the evening, the fluctuations in the line voltage should have been minimal.

4. Each reading of the intensity of the signal (eight were required to get k/k') involved recording the reading of a meter on the micro-microammeter. Care was taken in making these readings, but some error was obviously introduced. Also, in setting the wavelength dial some human error was introduced.

Errors in k'/ρ_p

Whereas errors in k/k' introduced fluctuations in the data points (Figures 10 through 15), an error in k'/ρ_p would throw all of the data points off by the same factor. k' was subject to the same errors discussed above, but the greatest source of error in the magnitude of the k/ρ_p values was probably in the measurement of ρ_p. ρ_p varied from about 6 $\mu gm/cm^3$ with

50 percent attenuation to about 20 $\mu gm/cm^3$ with 90 percent attenuation.

It should be pointed out, however, that the purpose of this research was directed toward establishing the wavelength dependence of k/ρ_p at various temperatures, rather than its magnitude. It is well known that the magnitude of k/ρ_p depends on how the aerosol is produced, and experimental measurements by others have ranged from 10,000 cm^2/gm to 50,000 cm^2/gm[11]. The value of this research lies in establishing that a carbon aerosol has been produced for which k/ρ_p is essentially independent of wavelength up to $1500^\circ F$. Factors introducing errors in ρ_p include the deposition of particles on the tube walls before reaching the filter, changes in the aerosol concentration in the chimney due to the sample being withdrawn, air leaks in the sampling system, and the uncertainty in the gas temperature in the reservoir jug after the sample has been pulled.

The measured values of k'/ρ_p ranged from 2 x 10^4 to 4 x 10^4, both at room temperature and at higher temperatures. Since all major factors introducing error into the value for ρ_p tend to make ρ_p appear too large, k'/ρ_p should be closer to the lower value of 2 x 10^4 cm^2/gm. A careful analysis of the density data obtained throughout the course of this experiment has led the author to accept the value of

$$k'/\rho_p = 2 \times 10^4 \ cm^2/gm \pm 50\% \quad . \tag{23}$$

This relatively large error in ρ_p could be reduced considerably by using a more sophisticated sampling mechanism.

Destructive Test

Temperatures above 1525°F were not investigated because of possible damage to the spectrometer due to melting of the lithium fluoride window, and because of an increasing background signal. After all data had been taken, the spectrometer was filled with helium under a positive pressure of six inches of water to insure that a window meltdown would result in a gas flow out of the spectrometer, thus averting any damage to its internal components, and a destructive test of the furnace was run to ascertain the maximum gas temperature that could be reached with the present design. With the photomultiplier removed and nitrogen flowing, the heater power was turned on and the power slowly increased. The observation chamber was viewed through a piece of handi-wrap covering the photomultiplier housing.

As the power was increased, the gas temperature rose and the voltage across the tungsten filament increased. When the gas temperature reached 1000°F, the observation chamber was glowing red and the filament, which could be seen through the chimney, glowed like a light filament. At a gas temperature of 1850°F, the filament melted and shorted out on the bottom plate of the water jacket. The spike in the voltage curve resulted from the initial break of the filament, and the voltage dropped to zero as the melted filament shorted out. The details of this test are shown in Figure 16.
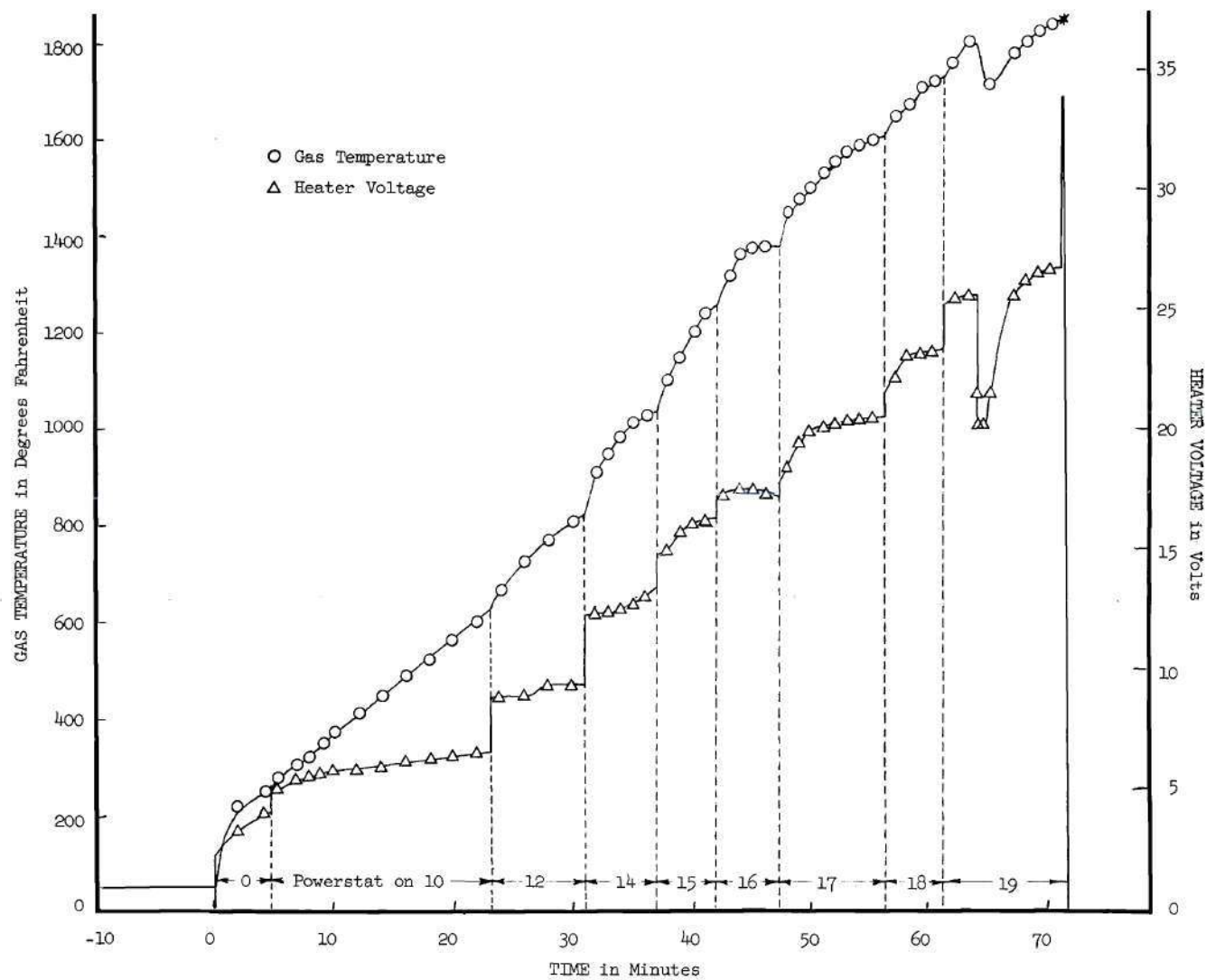
Figure 16. Destructive Test

CHAPTER V

CONCLUSIONS

The initial purpose of this research was to demonstrate the feasibility of using small carbon particles in hydrogen propellant to absorb the radiant energy from the hot gaseous core which is not absorbed by the hydrogen. Previously no measurements of the wavelength dependence of the optical properties of carbon aerosols had been reported in the vacuum ultraviolet region or at elevated temperatures. This project had as its objective the measurement of the mass absorption coefficient of a carbon particle cloud over all wavelengths of interest to the gaseous core concept (1000 Å to about 8000 Å) and at elevated temperatures.

The mass absorption coefficient, k/ρ_p, of a carbon particle cloud was measured and found to be essentially independent of wavelength and temperature over the wavelength range investigated, for temperatures below about $1500^{\circ}F$. The value of k/ρ_p was measured to be about 2×10^4 cm^2/gm. The application of the results of this experiment to the gaseous core nuclear rocket is greatly simplified by assuming that the apparent wavelength and temperature independence of k/ρ_p also applies to seeded hydrogen.

Ragsdale[15] suggests that the pressure inside the gaseous core rocket would be about 500 atmospheres, and the thickness of propellant surrounding the core may be about 100 cm. Since the particles are only useful for absorbing radiation at propellant temperatures below about $4500^{\circ}K$, one might consider the average temperature of the seeded gas in the core to

be about $3000^{\circ}K$, based on an entrance temperature of about $1500^{\circ}K$. Hydrogen at $3000^{\circ}K$ temperature and 500 atmospheres pressure has a density of 4×10^{-3} gm/cm^3.(16)

Letting the hydrogen density, ρ_H, be 4×10^{-3} gm/cm^3 and assuming the mass absorption coefficient, k/ρ_p, to be the value measured in this experiment, 2×10^4 cm^2/gm, one can then calculate the attenuation, I/I_o, of a beam of light at a distance x into the aerosol as a function of seed density, ρ_p, in grams of carbon seed per cubic centimeter of aerosol. The results of the calculations are given in Table 1 and presented in Figures 17 through 19.

Table 1. Attenuation Versus Seed Concentration

% Seed $\dfrac{\rho_p}{\rho_H} \times 10^{-2}$	ρ_p $\dfrac{gms}{cm^3}$	k_p cm^{-1}	$I/I_o = e^{-k_p x}$ x=1cm	5cm	10cm	50cm	100cm
0.01	4@-7	0.008	1.000	0.960	0.923	0.670	0.449
0.02	8@-7	0.016	0.990	0.923	0.852	0.449	0.201
0.05	2@-6	0.04	0.960	0.819	0.670	0.135	1.83@-2
0.1	4@-6	0.08	0.923	0.670	0.449	1.83@-2	3.35@-4
0.2	8@-6	0.16	0.852	0.449	0.201	3.35@-4	1.12@-7
0.5	2@-5	0.4	0.670	0.135	1.83@-2	2.06@-9	4.25@-18
1.0	4@-5	0.8	0.449	1.83@-2	3.35@-4	4.25@-8	-------
2.0	8@-5	1.6	0.201	3.35@-4	1.12@-7	-------	-------

Thus, to get a factor of 10,000 attenuation over a one meter distance, only about 0.1 percent by mass of carbon seed is required. This means that
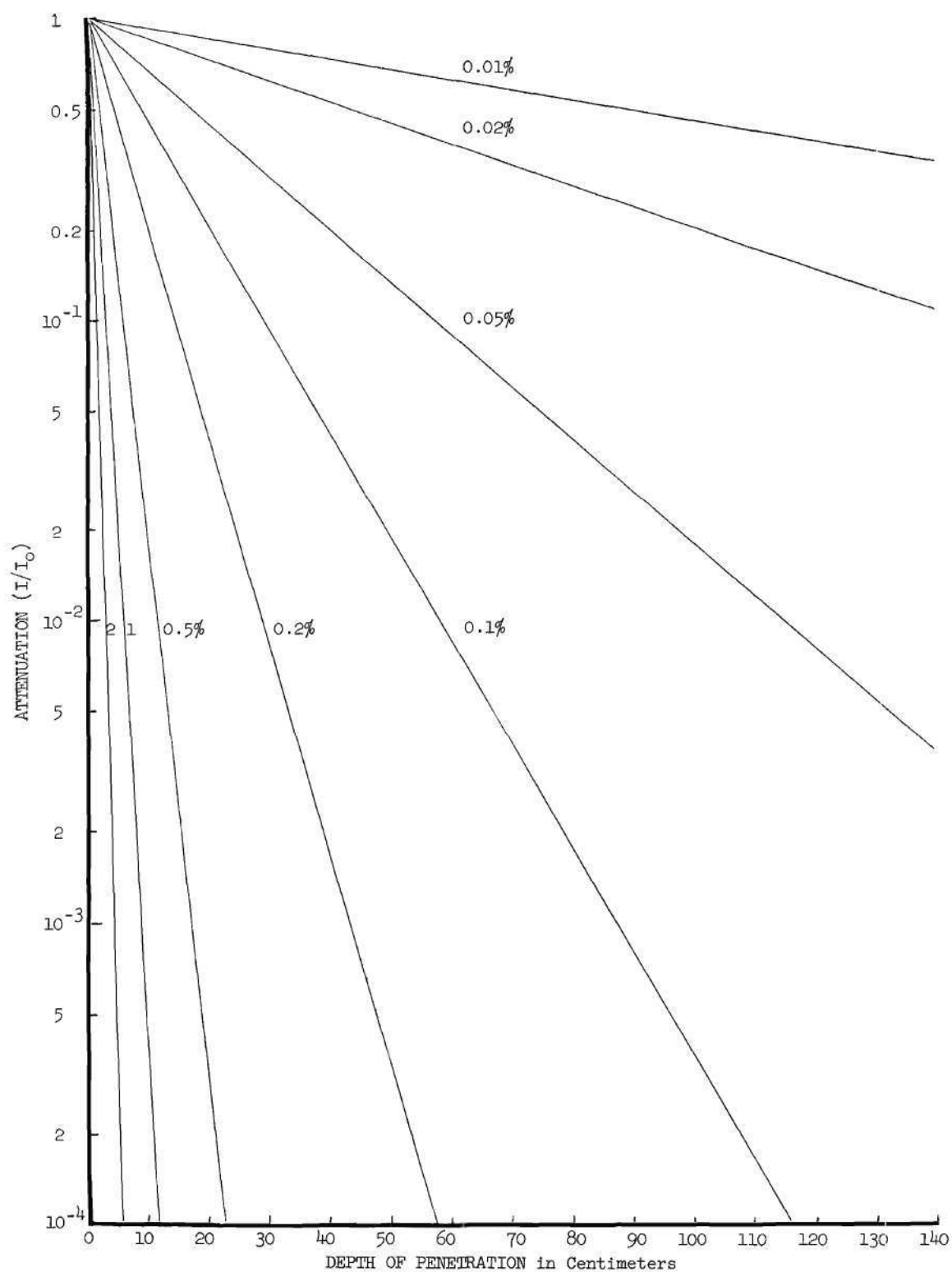
Figure 17. Energy Attenuation as a Function of Distance Through
the Propellant for Various Seed Densities
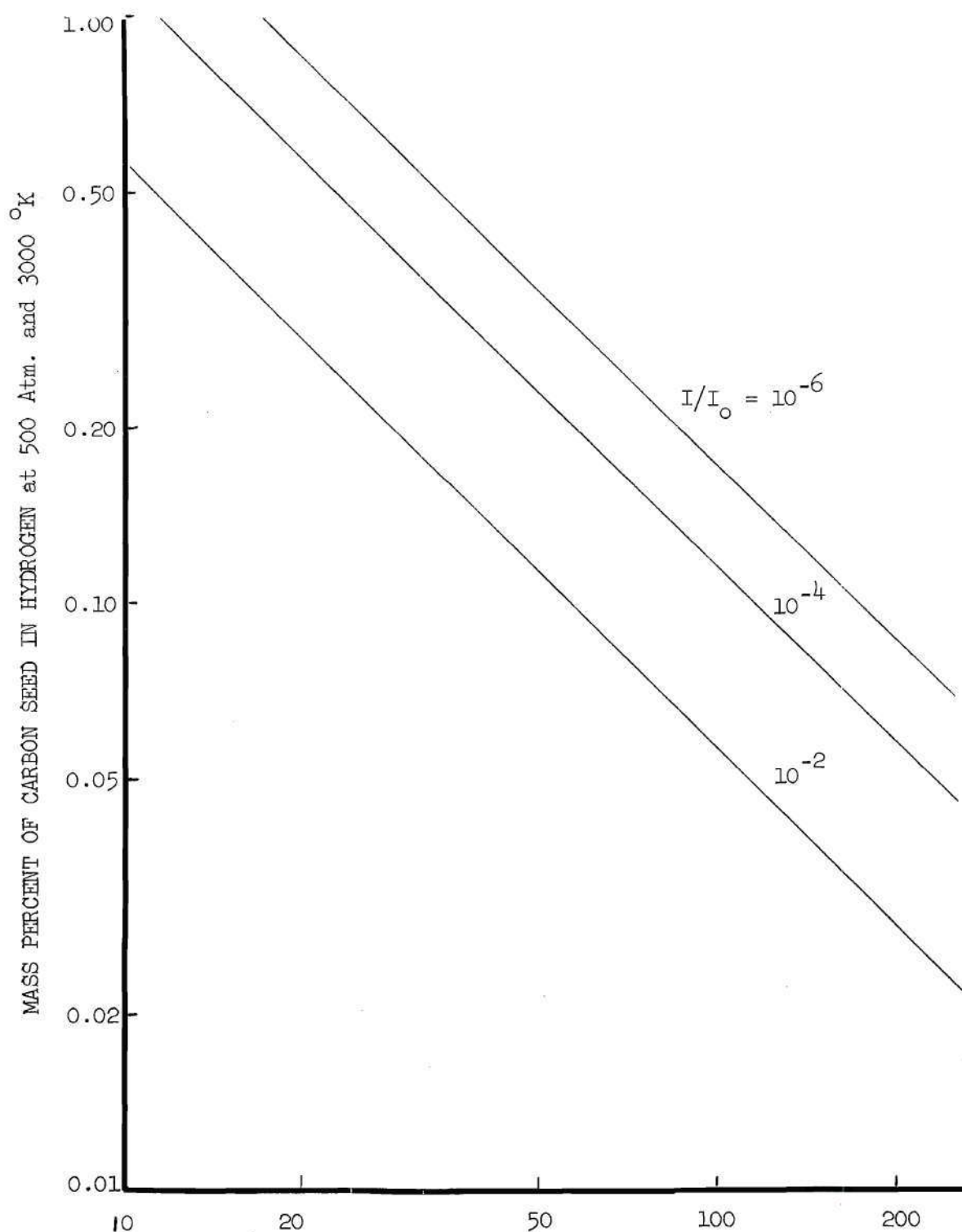
Figure 18.

PROPELLANT THICKNESS in Centimeters

Mass Percent of Carbon Seed Required for Attenuations of $10^{-2}, 10^{-4}$ and 10^{-6} as a Function of Propellant Thickness
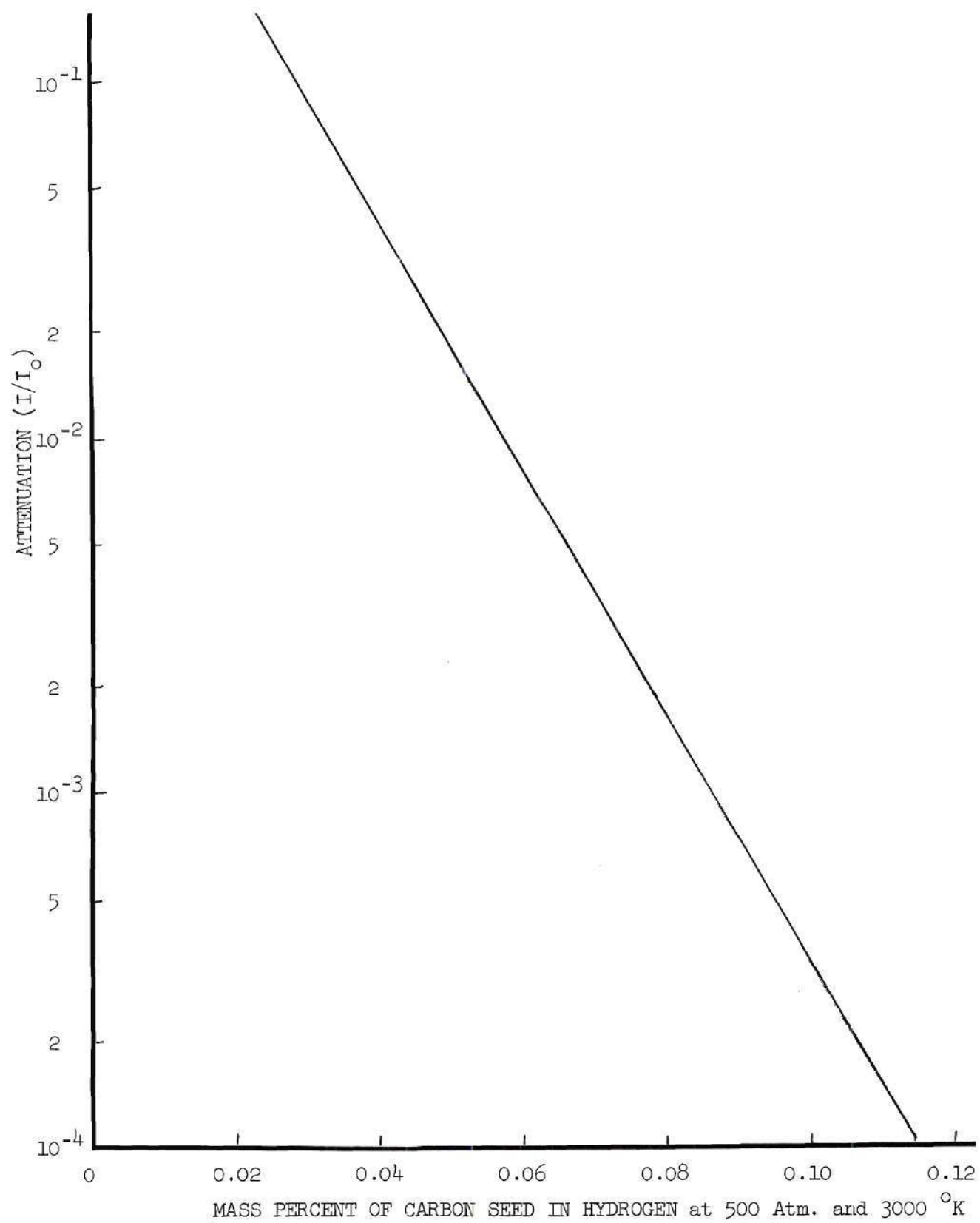
Figure 19.   Attenuation vs. Mass % Seed for One Meter of Propellant

only one pound of carbon is required per thousand pounds of hydrogen, which would have a negligible effect on specific impulse and would be quite satisfactory for the gaseous core rocket.

Actually, the energy from the core would not be radiated entirely perpendicular to the surface of the core. Much of the radiant energy must traverse a distance greater than the thickness of the propellant because it leaves the surface at an angle other than 90°. This means that the attenuation of the radiant energy is even greater for a particular seed concentration than is indicated above, unless the carbon particles become significantly less absorbing at temperatures between $1500^{\circ}F$ and $6500^{\circ}F$.

The spectrum emitted from the core would probably not be that of a black body, but as long as the absorption coefficient of the carbon particles is independent of wavelength, the spectrum of the emitted radiation is unimportant. It is interesting to note that the theory for spherical particles, which is discussed in detail in Appendix A, does not necessarily predict this wavelength independence. One might imagine the mass absorption coefficient of a real particle cloud to represent a sum of many of the curves presented in Figure 23 for different sizes such that the sum is wavelength independent. Also one must remember that in the real case the particles are not spheres but are irregularly shaped.

The results of this research indicate that, unless the absorption characteristics of the particle cloud change drastically at temperatures above $1500^{\circ}F$ but below the vaporization temperature, the carbon particles investigated would make a highly satisfactory seed material for gaseous core rocket applications.

CHAPTER VI

RECOMMENDATIONS

The experimental technique demonstrated by this project should be useful in obtaining attenuation data for much higher temperatures than those investigated here. A few minor modifications in the equipment arrangement should serve to greatly increase the operating temperature.

1. The furnace should be located between the source and the spectrometer rather than between the spectrometer and the photomultiplier as was the case here. With this arrangement the background signal would be practically eliminated because only that thermal radiation from the observation chamber which traversed the length of the spectrometer and was diffracted off the grating at the appropriate angle would be observed.

2. The filament and heating chamber should be raised so that the beam of light would pass across the top of the heating element. Then the gas would not cool down as much before being traversed by the light beam.

3. Separate vacuum systems should be used for the source and the spectrometer so that the source would operate at a relatively high pressure (several hundred microns of mercury) while the spectrometer would pump down to a good vacuum.

4. An automated data collecting system which could take data rapidly and punch them onto paper tape would greatly increase the accuracy of these measurements. The paper tape could then be used for rapid and accurate computer processing of large amounts of data.

5. A more precise, and probably more elaborate, means of measuring the seed density, ρ_p, is needed.

6. The aerosol generator used in this research was simple and produced a fairly uniform aerosol for a short time but offered little control of the aerosol density. A more sophisticated approach, as described in reference 10, could be taken to produce a steadier, finer aerosol.

7. At higher temperatures, above about $2500^{\circ}F$, thermocouples cannot be used for temperature measurements. Above $2500^{\circ}F$ the temperature can be measured with an optical pyrometer or by monitoring the resistance of a tungsten wire inside the observation chamber.

8. Flow meters would be useful in monitoring the gas flow rates so that given flow conditions could be reproduced easily.

9. For this type of work, it is important that the tungsten heating element be of a simple design and easily replaceable. Since one would like to operate with the heating element as hot as possible, the heating element would need to be replaced occasionally when it melts. The basic furnace design and especially the heating chamber design employed in this work is highly recommended because of the ease of making and installing the heating element.

10. If the arrangement in recommendation number 1 is used, a photomultiplier detector covered by a narrow band pass filter may be positioned beside the grating to give a signal proportional to the intensity of the light which passed through the aerosol. Since this photomultiplier would respond to a narrow band of wavelengths only, its signal could be related to the mass density, ρ_p, of the aerosol by $I/I_o = \exp(-kx)$ where $k = \text{const} \cdot \rho_p$. This arrangement would permit the continuous monitoring of the aerosol

concentration.

11. This experimental technique can be easily applied to seed materials other than carbon and carrier gases other than nitrogen. Burkig[13] suggests that iron and tantalum carbide may be useful seed materials. Experiments using hydrogen as the carrier gas would be more applicable to the gaseous core rocket problem.

APPENDICES

APPENDIX A

MIE THEORY OF SCATTERING

Background

In a paper published in 1908, G. Mie[21] obtained from Maxwell's equations a rigorous solution for the diffraction of a plane monochromatic wave by a homogeneous sphere of any diameter and of any composition situated in a homogeneous medium. An equivalent solution of the same problem was published shortly afterward by Peter Debye[22], and since then the subject has been treated in its different aspects by many writers.

Mie's solution, though derived for diffraction by a single sphere, also applies to diffraction by any number of spheres, provided that they are all of the same diameter and composition and provided also that they are randomly distributed and separated from each other by distances that are large compared to the particle radius. Under these circumstances there are no coherent phase relationships between the light that is scattered by the different spheres, and the total scattered energy is equal to the energy scattered by one sphere multiplied by their total number. Similarly, for a distribution of sizes, the energies scattered by the spheres of each particular size may be summed to obtain the total scattered energy.

The following detailed derivation of the Mie equations follows for the most part a brief outline of the solution in reference 19. References 17, 12, 23, 24, and 25 were also used extensively.

In this derivation the solution of Maxwell's equations is found

which describes the field arising from a plane monochromatic wave incident upon a spherical surface, across which the properties of the medium change abruptly. The incident wave and the boundary conditions are described in terms of a spherical polar coordinate system centered on the sphere, and the field represented as the sum of two subfields, each of which satisfies Maxwell's equations and the boundary conditions. Maxwell's equations together with the boundary conditions then separate into a set of ordinary differential equations, which are solved for the two subfields in the form of infinite series. The sum of the solutions for the two subfields is the solution for the actual field. The solution for the scattered wave is used to calculate the desired cross sections for spherical particles.

NOMENCLATURE

$\vec{H}(\vec{r},t)$ magnetic component of an electromagnetic wave

$\vec{E}(\vec{r},t)$ electric component of an electromagnetic wave

ϵ inductive capacity

μ magnetic permeability (=1 for non-magnetic materials)

σ electrical conductivity

ω frequency of the time varying fields

i $\sqrt{-1}$, as a superscript represents the incident wave

t time

c speed of light in vacuum

k_1 constant equal to $\frac{i\omega}{c}\left(\epsilon + i\,\frac{4\pi\sigma}{\omega}\right)$

k_2 constant equal to $\frac{i\omega}{c}$

k constant given by $k^2 = -k_1 \cdot k_2$, called the wave number

I as a superscript identifies quantities pertaining to the medium surrounding the sphere

II as a superscript identifies quantities pertaining to the sphere

x direction of the electric vector of the incoming wave

y direction of the magnetic vector of the incoming wave

z direction of propagation of the incoming wave

w as a superscript represents the wave within the sphere

s as a superscript represents the scattered wave

$\vec{i}$ unit vector in x direction

$\vec{j}$ unit vector in y direction

$\vec{k}$ unit vector in z direction

$\perp$ perpendicular component

$\parallel$ parallel component

a   radius of the sphere

r   distance from the center of the sphere to a field point

θ angle of scattering

ϕ angle between plane of observation and x axis

e   superscript which represents the "electric wave"

m   superscript which represents the "magnetic wave"

$^e\Pi, {}^m\Pi$ Debye's potentials-scalar functions from which the electric and magnetic waves may be derived

U   scalar function equal to $\frac{\partial}{\partial r}(r^e\pi)$

V   scalar function equal to $\frac{\partial}{\partial r}(r^m\pi)$

Π general function representing either $^e\Pi$ or $^m\Pi$

$R(r)$ functional dependence of Π on r

$\Theta(\theta)$ functional dependence of Π on θ

$\Phi(\phi)$ functional dependence of Π on ϕ

β constant equal to m^2 where m is any integer

α constant equal to $\ell(\ell+1)$ where ℓ is any integer greater than or equal to the absolute value of m

ξ $= \cos\theta$

$J_n(\rho)$ Bessel function of order n

$N_n(\rho)$ Neumann function of order n

$\Psi_n(\rho)$ $= \sqrt{\frac{\pi\rho}{2}}\, J_{n+\frac{1}{2}}(\rho)$

$\chi_n(\rho)$ $= \sqrt{\frac{\pi\rho}{2}}\, N_{n+\frac{1}{2}}(\rho)$

$\zeta_n^{(1)}(\rho)$ $= \Psi_n(\rho) - i\,\chi_n(\rho)$

$H_n^{(1)}$ Hankel function given by $H_n^{(1)} = J_n + i\,N_n$

$P_\ell^{(1)}$ Langendre polynomials

λ_o	wavelength of the light in vacuum
λ	wavelength of the light in medium surrounding the sphere
$\hat{n}$	complex refractive index of the sphere relative to the surrounding medium
q	$2\pi a/\lambda$
a_n, b_n	Mie coefficients
σ_e	extinction cross section
σ_s	scattering cross section
σ_a	absorption cross section
Re	denotes the real part
V	particle volume
ρ	density of sphere

DIFFRACTION BY A CONDUCTING SPHERE (MIE THEORY)

For small metallic particles refraction, absorption, and diffraction of light take place simultaneously. If the metallic particles were pure conductors, one would only be dealing with a problem of pure diffraction. For real metal particles, however, the effects that are due to the partial penetration of light into the particles are of particular physical interest.

In deriving Mie's formulae, one concerns himself with finding a solution of Maxwell's equations which describes the field arising from a plane monochromatic wave incident upon a spherical surface, across which the properties of the medium change abruptly. Using spherical polar coordinates one finds that Maxwell's equations, together with the boundary conditions, separate into a set of ordinary differential equations which may be taken to represent two subfields. These equations are then solved to obtain infinite series solutions.

Consider the diffraction of a plane, linearly polarized, monochromatic wave by a sphere of radius a, immersed in a homogeneous, isotropic medium. We assume the medium to be a non-conductor and both medium and sphere non-magnetic.

Maxwell's equations[*] include, for no sources,

$$\nabla \times \vec{H}(t) = \frac{4\pi}{c} \vec{J}(t) + \frac{1}{c} \frac{\partial \vec{D}(t)}{\partial t} \tag{24}$$

---

[*] Stratton[25], p. 178

$$\nabla \times \vec{E}(t) + \frac{1}{c} \frac{\partial \vec{B}(t)}{\partial t} = 0 \tag{25}$$

$$\nabla \cdot \vec{D}(t) = 0 \tag{26}$$

$$\nabla \cdot \vec{B}(t) = 0 \tag{27}$$

where

$$\vec{D}(t) = \varepsilon \vec{E}(t) \tag{28}$$

$$\vec{B}(t) = \mu \vec{H}(t) \tag{29}$$

$$\vec{J}(t) = \sigma \vec{E}(t) \tag{30}$$

μ, the permeability, is 1 for non-magnetic materials, so $\vec{B}$ is equal to $\vec{H}$.[*]
For plane waves incident on the sphere, the time dependence is taken to
be $e^{-i\omega t}$. The time dependence will be the same inside the sphere, so both
inside and outside the sphere

$$\vec{E}(t) = \vec{E} e^{-i\omega t} \tag{31}$$

$$\vec{H}(t) = \vec{H} e^{-i\omega t} \tag{32}$$

---

[*] Stratton[(25)], p. 153

$\vec{E}$ and $\vec{H}$ are now time independent. Insert Equations (28) and (30) into Equation (24).

$$\nabla \times \vec{H}(t) = \frac{4\pi\sigma}{c} \vec{E}(t) + \frac{\varepsilon}{c} \frac{\partial \vec{E}(t)}{\partial t} \tag{33}$$

Insert Equation (29) into Equation (25).

$$\nabla \times \vec{E}(t) = -\frac{1}{c} \frac{\partial \vec{H}(t)}{\partial t} \tag{34}$$

Substituting Equation (31) into Equation (33) one gets

$$\nabla \times \vec{H} = \frac{4\pi\sigma}{c} \vec{E} - \frac{i\omega\varepsilon}{c} \vec{E} \tag{35}$$

Also, substituting Equation (32) into Equation (34) produces

$$\nabla \times \vec{E} = \frac{i\omega}{c} \vec{H} \tag{36}$$

Equations (35) and (36) are Maxwell's equations in their time-free form, which may also be written

$$\nabla \times \vec{H} = -k_1 \vec{E} \tag{37}$$

$$\nabla \times \vec{E} = k_2 \vec{H} \tag{38}$$

where

$$k_1 = \frac{i\omega}{c}\left(\varepsilon + i\,\frac{4\pi\sigma}{\omega}\right) \tag{39}$$

and

$$k_2 = \frac{i\omega}{c} \tag{40}$$

Consider Equations (37) and (38). Insert Equations (28) and (29) into Equations (26) and (27), and remembering that ε and μ are assumed to be constant, one has for the case of no sources,

$$\nabla \cdot \vec{E} = 0 \tag{41}$$

$$\nabla \cdot \vec{H} = 0 \tag{42}$$

Take the curl of Equations (37) and (38),

$$\nabla \times \nabla \times \vec{H} = -k_1 \nabla \times \vec{E} \tag{43}$$

$$\nabla \times \nabla \times \vec{E} = k_2 \nabla \times \vec{H} \tag{44}$$

Substitute Equations (37) and (38) into Equations (43) and (44).

$$\nabla \times \nabla \times \vec{H} = -k_1 k_2 \vec{H} \tag{45}$$

$$\nabla \times \nabla \times \vec{E} = -k_1 k_2 \vec{E} \tag{46}$$

Since

$$\nabla \times (\nabla \times \vec{A}) = \nabla(\nabla \cdot \vec{A}) - \nabla^2 \vec{A} \tag{47}$$

where $\vec{A}$ is any vector, substitute Equations (41), (42), (45), and (46) into Equation (47) to get Equations (48) and (49).

$$\nabla^2 \vec{H} = k_1 k_2 \vec{H} \tag{48}$$

$$\nabla^2 \vec{E} = k_1 k_2 \vec{E} \tag{49}$$

Let u represent any Cartesian component of $\vec{E}$ or $\vec{H}$, then one has

$$\nabla^2 u = k_1 k_2 u = -k^2 u \tag{50}$$

where k^2 is defined by

$$k^2 = -k_1 k_2 \tag{51}$$

If one considers a wave propagating in only one direction, say, the z direction, then the solution for $u(z,t)$ is

$$u(z,t) = A e^{ikz - i\omega t} + B e^{-ikz - i\omega t} \tag{52}$$

where k is given by Equation (51). k is called the wave number. It is real outside the sphere and complex inside the sphere.
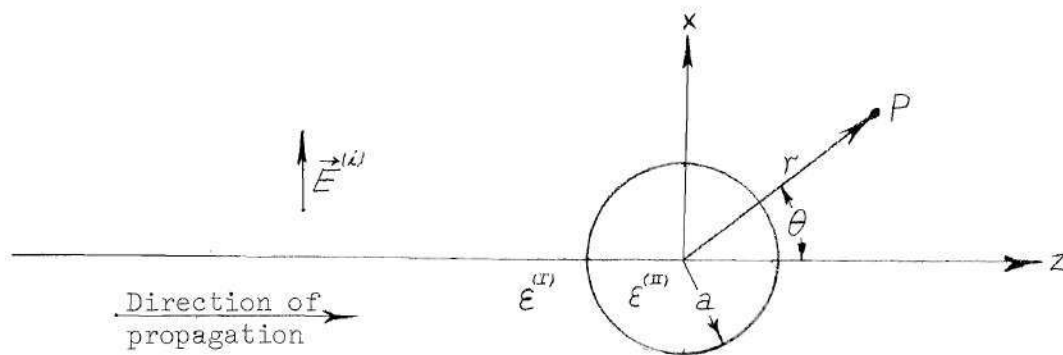
Figure 20.   Diffraction from a Sphere

Let the superscript I refer to quantities pertaining to the medium surrounding the sphere and II refer to the sphere.

$$\sigma^{(I)} = 0 \tag{53}$$

Let z be the direction of propagation of a plane wave and x be the direction of its electric vector.

Let the amplitude of the electric vector of the incident wave be normalized to unity, i.e.,

$$\left| \vec{E}^{(i)} \right| = \left| e^{i k^{(I)} z} \right| = 1 \tag{54}$$

Let superscript (i) represent the incident wave, (w) represent the wave within the sphere, and (s) represent the scattered wave. Thus, one has

$$E_x^{(i)} = e^{i k^{(I)} z} \tag{55}$$

and since

$$\vec{H}^{(i)} = \frac{1}{k_z^{(I)}} \nabla \times \vec{E}^{(i)} = \frac{1}{k_z^{(I)}} \begin{vmatrix} \vec{i} & \vec{j} & \vec{k} \\ \frac{\partial}{\partial x} & \frac{\partial}{\partial y} & \frac{\partial}{\partial z} \\ e^{ikz^{(I)}} & 0 & 0 \end{vmatrix} = \frac{1}{k_z^{(I)}} \frac{\partial}{\partial z} e^{ikz^{(I)}} \vec{j} = \frac{ik^{(I)}}{k_z^{(I)}} e^{ikz^{(I)}} \vec{j} \qquad (56)$$

The six components of the incident field vectors are

$$E_x^{(i)} = e^{ikz^{(I)}} \qquad (57)$$

$$H_y^{(i)} = \frac{ik^{(I)}}{k_z^{(II)}} e^{ikz^{(I)}} \qquad (58)$$

$$E_y^{(i)} = E_z^{(i)} = H_x^{(i)} = H_z^{(i)} = 0 \qquad (59)$$

Gauss' theorem states that for any vector $\vec{A}$

$$\oint \vec{A} \cdot d\vec{a} = \int \nabla \cdot \vec{A} \, dv \qquad (60)$$

Using Equations (41) and (42), Equation (60) becomes Equations (61) and (62).

$$\oint \vec{H} \cdot d\vec{a} = \int \nabla \cdot \vec{H} \, dv = 0 \qquad (61)$$

$$\oint \vec{E} \cdot d\vec{a} = \int \nabla \cdot \vec{E} \, dv = 0 \qquad (62)$$

If one considers a small element of volume as shown, then
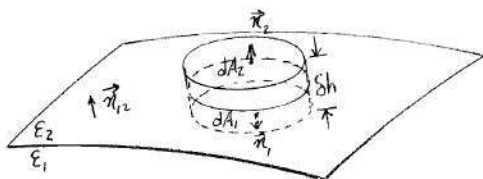
using Equation (61) he has

$$\oint \vec{H} \cdot \vec{da} = \vec{H}^{(1)} \cdot \vec{n}_1 \delta A_1 + \vec{H}^{(2)} \cdot \vec{n}_2 \delta A_2 + \text{contribution from walls} = 0. \quad (63)$$

Let $\delta h \to 0$, then the contribution from the walls approaches zero and at the surface,

$$(\vec{H}^{(1)} \cdot \vec{n}_1 + \vec{H}^{(2)} \cdot \vec{n}_2) \, \delta A = 0 \quad (64)$$

Since at the surface - $\vec{n}_1 = \vec{n}_2 = \vec{n}_{12}$, and $\delta A \neq 0$, Equation (64) implies Equation (65)

$$\vec{n}_{12} \cdot (\vec{H}^{(2)} - \vec{H}^{(1)}) = 0 \quad (65)$$

Thus, the normal component of $\vec{H}$ is continuous at the interface between two non-magnetic materials. The same argument shows that the normal component of $\epsilon \, \vec{E}$ is continuous at the interface.

Next, examine the behavior of the tangential components.
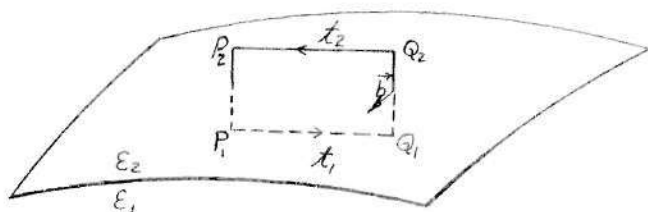
Consider the rectangular path with points P_1 and Q_1 in material 1, and points P_2 and Q_2 in material 2. Let $\vec{b}$ be the unit vector perpendicular to the plane of the rectangle. Stokes' theorem states that for any vector $\vec{A}$,

$$\oint \vec{A} \cdot \vec{dr} = \int (\nabla \times \vec{A}) \cdot \vec{da} \tag{66}$$

so

$$\oint \vec{E} \cdot \vec{dr} = \int (\nabla \times \vec{E}) \cdot \vec{b}\, da = -\frac{1}{c} \int \frac{\partial \vec{H}}{\partial t} \cdot \vec{b}\, da \tag{67}$$

The second and third integrals are taken throughout the area of the rectangle, and the first along its boundary.

Let the length P_1 to $Q_1 = \delta \ell_1$, then the length P_2 to $Q_2 = \delta \ell_2$, then if $\delta \ell_1$ and $\delta \ell_2$ are small, $\vec{E}$ may be replaced by constant values $\vec{E}^{(1)}$ and $\vec{E}^{(2)}$ along each of these segments. Similarly, $\frac{\partial \vec{B}}{\partial t}$ may be replaced by constant values. Equation (67) then gives

$$\vec{E}^{(1)} \cdot \vec{t}_1 \delta \ell_1 + \vec{E}^{(2)} \cdot \vec{t}_2 \delta \ell_2 + \text{contribution from ends} = -\frac{1}{c} \frac{\partial \vec{B}}{\partial t} \cdot \vec{b}\, \delta \ell\, \delta h \tag{68}$$

where $\delta \ell$ is the length of $\delta \ell_1$ or $\delta \ell_2$. Now if the height of the rectangle, δh, is shrunk to zero, the contribution from the ends shrinks to zero.

Also, if $\frac{\partial \vec{B}}{\partial t}$ remains finite, the last term vanishes and Equation (68) becomes

$$(\vec{E}^{(1)} \cdot \vec{t}_1 + \vec{E}^{(2)} \cdot \vec{t}_2) \delta l = 0 \tag{69}$$

Let $\vec{n}_{12}$ be the normal from medium 1 to medium 2, so

$$-\vec{t} = \vec{t}_1 = -\vec{b} \times \vec{n}_{12} \tag{70}$$

$$\vec{t} = \vec{t}_2 = \vec{b} \times \vec{n}_{12} \tag{71}$$

Thus, Equation (69) becomes

$$\vec{b} \cdot [\vec{n}_{12} \times (\vec{E}^{(2)} - \vec{E}^{(1)})] = 0 \tag{72}$$

Since the orientation of the rectangle and consequently that of the unit vector $\vec{b}$ is arbitrary, it follows that

$$\vec{n}_{12} \times (\vec{E}^{(2)} - \vec{E}^{(1)}) = 0 \tag{73}$$

thus, the tangential component of the electric vector is continuous across the surface. The analysis of the tangential component of the $\vec{H}$ vector is the same.

Thus, in the case of the conducting sphere, one has the following four boundary conditions at $r = a$.

$$E_{tan}^{(1)} = E_{tan}^{(2)} \tag{74}$$

$$H_{tan}^{(1)} = H_{tan}^{(2)} \tag{75}$$

$$\varepsilon^{(1)} E_{\perp}^{(1)} = \varepsilon^{(2)} E_{\perp}^{(2)} \tag{76}$$

$$H_{\perp}^{(1)} = H_{\perp}^{(2)} \tag{77}$$

In order to satisfy these boundary conditions, one must assume that in addition to incident field $\vec{E}^{(i)}$, $\vec{H}^{(i)}$ and the field within the sphere $\vec{E}^{(w)}$, $\vec{H}^{(w)}$, there is a scattered (or diffracted) field $\vec{E}^{(s)}$, $\vec{H}^{(s)}$ in the medium surrounding the sphere. Thus, the total electric field is given by Equation (78) outside the sphere,

$$\vec{E} = \vec{E}^{(i)} + \vec{E}^{(s)} \tag{78}$$

and by Equation (79) inside the sphere.

$$\vec{E} = \vec{E}^{(w)} \tag{79}$$

with similar expressions for $\vec{H}$.

Since the boundary conditions must hold for all time, all the six vectors must have the same time dependence. Obviously, if they did not have the same time dependence, then E_{tan} and $\varepsilon E_{\perp}$ would not always be con-

tinuous at the surface of the sphere. Thus, the time dependence of all six vectors is $e^{-i\omega t}$.

Now introduce spherical polar coordinates r, θ, φ such that

$$x = r \sin\theta \cos\phi \tag{80}$$

$$y = r \sin\theta \sin\phi \tag{81}$$

$$z = r \cos\theta \tag{82}$$

Let $\vec{i}$, $\vec{j}$, and $\vec{k}$ be the orthonormal basis vectors of our Cartesian coordinate system, and $\vec{1}_r$, $\vec{1}_\theta$, and $\vec{1}_\phi$ be the basis vectors of the spherical system. Then in the rectangular system, for any vector $\vec{A}$

$$\nabla \times \vec{A} = \begin{vmatrix} \vec{i} & \vec{j} & \vec{k} \\ \dfrac{\partial}{\partial x} & \dfrac{\partial}{\partial y} & \dfrac{\partial}{\partial z} \\ A_x & A_y & A_z \end{vmatrix} \tag{83}$$

In the spherical polar coordinate system, the curl is

$$\nabla \times \vec{A} = \begin{vmatrix} \dfrac{\vec{1}_r}{r^2 \sin\theta} & \dfrac{\vec{1}_\theta}{r \sin\theta} & \dfrac{\vec{1}_\phi}{r} \\ \dfrac{\partial}{\partial r} & \dfrac{\partial}{\partial \theta} & \dfrac{\partial}{\partial \phi} \\ A_r & r A_\theta & r \sin\theta A_\phi \end{vmatrix} \tag{84}$$

The components of $\vec{A}$ are transformed from the Cartesian to the spherical

system by

$$A_r = A_x \sin\theta \cos\phi + A_y \sin\theta \sin\phi + A_z \cos\theta \qquad (85)$$

$$A_\theta = A_x \cos\theta \cos\phi + A_y \cos\theta \sin\phi - A_z \sin\theta \qquad (86)$$

$$A_\phi = -A_x \sin\phi + A_y \cos\phi \qquad (87)$$

Applying Equation (84), Equations (37) and (38) become Equations (88) through (93).

$$-k_1 E_r = \frac{1}{r^2 \sin\theta} \left\{ \frac{\partial}{\partial\theta}(r\sin\theta H_\phi) - \frac{\partial}{\partial\phi}(rH_\theta) \right\} \qquad (88)$$

$$-k_1 E_\theta = \frac{1}{r\sin\theta} \left\{ \frac{\partial H_r}{\partial\phi} - \frac{\partial}{\partial r}(rH_\phi \sin\theta) \right\} \qquad (89)$$

$$-k_1 E_\phi = \frac{1}{r} \left\{ \frac{\partial}{\partial r}(rH_\theta) - \frac{\partial}{\partial\theta}H_r \right\} \qquad (90)$$

$$k_2 H_r = \frac{1}{r^2 \sin\theta} \left\{ \frac{\partial}{\partial\theta}(r\sin\theta E_\phi) - \frac{\partial}{\partial\phi}(rE_\theta) \right\} \qquad (91)$$

$$k_2 H_\theta = \frac{1}{r\sin\theta} \left\{ \frac{\partial E_r}{\partial\phi} - \frac{\partial}{\partial r}(rE_\phi \sin\theta) \right\} \qquad (92)$$

$$k_2 H_\phi = \frac{1}{r} \left\{ \frac{\partial}{\partial r}(rE_\theta) - \frac{\partial E_r}{\partial\theta} \right\} \qquad (93)$$

The boundary conditions at r = a, Equations (74) through (77), become Equations (94) through (99).

$$E_\theta^{(I)} = E_\theta^{(II)} \qquad (94)$$

$$H_\theta^{(I)} = H_\theta^{(II)} \qquad (95)$$

$$E_\phi^{(I)} = E_\phi^{(II)} \qquad (96)$$

$$H_\phi^{(I)} = H_\phi^{(II)} \qquad (97)$$

$$\epsilon_1 E_r^{(I)} = \epsilon_2 E_r^{(II)} \qquad (98)$$

$$H_r^{(I)} = H_r^{(II)} \qquad (99)$$

Equations (88) through (93) and boundary conditions, Equations (94) through (99), are the basic equations of the problem of the scattering of electromagnetic radiation by a conducting sphere.

The first step toward solving these equations will be to represent the $\vec{E}$ and $\vec{H}$ fields as a superposition of two linearly independent fields $(^e\vec{H}, \,^e\vec{H})$ and $(^m\vec{E}, \,^m\vec{H})$ each satisfying Equations (88) through (93) such that

$$\vec{E} = \,^e\vec{E} + \,^m\vec{E} \qquad (100)$$

$$\vec{H} = {}^{e}\vec{H} + {}^{m}\vec{H} \tag{101}$$

$$^{e}H_r = 0 \tag{102}$$

$$^{m}E_r = 0 \tag{103}$$

$$^{e}E_r = E_r \tag{104}$$

and

$$^{m}H_r = H_r \tag{105}$$

Write these fields as vectors,

$$\vec{E} = \begin{bmatrix} E_r \\ E_\theta \\ E_\phi \end{bmatrix} \tag{106}$$

$$^{e}\vec{E} = \begin{bmatrix} E_r \\ ^{e}E_\theta \\ ^{e}E_\phi \end{bmatrix} \tag{107}$$

$$^{m}\vec{E} = \begin{bmatrix} 0 \\ ^{m}E_\theta \\ ^{m}E_\phi \end{bmatrix} \tag{108}$$

$$\vec{H} = \begin{bmatrix} H_r \\ H_\theta \\ H_\phi \end{bmatrix} \tag{109}$$

$$^e\vec{H} = \begin{bmatrix} O \\ ^eH_\theta \\ ^eH_\phi \end{bmatrix} \tag{110}$$

$$^m\vec{H} = \begin{bmatrix} H_r \\ ^mH_\theta \\ ^mH_\phi \end{bmatrix} \tag{111}$$

Since $^e\vec{E}$, $^e\vec{H}$, and $^m\vec{E}$, $^m\vec{H}$ each are taken to satisfy Equations (88) through (93), then $\vec{E}$ and $\vec{H}$ also do and the representation of the field as two sub-fields is consistent with the equations of the problem.

Now look at the electric wave, $(^e\vec{E}, \; ^e\vec{H})$, which is assumed to obey Maxwell's equations. Since $^e\vec{H}_r$ is zero, Equations (89) and (90) become

$$k_1\,^eE_\theta = \frac{1}{r}\frac{\partial}{\partial r}\left(r\,^eH_\phi\right) \tag{112}$$

$$k_1\,^eE_\phi = -\frac{1}{r}\frac{\partial}{\partial r}\left(r\,^eH_\theta\right) \tag{113}$$

Substituting Equation (112) into Equation (93) yields

$$k_2\,^eH_\phi = \frac{1}{r}\left\{\frac{\partial}{\partial r}\left[\frac{1}{k_1}\frac{\partial}{\partial r}\left(r\,^eH_\phi\right)\right] - \frac{\partial E_r}{\partial \theta}\right\} \tag{114}$$

which becomes

$$k_2 \, {}^e H_\phi = \frac{1}{k_1 r} \frac{\partial^2}{\partial r^2} (r \, {}^e H_\phi) - \frac{1}{r} \frac{\partial E_r}{\partial \theta} \tag{115}$$

or

$$\frac{\partial^2}{\partial r^2} (r \, {}^e H_\phi) - k_1 k_2 r \, {}^e H_\phi = k_1 \frac{\partial E_r}{\partial \theta} \tag{116}$$

but k^2 is $-k_1 k_2$ by Equation (51), where k is the wave number; so,

$$\left(\frac{\partial^2}{\partial r^2} + k^2 \right) (r \, {}^e H_\phi) = k_1 \frac{\partial E_r}{\partial \theta} \tag{117}$$

Similarly, substitute Equation (113) into Equation (92)

$$k_2 \, {}^e H_\phi = \frac{1}{r \sin\theta} \left\{ \frac{\partial E_r}{\partial \phi} + \frac{\partial}{\partial r} \left[\frac{1}{k_1} \frac{\partial}{\partial r} (r \, {}^e H_\theta) \sin\theta \right] \right\} \tag{118}$$

which becomes

$$k_2 \, {}^e H_\theta = \frac{1}{r \sin\theta} \frac{\partial E_r}{\partial \phi} + \frac{1}{k_1 r} \frac{\partial^2}{\partial r^2} (r \, {}^e H_\theta) \tag{119}$$

or

$$\frac{\partial^2}{\partial r^2} (r \, {}^e H_\theta) - k_1 k_2 r \, {}^e H_\theta = -\frac{k_1}{\sin\theta} \frac{\partial E_r}{\partial \phi} \tag{120}$$

so finally,

$$\left(\frac{\partial^2}{\partial r^2} + k^2\right)\left(r\,^eH_\theta\right) = -\frac{k_1}{\sin\theta}\frac{\partial E_r}{\partial \phi} \tag{121}$$

Equations (88), (117), and (121) constitute a complete system of equations for E_r, $^eH_\theta$, and $^eH_\phi$. This system of equations is written

$$\frac{1}{r^2\sin\theta}\left\{\frac{\partial}{\partial\theta}\left(r\sin\theta\,H_\phi\right) - \frac{\partial}{\partial\phi}\left(rH_\theta\right)\right\} = -k_1 E_r \tag{88}$$

$$\left(\frac{\partial^2}{\partial r^2} + k^2\right)\left(r\,^eH_\phi\right) = k_1\frac{\partial E_r}{\partial \theta} \tag{117}$$

$$\left(\frac{\partial^2}{\partial r^2} + k^2\right)\left(r\,^eH_\theta\right) = -\frac{k_1}{\sin\theta}\frac{\partial E_r}{\partial \phi} \tag{121}$$

Only those solutions of this system of equations which satisfy the condition $\nabla \cdot {}^e\vec{H} = 0$, Equation (27), represent physical fields, so one is restricted to such solutions. Since $^eH_r = 0$,

$$\nabla \cdot {}^e\vec{H} = \frac{1}{r\sin\theta}\left\{\frac{\partial\,^eH_\phi}{\partial\phi} + \frac{\partial}{\partial\theta}\left(^eH_\theta\sin\theta\right)\right\} = 0 \tag{122}$$

for any value of r and θ, so

$$\frac{\partial}{\partial\theta}\left(\sin\theta\,^eH_\theta\right) + \frac{\partial}{\partial\phi}\left(^eH_\phi\right) = 0 \tag{123}$$

Now substitute Equations (102), (112), and (113) into Equation (91)

$$O = \frac{1}{k_2 r^2 \sin\theta} \left\{ \frac{\partial}{\partial \theta} \left[-\frac{1}{k_1} \frac{\partial}{\partial r} (r \, ^eH_\theta) \sin\theta \right] - \frac{\partial}{\partial \phi} \left[\frac{1}{k_1} \frac{\partial}{\partial r} (r \, ^eH_\phi) \right] \right\} \tag{124}$$

which becomes

$$O = \frac{1}{k^2 r^2 \sin\theta} \frac{\partial}{\partial r} \left\{ r \left[\frac{\partial}{\partial \theta} (\sin\theta \, ^eH_\theta) + \frac{\partial}{\partial \phi} (^eH_\phi) \right] \right\} \tag{125}$$

which is satisfied because of Equation (123).

Equations (112) through (125) refer to the components of the $^e\vec{E}$, $^e\vec{H}$ field. The $^m\vec{E}$, $^m\vec{H}$ field could have been applied to obtain the complementary set of equations with $^mE_r = 0$ and $^mH_r = H_r$. The procedure is the same.

The solution $(^e\vec{E}, ^e\vec{H})$ with a vanishing radial magnetic field is called the electric wave (or transverse magnetic wave) and the solution $(^m\vec{E}, ^m\vec{H})$ with a vanishing radial electric field is called the magnetic wave (or transverse electric wave). Now it will be shown that there exists scalar potentials $^e\Pi$ and $^m\Pi$ from which they may be derived. $^e\Pi$ and $^m\Pi$ are called Debye's potentials.

Looking again at Equations (123) and (125), one sees that

$$\frac{\partial}{\partial \theta} (r \, ^eE_\phi \sin\theta) = \frac{\partial}{\partial \phi} (r \, ^eE_\theta) \tag{126}$$

Then, there exists a scalar function U such that

$$\frac{\partial U}{\partial \phi} = r \, ^eE_\phi \sin\theta \tag{127} \qquad\qquad \frac{\partial U}{\partial \theta} = r \, ^eE_\theta \tag{128}$$

Equation (126) may be written

$$\frac{\partial}{\partial\theta}\left(\frac{\partial U}{\partial\phi}\right) = \frac{\partial}{\partial\phi}\left(\frac{\partial U}{\partial\theta}\right) \tag{129}$$

which is an identity. Thus,

$$^e E_\phi = \frac{1}{r\sin\theta}\frac{\partial U}{\partial\theta} \tag{130}$$

$$^e E_\theta = \frac{1}{r}\frac{\partial U}{\partial\theta} \tag{131}$$

Now let

$$U = \frac{\partial}{\partial r}\left(r\,^e\Pi\right) \tag{132}$$

Then Equations (130) and (131) become

$$^e E_\theta = \frac{1}{r}\frac{\partial^2(r\,^e\Pi)}{\partial r\,\partial\theta} \tag{133}$$

$$^e E_\phi = \frac{1}{r\sin\theta}\frac{\partial^2(r\,^e\Pi)}{\partial r\,\partial\phi} \tag{134}$$

Substituting Equation (133) into Equation (112) yields

$$\frac{k_1}{r}\frac{\partial^2(r\,^e\Pi)}{\partial r\,\partial\theta} = \frac{1}{r}\frac{\partial}{\partial r}\left(r\,^e H_\phi\right) \tag{135}$$

or

$$k_i \frac{\partial}{\partial r}\left[r \frac{\partial^e \Pi}{\partial \theta} \right] = \frac{\partial}{\partial r}(r\, {}^e H_\phi)$$

(136)

This equation is satisfied by

$${}^e H_\phi = k_i \frac{\partial^e \Pi}{\partial \theta} = \frac{k_i}{r} \frac{\partial(r^e \Pi)}{\partial \theta}$$

(137)

Similarly, using Equation (134) it may be shown that Equation (113) is satisfied by

$${}^e H_\phi = -\frac{k_i}{\sin\theta} \frac{\partial^e \Pi}{\partial \phi} = -\frac{k_i}{r\sin\theta} \frac{\partial(r^e \Pi)}{\partial \phi}$$

(138)

Now substitute Equations (137) and (138) into Equation (88)

$$-k_i\, {}^e E_r = \frac{1}{r^2\sin\theta}\left\{ r k_i \frac{\partial}{\partial \theta}\left(\sin\theta \frac{\partial^e \Pi}{\partial \theta}\right) - \frac{r k_i}{\sin\theta} \frac{\partial^{2\,e} \Pi}{\partial \phi^2} \right\}$$

(139)

or

$${}^e E_r = -\frac{1}{r\sin\theta}\left\{ \frac{\partial}{\partial \theta}\left(\sin\theta \frac{\partial^e \Pi}{\partial \theta}\right) + \frac{1}{\sin\theta} \frac{\partial^{2\,e} \Pi}{\partial \phi^2} \right\}$$

(140)

Substitute Equations (138) and (140) into Equation (117) to get

$$\left(\frac{\partial^2}{\partial r^2}+k^2\right)\left[\frac{-k_i}{\sin\theta} \frac{\partial}{\partial \phi}(r^e \Pi)\right] = \frac{k_i}{r\sin^2\theta} \frac{\partial}{\partial \phi}\left[\frac{\partial}{\partial \theta}\left(\sin\theta \frac{\partial^e \Pi}{\partial \theta}\right) + \frac{1}{\sin\theta} \frac{\partial^{2\,e} \Pi}{\partial \phi^2} \right]$$

(141)

which may be written

$$-\frac{k_1}{\sin\theta}\frac{\partial}{\partial\phi}\left[\frac{\partial^2}{\partial r^2}(r\,{}^e\Pi) - \frac{k_1 k^2}{\sin\theta}\frac{\partial}{\partial\phi}(r\,{}^e\Pi)\right] = \frac{k_1}{r\sin^2\theta}\frac{\partial}{\partial\phi}\left[\frac{\partial}{\partial\theta}\left(\sin\theta\,\frac{\partial\,{}^e\Pi}{\partial\theta}\right) + \frac{1}{\sin\theta}\frac{\partial^2\,{}^e\Pi}{\partial\phi^2}\right] \qquad (142)$$

or, multiplying Equation (142) by $\sin\theta/k_1 r$, one may write

$$\frac{\partial}{\partial\phi}\left[\frac{1}{r}\frac{\partial^2}{\partial r^2}(r\,{}^e\Pi) + \frac{1}{r^2\sin\theta}\frac{\partial}{\partial\theta}\left(\sin\theta\,\frac{\partial\,{}^e\Pi}{\partial\theta}\right) + \frac{1}{r^2\sin^2\theta}\frac{\partial^2\,{}^e\Pi}{\partial\phi^2} + k^2\,{}^e\Pi\right] = 0 \qquad (143)$$

Also, substitute Equations (137) and (140) into Equation (121) to get

$$\left(\frac{\partial^2}{\partial r^2} + k^2\right)k_1\frac{\partial}{\partial\theta}(r\,{}^e\Pi) = k_1\frac{\partial}{\partial\theta}\left\{-\frac{1}{r\sin\theta}\left[\frac{\partial}{\partial\theta}\left(\sin\theta\,\frac{\partial\,{}^e\Pi}{\partial\theta}\right) + \frac{1}{\sin\theta}\frac{\partial^2\,{}^e\Pi}{\partial\phi^2}\right]\right\} \qquad (144)$$

or

$$\frac{\partial}{\partial\theta}\left[\frac{1}{r}\frac{\partial^2}{\partial r^2}(r\,{}^e\Pi) + \frac{1}{r^2\sin\theta}\frac{\partial}{\partial\theta}\left(\sin\theta\,\frac{\partial\,{}^e\Pi}{\partial\theta}\right) + \frac{1}{r^2\sin^2\theta}\frac{\partial^2\,{}^e\Pi}{\partial\phi^2} + k^2\,{}^e\Pi\right] = 0 \qquad (145)$$

Equations (143) and (145) express the vanishing of the ϕ and θ derivatives of the same expression. These equations may, therefore, be satisfied by equating this expression to zero.

$$\frac{1}{r}\frac{\partial^2(r\,{}^e\Pi)}{\partial r^2} + \frac{1}{r^2\sin\theta}\frac{\partial}{\partial\theta}\left(\sin\theta\,\frac{\partial\,{}^e\Pi}{\partial\theta}\right) + \frac{1}{r^2\sin^2\theta}\frac{\partial^2\,{}^e\Pi}{\partial\phi^2} + k^2\,{}^e\Pi = 0 \qquad (146)$$

This equation may be rewritten

$$-\frac{1}{r\sin\theta}\left[\frac{\partial}{\partial\theta}\left(\sin\theta\,\frac{\partial^e\Pi}{\partial\theta}\right)+\frac{1}{\sin\theta}\frac{\partial^{2\,e}\Pi}{\partial\phi^2}\right]=\frac{\partial^2(r^e\Pi)}{\partial r^2}+k^2r^e\Pi \tag{147}$$

which means that Equation (140) may be written as

$$^eE_r=\frac{\partial^2(r^e\Pi)}{\partial r^2}+k^2r^e\Pi \tag{148}$$

Expressions for all the components of the electric wave ($^e\vec{E}$, $^e\vec{H}$) have now been obtained in terms of a single scalar function $^e\Pi$. These components are given by

$$^eE_r=\frac{\partial^2(r^e\Pi)}{\partial r^2}+k^2r^e\Pi \tag{148}$$

$$^eE_\theta=\frac{1}{r}\frac{\partial^2(r^e\Pi)}{\partial r\,\partial\theta} \tag{133}$$

$$^eE_\phi=\frac{1}{r\sin\theta}\frac{\partial^2(r^e\Pi)}{\partial r\,\partial\phi} \tag{134}$$

$$^eH_r=0 \tag{102}$$

$$^eH_\theta=-\frac{k_1}{r\sin\theta}\frac{\partial(r^e\Pi)}{\partial\phi} \tag{138}$$

$$^e\!H_\phi = \frac{k_1}{r}\frac{\partial(r\,^e\Pi)}{\partial\theta} \tag{137}$$

In order to verify that a solution to the set of equations has been found, substitute these last six equations and Equation (146) into Equations (88) to (93).

First, substituting Equations (137), (138), and (148) into Equation (88), yields

$$-k_1\frac{\partial^2(r\,^e\Pi)}{\partial r^2} - k^2 k_1 r\,^e\Pi = \frac{1}{r^2\sin\theta}\left\{\frac{\partial}{\partial\theta}\left[k_1\sin\theta\frac{\partial(r\,^e\Pi)}{\partial\theta}\right] - \frac{\partial}{\partial\phi}\left[-\frac{k_1}{\sin\theta}\frac{\partial(r\,^e\Pi)}{\partial\phi}\right]\right\} \tag{149}$$

or

$$\frac{\partial^2(r\,^e\Pi)}{\partial r^2} + \frac{1}{r\sin\theta}\frac{\partial}{\partial\theta}\left(\sin\theta\frac{\partial\,^e\Pi}{\partial\theta}\right) + \frac{1}{r\sin^2\theta}\frac{\partial^2\,^e\Pi}{\partial\phi^2} + k^2 r\,^e\Pi = 0 \tag{150}$$

Equation (150) is satisfied because of Equation (146), so Equations (137), (138), and (148) are indeed solutions for Equation (88).

Similarly, substitute Equations (133), (102), and (137) into Equation (89) to get

$$-\frac{k_1}{r}\frac{\partial^2(r\,^e\Pi)}{\partial r\partial\theta} = -\frac{1}{r\sin\theta}\frac{\partial}{\partial r}\left[k_1\sin\theta\frac{\partial}{\partial\theta}(r\,^e\Pi)\right] \tag{151}$$

or

$$-\frac{k_1}{r}\frac{\partial^2(r\,^e\Pi)}{\partial r\partial\theta} = -\frac{k_1}{r}\frac{\partial^2(r\,^e\Pi)}{\partial r\partial\theta} \tag{152}$$

which is an identity; hence, Equation (89) is solved.

Substitute Equations (134), (138), and (102) into Equation (90).

$$-\frac{k_1}{r\sin\theta}\frac{\partial^2(r^e\Pi)}{\partial r\partial\phi} = \frac{1}{r}\frac{\partial}{\partial r}\left[-\frac{k_1}{\sin\theta}\frac{\partial(r^e\Pi)}{\partial\phi}\right] \tag{153}$$

which is written

$$-\frac{k_1}{r\sin\theta}\frac{\partial^2(r^e\Pi)}{\partial r\partial\phi} = -\frac{k_1}{r\sin\theta}\frac{\partial^2(r^e\Pi)}{\partial r\partial\phi} \tag{154}$$

Substitute Equations (102), (134), and (133) into Equation (91).

$$\frac{1}{r^2\sin\theta}\left\{\frac{\partial}{\partial\theta}\left[\frac{\partial^2(r^e\Pi)}{\partial r\partial\phi}\right] - \frac{\partial}{\partial\phi}\left[\frac{\partial^2(r^e\Pi)}{\partial r\partial\theta}\right]\right\} = 0 \tag{155}$$

which becomes

$$\frac{1}{r^2\sin\theta}\left\{\frac{\partial^3(r^e\Pi)}{\partial r\partial\theta\partial\phi} - \frac{\partial^3(r^e\Pi)}{\partial r\partial\theta\partial\phi}\right\} = 0 \tag{156}$$

Substitute Equations (138), (148), and (134) into Equation (92).

$$-\frac{k_1k_2}{r\sin\theta}\frac{\partial(r^e\Pi)}{\partial\phi} = \frac{1}{r\sin\theta}\left\{\frac{\partial}{\partial\phi}\left[\frac{\partial^2(r^e\Pi)}{\partial r^2} + k^2 r^e\Pi\right] - \frac{\partial}{\partial r}\left[\frac{\partial^2(r^e\Pi)}{\partial r\partial\phi}\right]\right\} \tag{157}$$

which can be written

$$k^2\frac{\partial(r^e\Pi)}{\partial\phi} = \frac{\partial^3(r^e\Pi)}{\partial r^2\partial\phi} + k^2\frac{\partial(r^e\Pi)}{\partial\phi} - \frac{\partial^3(r^e\Pi)}{\partial r^2\partial\phi} \tag{158}$$

And finally, substitute Equations (137), (133), and (148) into Equation (93).

$$\frac{k_1 k_2}{r} \frac{\partial (r\,^e\Pi)}{\partial \theta} = \frac{1}{r} \left\{ \frac{\partial}{\partial r} \left[\frac{\partial^2 (r\,^e\Pi)}{\partial r\, \partial \theta} \right] - \frac{\partial}{\partial \theta} \left[\frac{\partial^2 (r\,^e\Pi)}{\partial r^2} + k^2 r\,^e\Pi \right] \right\} \qquad (159)$$

which is written

$$-\frac{k^2}{r} \frac{\partial (r\,^e\Pi)}{\partial \theta} = \frac{1}{r} \frac{\partial^3 (r\,^e\Pi)}{\partial r^2 \partial \theta} - \frac{1}{r} \frac{\partial^3 (r\,^e\Pi)}{\partial r^2 \partial \theta} - \frac{k^2}{r} \frac{\partial (r\,^e\Pi)}{\partial \theta} \qquad (160)$$

It has now been shown that $(^e\vec{E}, \,^e\vec{H})$, given by Equations (102), (133), (134),(137),(138)and(148),in terms of $^e\Pi$, is a solution of the set of Equations (88) through (93), which are Maxwell's equations in spherical polar coordinates.

In a similar way the magnetic wave $(^m\vec{E}, \,^m\vec{H})$ may be considered, and it is found that this wave can be derived from a scalar potential function, $^m\Pi$, which satisfies the same differential Equation (146) as $^e\Pi$. With $^m E_r = 0$, Equations (92) and (93) become

$$k_2\,^mH_\theta = -\frac{1}{r \sin\theta} \frac{\partial}{\partial r}(r E_\phi \sin\theta) = -\frac{1}{r} \frac{\partial}{\partial r}(r\,^mE_\phi) \qquad (161)$$

$$k_2\,^mH_\phi = \frac{1}{r} \frac{\partial}{\partial r}(r\,^mE_\phi) \qquad (162)$$

Now substitute Equation (162) into Equation (89).

$$-k_1{}^m E_\theta = \frac{1}{r\sin\theta}\left\{\frac{\partial H_r}{\partial\phi} - \frac{\partial}{\partial r}\left[\frac{\sin\theta}{k_2}\frac{\partial}{\partial r}\left(r\,{}^m E_\theta\right)\right]\right\} \qquad (163)$$

or

$$-k_1 k_2\, r\,{}^m E_\theta = \frac{k_2}{\sin\theta}\frac{\partial\,{}^m H_r}{\partial\phi} - \frac{\partial^2\left(r\,{}^m E_\theta\right)}{\partial r^2} \qquad (164)$$

or

$$\left(\frac{\partial^2}{\partial r^2} + k^2\right)\left(r\,{}^m E_\theta\right) = \frac{k_2}{\sin\theta}\frac{\partial\,{}^m H_r}{\partial\phi} \qquad (165)$$

Similarly, substitute Equation (162) into Equation (90).

$$-k_1{}^m E_\phi = \frac{1}{r}\left\{\frac{\partial}{\partial r}\left[-\frac{1}{k_2\sin\theta}\frac{\partial}{\partial r}\left(r E_\phi\sin\theta\right)\right] - \frac{\partial\,{}^m H_r}{\partial\theta}\right\} \qquad (166)$$

or

$$-k_1 k_2\, r\,{}^m E_\phi = -\frac{\partial^2}{\partial r^2}\left(r\,{}^m E_\phi\right) - k_2\frac{\partial\,{}^m H_r}{\partial\theta} \qquad (167)$$

or

$$\left(\frac{\partial^2}{\partial r^2} + k^2\right)\left(r\,{}^m E_\phi\right) = -k_2\frac{\partial\,{}^m H_r}{\partial\theta} \qquad (168)$$

Equations (165), (168), and (91) constitute a complete system of equations for ${}^m H_r$, ${}^m E_\theta$, and ${}^m E_\phi$. Equation (88) becomes

$$\frac{1}{k^2 r^2 \sin\theta} \left\{ \frac{\partial}{\partial\theta} \left[\sin\theta \frac{\partial}{\partial r}(r\,{}^m E_\theta) \right] + \frac{\partial}{\partial\phi} \left[\frac{\partial}{\partial r}(r\,{}^m E_\phi) \right] \right\} = 0 \tag{169}$$

or

$$\frac{1}{k^2 r^2 \sin\theta} \frac{\partial}{\partial r} \left[\frac{\partial}{\partial\theta}(r\sin\theta\,{}^m E_\theta) + \frac{\partial}{\partial\phi}(r\,{}^m E_\phi) \right] = 0 \tag{170}$$

This equation is satisfied because for physical fields and no sources

$$\nabla \cdot {}^m\vec{E} = 0 \tag{171}$$

and in spherical polar coordinates, this is written

$$\frac{1}{r\sin\theta} \left[\frac{\partial}{\partial\theta}(\sin\theta\,{}^m E_\theta) + \frac{\partial}{\partial\phi}\,{}^m E_\phi \right] = 0 \tag{172}$$

since ${}^m E_r = 0$.

Looking again at Equation (88) and letting ${}^m E_r = 0$, one sees that

$$\frac{\partial}{\partial\theta}(\sin\theta\,{}^m H_\phi) = \frac{\partial}{\partial\phi}\,{}^m H_\theta \tag{173}$$

It follows from Equation (173) that ${}^m H_\phi$ and ${}^m H_\theta$ may be represented as the gradient of a single scalar function v.

$$\,{}^m H_\phi = \frac{1}{r\sin\theta} \frac{\partial r}{\partial\phi} \tag{174}$$

$$\,{}^m H_\theta = \frac{1}{r} \frac{\partial V}{\partial\theta} \tag{175}$$

Now, as before, let

$$V = \frac{\partial (r^m \Pi)}{\partial r} \qquad ; \qquad (176)$$

then Equations (174) and (175) become

$$^mH_\phi = \frac{1}{r \sin\theta} \frac{\partial^2 (r^m \Pi)}{\partial r \partial \phi} \qquad (177)$$

$$^mH_\theta = \frac{1}{r} \frac{\partial^2 (r^m \Pi)}{\partial r \partial \theta} \qquad (178)$$

Substituting Equation (178) into Equation (161) yields

$$\frac{k_2}{r} \frac{\partial^2 (r^m \Pi)}{\partial r \partial \theta} = -\frac{1}{r} \frac{\partial}{\partial r} (r^m \Pi) \qquad (179)$$

or

$$k_2 \frac{\partial}{\partial r} \left[\frac{\partial (r^m \Pi)}{\partial \theta} \right] = -\frac{\partial}{\partial r} (r^m E_\phi) \qquad (180)$$

This equation is satisfied by

$$^mE_\phi = -k_2 \frac{\partial^m \Pi}{\partial \theta} = -\frac{k_2}{r} \frac{\partial (r^m \Pi)}{\partial \theta} \qquad (181)$$

Substituting Equation (177) into Equation (162) yields

$$\frac{k_2}{r \sin\theta} \frac{\partial^2 (r^m \Pi)}{\partial r \partial \phi} = \frac{1}{r} \frac{\partial}{\partial r} (r^m E_\theta) \qquad (182)$$

$$\frac{k_2}{\sin\theta}\frac{\partial}{\partial r}\left[\frac{\partial(r^{m}\Pi)}{\partial\phi}\right] = \frac{\partial}{\partial r}(r^{m}E_\theta) \tag{183}$$

which is satisfied by

$$^{m}E_\theta = \frac{k_2}{\sin\theta}\frac{\partial^{m}\Pi}{\partial\phi} \tag{184}$$

Now substitute Equations (181) and (184) into Equation (91).

$$k_2\,^{m}H_r = \frac{1}{r^2\sin\theta}\left\{\frac{\partial}{\partial\theta}\left[-k_2\sin\theta\,\frac{\partial(r^{m}\Pi)}{\partial\theta}\right] - \frac{\partial}{\partial\phi}\left[\frac{k_2}{\sin\theta}\frac{\partial(r^{m}\Pi)}{\partial\phi}\right]\right\} \tag{185}$$

or

$$^{m}H_r = -\frac{1}{r\sin\theta}\left[\frac{\partial}{\partial\theta}\left(\sin\theta\,\frac{\partial^{m}\Pi}{\partial\theta}\right) + \frac{1}{\sin\theta}\frac{\partial^{2\,m}\Pi}{\partial\phi^2}\right] \tag{186}$$

Substitute now Equations (184) and (186) into Equation (165).

$$\left(\frac{\partial^2}{\partial r^2}+k^2\right)\frac{r\,k_2}{\sin\theta}\frac{\partial^{m}\Pi}{\partial\phi} = -\frac{k_2}{r\sin^2\theta}\frac{\partial}{\partial\phi}\left[\frac{\partial}{\partial\theta}\left(\sin\theta\,\frac{\partial^{m}\Pi}{\partial\theta}\right) + \frac{1}{\sin\theta}\frac{\partial^{2\,m}\Pi}{\partial\phi^2}\right] \tag{187}$$

or

$$\frac{\partial}{\partial\phi}\left[\frac{1}{r}\frac{\partial^2(r^{m}\Pi)}{\partial r^2} + \frac{1}{r^2\sin\theta}\frac{\partial}{\partial\theta}\left(\sin\theta\,\frac{\partial^{m}\Pi}{\partial\theta}\right) + \frac{1}{r^2\sin^2\theta}\frac{\partial^{2\,m}\Pi}{\partial\phi^2} + k^{2\,m}\Pi\right] = 0 \tag{188}$$

Substitute Equations (181) and (186) into Equation (168).

$$\left(\frac{\partial^2}{\partial r^2}+k^2\right)\left(-k_2 r\frac{\partial\,^m\Pi}{\partial\theta}\right) = -k_2\frac{\partial}{\partial\theta}\left\{\frac{-1}{r\sin\theta}\left[\frac{\partial}{\partial\theta}\left(\sin\theta\frac{\partial\,^m\Pi}{\partial\theta}\right)+\frac{1}{\sin\theta}\frac{\partial^2\,^m\Pi}{\partial\phi^2}\right]\right\} \tag{189}$$

$$\frac{\partial}{\partial\theta}\left[\frac{1}{r}\frac{\partial^2(r\,^m\Pi)}{\partial r^2}+\frac{1}{r^2\sin\theta}\frac{\partial}{\partial\theta}\left(\sin\theta\frac{\partial\,^m\Pi}{\partial\theta}\right)+\frac{1}{r^2\sin^2\theta}\frac{\partial^2\,^m\Pi}{\partial\phi^2}+k^2\,^m\Pi\right] \tag{190}$$

Equations (188) and (190) express the vanishing of the ϕ and θ derivatives, repsectively, of the same expression. These equations are satisfied if the expression is zero; so let

$$\frac{1}{r}\frac{\partial^2(r\,^m\Pi)}{\partial r^2}+\frac{1}{r^2\sin\theta}\frac{\partial}{\partial\theta}\left(\sin\theta\frac{\partial\,^m\Pi}{\partial\theta}\right)+\frac{1}{r^2\sin^2\theta}\frac{\partial^2\,^m\Pi}{\partial\phi^2}+k^2\,^m\Pi = 0 \tag{191}$$

This equation, which is identical to Equation (146), is just the wave equation written in spherical polar coordinates:

$$\nabla^2\,^e\Pi + k^2\,^e\Pi = 0 \tag{192}$$

$$\nabla^2\,^m\Pi + k^2\,^m\Pi = 0 \tag{193}$$

By means of Equation (193), Equation (186) may be rewritten as

$$^mH_r = \frac{\partial^2(r\,^m\Pi)}{\partial r^2}+k^2 r\,^m\Pi \tag{194}$$

Expressions for all the components of the magnetic wave ($^m\vec{E}$, $^m\vec{H}$)

have now been obtained in terms of a single scalar function $^m\Pi$. These components are given by

$$^m E_r = 0 \qquad (103)$$

$$^m E_\theta = \frac{k_2}{r\sin\theta}\frac{\partial(r\,^m\Pi)}{\partial\phi} \qquad (184)$$

$$^m E_\phi = -\frac{k_2}{r}\frac{\partial(r\,^m\Pi)}{\partial\theta} \qquad (181)$$

$$^m H_r = \frac{\partial^2(r\,^m\Pi)}{\partial r^2} + k^2 r\,^m\Pi \qquad (194)$$

$$^m H_\theta = \frac{1}{r}\frac{\partial^2(r\,^m\Pi)}{\partial r\,\partial\theta} \qquad (178)$$

$$^m H_\phi = \frac{1}{r\sin\theta}\frac{\partial^2(r\,^m\Pi)}{\partial r\,\partial\phi} \qquad (177)$$

In order to varify that a solution of the set of Equations (88) through (93) has been found, substitute these last six equations and Equation (193) into Equation (88) through Equation (93). First, substitute Equations (103), (177), and (178) into Equation (88), to get

$$\frac{1}{r^2\sin\theta}\left\{\frac{\partial}{\partial\theta}\left[\frac{\partial^2(r\,^m\Pi)}{\partial r\,\partial\phi}\right] - \frac{\partial}{\partial\phi}\left[\frac{\partial^2(r\,^m\Pi)}{\partial r\,\partial\theta}\right]\right\} = 0 \qquad (195)$$

or

$$\frac{\partial^3(r^m\Pi)}{\partial r \partial\theta \partial\phi} = \frac{\partial^3(r^m\Pi)}{\partial r \partial\theta \partial\phi} \tag{196}$$

so Equation (88) is satisfied by Equations (103), (177), and (178). Now substitute Equations (184), (194), and (177) into Equation (89) to get

$$-\frac{k_1 k_2}{r\sin\theta}\frac{\partial(r^m\Pi)}{\partial\phi} = \frac{1}{r\sin\theta}\left\{\frac{\partial}{\partial\phi}\left[\frac{\partial^2(r^m\Pi)}{\partial r^2} + k^2 r^m\Pi\right] - \frac{\partial}{\partial r}\left[\frac{\partial^2(r^m\Pi)}{\partial r \partial\phi}\right]\right\} \tag{197}$$

or

$$k^2\frac{\partial(r^m\Pi)}{\partial\phi} + \frac{\partial^3(r^m\Pi)}{\partial r^2\partial\phi} = k^2\frac{\partial(r^m\Pi)}{\partial\phi} + \frac{\partial^3(r^m\Pi)}{\partial r^2\partial\phi} \tag{198}$$

so Equation (89) is satisfied. Now substitute Equations (181), (178), and (194) into Equation (90).

$$\frac{k_1 k_2}{r}\frac{\partial(r^m\Pi)}{\partial\theta} = \frac{1}{r}\left\{\frac{\partial}{\partial r}\left[\frac{\partial^2(r^m\Pi)}{\partial r \partial\theta}\right] - \frac{\partial}{\partial\theta}\left[\frac{\partial^2(r^m\Pi)}{\partial r^2} + k^2 r^m\Pi\right]\right\} \tag{199}$$

or

$$-k^2\frac{\partial(r^m\Pi)}{\partial\theta} + \frac{\partial^3(r^m\Pi)}{\partial r^2\partial\theta} = -k^2\frac{\partial(r^m\Pi)}{\partial\theta} + \frac{\partial^3(r^m\Pi)}{\partial r^2\partial\theta} \tag{200}$$

so Equation (90) is satisfied. Now substitute Equations (194), (181), and (184) into Equation (91).

$$k_2 \frac{\partial^2 (r^m\Pi)}{\partial r^2} + k_2 k r^{2\,m}\Pi = \frac{1}{r^2 \sin\theta}\left\{\frac{\partial}{\partial\theta}\left[-k_2 \sin\theta \frac{\partial(r^m\Pi)}{\partial\theta}\right] - \frac{\partial}{\partial\phi}\left[\frac{k_2}{\sin\theta}\frac{\partial(r^m\Pi)}{\partial\phi}\right]\right\} \quad (201)$$

or

$$\frac{1}{r}\frac{\partial^2 (r^m\Pi)}{\partial r^2} + \frac{1}{r^2 \sin\theta}\frac{\partial}{\partial\theta}\left(\sin\theta \frac{\partial^m\Pi}{\partial\theta}\right) + \frac{1}{r^2 \sin^2\theta}\frac{\partial^{2\,m}\Pi}{\partial\phi^2} + k^{2\,m}\Pi = 0 \quad (202)$$

This is Equation (193), so Equation (91) is satisfied. Now substitute Equations (103), (181), and (178) into Equation (92) to get

$$\frac{k_2}{r}\frac{\partial^2 (r^m\Pi)}{\partial r \partial\theta} = -\frac{1}{r\sin\theta}\frac{\partial}{\partial r}\left[-k_2 \sin\theta \frac{\partial(r^m\Pi)}{\partial\theta}\right] \quad (203)$$

or

$$\frac{\partial^2 (r^m\Pi)}{\partial r \partial\theta} = \frac{\partial^2 (r^m\Pi)}{\partial r \partial\theta} \quad (204)$$

so Equation (92) is satisfied. Now substitute Equations (103), (177), and (184) into Equation (93).

$$\frac{k_2}{r\sin\theta}\frac{\partial^2 (r^m\Pi)}{\partial r \partial\phi} = \frac{1}{r}\frac{\partial}{\partial r}\left[\frac{k_2}{\sin\theta}\frac{\partial(r^m\Pi)}{\partial\phi}\right] \quad (205)$$

or

$$\frac{\partial^2 (r^m\Pi)}{\partial r \partial\phi} = \frac{\partial^2 (r^m\Pi)}{\partial r \partial\phi} \quad (206)$$

so Equation (93) is satisfied.

It has now been shown that $(^{m}\vec{E}, {}^{m}\vec{H})$, given by Equations (103), (177), (178), (181), (184), and (194) in terms of $^{m}\Pi$, is a solution of Equations (88) through (93). Since $(^{e}\vec{E}, {}^{e}\vec{H})$, given by Equations (102), (133), (134), (137), (138), and (148) in terms of $^{m}\Pi$, is also a solution of Equations (88) through (93), then the sum of these two solutions is a solution. Thus, $\vec{E}$ and $\vec{H}$ are solutions of Equations (88) through (93), where $\vec{E}$ and $\vec{H}$ are given by

$$\vec{E} = {}^{e}\vec{E} + {}^{m}\vec{E} \tag{207}$$

$$\vec{H} = {}^{e}\vec{H} + {}^{m}\vec{H} \tag{208}$$

The components of $\vec{E}$ and $\vec{H}$ are now written as:

$$E_r = {}^{e}E_r + {}^{m}E_r = \frac{\partial^2(r\,{}^{e}\Pi)}{\partial r^2} + k^2 r\,{}^{e}\Pi \tag{209}$$

$$E_\theta = {}^{e}E_\theta + {}^{m}E_\theta = \frac{1}{r}\frac{\partial^2(r\,{}^{e}\Pi)}{\partial r\partial\theta} + \frac{k_2}{r\sin\theta}\frac{\partial(r\,{}^{m}\Pi)}{\partial\phi} \tag{210}$$

$$E_\phi = {}^{e}E_\phi + {}^{m}E_\phi = \frac{1}{r\sin\theta}\frac{\partial^2(r\,{}^{e}\Pi)}{\partial r\partial\phi} - \frac{k_2}{r}\frac{\partial(r\,{}^{m}\Pi)}{\partial\theta} \tag{211}$$

$$H_r = {}^{e}H_r + {}^{m}H_r = \frac{\partial^2(r\,{}^{m}\Pi)}{\partial r^2} + k^2 r\,{}^{m}\Pi \tag{212}$$

$$H_\theta = {}^eH_\theta + {}^mH_\theta = - \frac{k_1}{r \sin\theta} \frac{\partial(r {}^e\Pi)}{\partial\phi} + \frac{1}{r} \frac{\partial^2(r {}^m\Pi)}{\partial r \partial\theta} \tag{213}$$

$$H_\phi = {}^eH_\phi + {}^mH_\phi = \frac{k_1}{r} \frac{\partial(r {}^e\Pi)}{\partial\theta} + \frac{1}{r \sin\theta} \frac{\partial^2(r {}^m\Pi)}{\partial r \partial\phi} \tag{214}$$

Looking again at Equations (146) and (193), remember that both potentials, ${}^e\Pi$ and ${}^m\Pi$ are solutions of the wave equation

$$\nabla^2\Pi + k^2\Pi = 0 \tag{215}$$

written in polar coordinates.

The boundary conditions Equations (94) through (99) state that E_θ, E_ϕ, εE_r, H_θ, H_ϕ, and H_r shall be continuous across the spherical surface $r = a$. Equation (210) shows E_θ is continuous across $r = a$ if $\frac{\partial(r {}^e\Pi)}{\partial r}$ and $k_2 r \, {}^m\Pi$ are continuous across $r = a$. Equation (211) shows E_ϕ is continuous across $r = a$ if these same conditions hold. Equations (213) and (214) show that H_θ and H_ϕ are continuous across $r = a$ if $\frac{\partial(r {}^m\Pi)}{\partial r}$ and $k_1 r \, {}^e\Pi$ are continuous across $r = a$. Thus, in order that the components E_θ, E_ϕ, H_θ, and H_ϕ shall be continuous over $r = a$, it is sufficient that the four quantities

$$k_1 r \, {}^e\Pi \qquad k_2 r \, {}^m\Pi \qquad \frac{\partial}{\partial r}(r {}^e\Pi) \qquad \frac{\partial}{\partial r}(r {}^m\Pi) \tag{216}$$

shall be continuous across this surface. Thus, these boundary conditions split into independent conditions for ${}^e\Pi$ and ${}^m\Pi$. The diffraction problem is thus reduced to the problem of finding two mutually independent solutions

of the wave equation, with prescribed boundary conditions.

Solve the Wave Equation (215) for Π by separation of variables. Let

$$\Pi = R(r)\,\Theta(\theta)\,\Phi(\phi) \tag{217}$$

and substitute into Equation (215).

$$\nabla^2 \Pi + k^2 \Pi = 0 \tag{218}$$

or

$$\frac{1}{r}\frac{\partial^2(r\Pi)}{\partial r^2} + \frac{1}{r^2 \sin\theta}\frac{\partial}{\partial\theta}\left(\sin\theta\frac{\partial\Pi}{\partial\theta}\right) + \frac{1}{r^2 \sin^2\theta}\frac{\partial^2\Pi}{\partial\phi^2} + k^2\Pi = 0 \tag{219}$$

or

$$\frac{\Theta\Phi}{r}\frac{d^2(rR)}{dr^2} + \frac{R\Phi}{r^2 \sin\theta}\frac{d}{d\theta}\left(\sin\theta\frac{d\Theta}{d\theta}\right) + \frac{R\Theta}{r^2 \sin^2\theta}\frac{d^2\Phi}{d\phi^2} + k^2 R\Theta\Phi = 0 \tag{220}$$

or

$$\frac{1}{rR}\frac{d^2(rR)}{dr^2} + \frac{1}{\Theta r^2 \sin\theta}\frac{d}{d\theta}\left(\sin\theta\frac{d\Theta}{d\theta}\right) + \frac{1}{\Phi r^2 \sin^2\theta}\frac{d^2\Phi}{d\phi^2} + k^2 = 0 \tag{221}$$

or

$$\frac{r\sin^2\theta}{R}\frac{d^2(rR)}{dr^2} + \frac{\sin\theta}{\Theta}\frac{d}{d\theta}\left(\sin\theta\frac{d\Theta}{d\theta}\right) + \frac{1}{\Phi}\frac{d^2\Phi}{d\phi^2} + k^2 r^2 \sin^2\theta = 0 \tag{222}$$

The Φ term is independent of the Θ and R terms, since r, θ and φ are independent variables, so the Φ term must be a constant, and we may write

Equation (222) as two independent equations.

$$\frac{r \sin^2\theta}{R} \frac{d^2(rR)}{dr^2} + \frac{\sin\theta}{\Theta} \frac{d}{d\theta}\left(\sin\theta \frac{d\Theta}{d\theta}\right) + k^2 r^2 \sin^2\theta = \beta \qquad (223)$$

$$\frac{1}{\Phi} \frac{d^2\Phi}{d\phi^2} = -\beta \qquad (224)$$

where β is a constant. Equation (224) is written

$$\frac{d^2\Phi}{d\phi^2} + \beta\Phi = 0 \qquad (225)$$

Divide Equation (223) by $\sin^2\theta$ to get

$$\frac{r}{R} \frac{d^2(rR)}{dr^2} + \frac{1}{\sin\theta \, \Theta} \frac{d}{d\theta}\left(\sin\theta \frac{d\Theta}{d\theta}\right) + k^2 r^2 - \frac{\beta}{\sin^2\theta} = 0 \qquad (226)$$

Since θ and r are independent variables, write Equation (226) as two independent equations

$$\frac{r}{R} \frac{d^2(rR)}{dr^2} + k^2 r^2 = \alpha \qquad (227)$$

$$\frac{1}{\sin\theta \, \Theta} \frac{d}{d\theta}\left(\sin\theta \frac{d\Theta}{d\theta}\right) - \frac{\beta}{\sin^2\theta} = -\alpha \qquad (228)$$

Equation (227) may be written

$$\frac{d^2(rR)}{dr^2} + \left(k^2 - \frac{\alpha}{r^2}\right) rR = 0 \tag{229}$$

and Equation (228) may be written

$$\frac{1}{\sin\theta}\frac{d}{d\theta}\left(\sin\theta\frac{d\Theta}{d\theta}\right) + \left(\alpha - \frac{\beta}{\sin^2\theta}\right)\Theta = 0 \tag{230}$$

As the field $\vec{E}$, $\vec{H}$ is a single valued function of position, so Π must also be single valued. This requirement imposes restrictions on Φ and Θ, as will be shown.

First consider the simplest of our three equations, the Φ Equation (225).

$$\frac{d^2\Phi}{d\phi^2} + \beta\Phi = 0 \tag{231}$$

The general solution of this equation is

$$\Phi(\phi) = a\cos(\sqrt{\beta}\,\phi) + b\,\sin(\sqrt{\beta}\,\phi) \tag{232}$$

where ϕ is in radians. Since ϕ can take on any value from $-\infty$ to $+\infty$, in order for Φ to be single valued, it is necessary that

$$\Phi(\phi) = \Phi(\phi + 2\pi n) \tag{233}$$

for all values of ϕ, where n is any integer from $-\infty$ to $+\infty$, this holds true only if

$$\beta = m^2 \tag{234}$$

where m is any integer. Thus, the single valued solution of Equation (275) is

$$\Phi(\phi) = a_m \cos(m\phi) + b_m \sin(m\phi) \tag{235}$$

Now examine Equation (230)

$$\frac{1}{\sin\theta} \frac{d}{d\theta}\left(\sin\theta \frac{d\Theta}{d\theta}\right) + \left(\alpha - \frac{\beta}{\sin^2\theta}\right)\Theta = 0 \tag{236}$$

becomes

$$\frac{1}{\sin\theta} \frac{d}{d\theta}\left(\sin\theta \frac{d\Theta}{d\theta}\right) + \left(\alpha - \frac{m^2}{\sin^2\theta}\right)\Theta = 0 \tag{237}$$

Here remember $\Theta = \Theta(\theta)$, and for the same reason that $\Phi(\phi)$ must be single valued, so must $\Theta(\theta)$ be single valued, for all values of θ from $-\infty$ to $+\infty$. It turns out that $\Theta(\theta)$ is single valued when, and only when

$$\alpha = \ell(\ell+1) \tag{238}$$

where ℓ is an integer $\geq |m|$. Now, to facilitate solving the equation, let

$$\xi = \cos\theta \tag{239}$$

Then

$$d\xi = -\sin\theta\, d\theta \tag{240}$$

or

$$\frac{d}{d\xi} = -\frac{1}{\sin\theta}\frac{d}{d\theta} \tag{241}$$

Also,

$$\sin\theta\frac{d}{d\theta} = \sin^2\theta\frac{d}{\sin\theta\, d\theta} = -(1-\cos^2\theta)\left(-\frac{1}{\sin\theta}\frac{d}{d\theta}\right) = -(1-\xi^2)\frac{d}{d\xi} \tag{242}$$

Substituting Equations (238), (241), and (242) into Equation (237) produces

$$\frac{d}{d\xi}\left[(1-\xi^2)\frac{d\Theta}{d\xi}\right] + \left[\ell(\ell+1) - \frac{m^2}{1-\xi^2}\right]\Theta = 0 \tag{243}$$

$\Theta(\xi)$ must be zero at the singular points $\xi = \pm 1$ (because $\dfrac{m^2}{1-\xi^2} = \infty$ for $m > 0$ and $\ell(\ell+1)\,\Theta = 0$, $\ell > 0$, for $m = 0$, at $\xi = \pm 1$). Thus, to find an analytic expression for Θ, try to find a series solution about the points $\xi = \pm 1$ (north and south poles of the unit sphere) in powers of $\xi \mp 1$:

$$\Theta(\xi) = (\xi \mp 1)^{\lambda}\sum_{n=0}^{\infty} a_n(\xi \mp 1)^n \tag{244}$$

Note:

$$\frac{d(\xi \mp 1)}{d\xi} = 1 \tag{245}$$

or

$$d(\xi \mp 1) = d\xi \tag{246}$$

so

$$\frac{d\Theta}{d\xi} = (\xi \mp 1)^{\lambda-1} \sum_{n=0}^{\infty} (\lambda+n) a_n (\xi \mp 1)^n \tag{247}$$

$$\frac{d^2\Theta}{d\xi^2} = (\xi \mp 1)^{\lambda-2} \sum_{n=0}^{\infty} (\lambda+n)(\lambda+n-1) a_n (\xi \mp 1)^n \tag{248}$$

Write Equation (243) as

$$\left(1-\xi^2\right)\frac{d^2\Theta}{d\xi^2} - 2\xi\frac{d\Theta}{d\xi} + \left[\ell(\ell+1) - \frac{m^2}{1-\xi^2}\right]\Theta = 0 \tag{249}$$

and substitute in Equations (244), (247), and (248)

$$\sum_{n=0}^{\infty}\left\{(1-\xi^2)(\xi\mp1)^{\lambda+n-2}(\lambda+n)(\lambda+n-1)a_n - 2\xi(\xi\mp1)^{\lambda+n-1}(\lambda+n)a_n + \left[\ell(\ell+1)-\frac{m^2}{1-\xi^2}\right](\xi\mp1)^{\lambda+n}a_n\right\} = 0 . \tag{250}$$

$$\xi = 1 \pm (\xi \mp 1) \tag{251}$$

Square both sides to get

$$\xi^2 = 1 \pm 2(\xi \mp 1) + (\xi \mp 1)^2 \tag{252}$$

so

$$\left(1-\xi^2\right) = \mp 2\left(\xi \mp 1\right) - \left(\xi \mp 1\right)^2 \tag{253}$$

and

$$-2\xi = -2 \mp 2\left(\xi \mp 1\right) \tag{254}$$

and one may write

$$-\frac{m^2}{1-\xi^2} = \frac{m^2}{\pm 2\left(\xi \mp 1\right)+\left(\xi \mp 1\right)^2} \tag{255}$$

Series Equation (250) must vanish term by term. The lowest term is the $(\xi \mp 1)^{\lambda-1}$ term which yields

$$-2\lambda(\lambda-1) - 2\lambda + \frac{m^2}{2} = 0 \tag{256}$$

or

$$\lambda(\lambda-1) + \lambda - \frac{m^2}{4} = 0 \tag{257}$$

or

$$\lambda^2 = \frac{m^2}{4} \tag{258}$$

so

$$\lambda = \pm \frac{m}{2} \tag{259}$$

But the root $\lambda = -\frac{m}{2}$ must be excluded for Θ to be continuous, so

$$\lambda = + \frac{m}{2} \tag{260}$$

Now look for a solution of Equation (249) in the form

$$\Theta(\xi) = (1-\xi^2)^{\frac{m}{2}} \upsilon \tag{261}$$

since

$$(1-\xi^2) = (1-\xi)(1+\xi) \tag{262}$$

and see if a solution can be found. Equation (249) becomes

$$(1-\xi^2)\frac{d^2}{d\xi^2}\left[(1-\xi^2)^{\frac{m}{2}}\upsilon\right] - 2\xi\frac{d}{d\xi}\left[(1-\xi^2)^{\frac{m}{2}}\upsilon\right] + \left[l(l+1) - \frac{m^2}{1-\xi^2}\right]\left[(1-\xi^2)^{\frac{m}{2}}\upsilon\right] = 0 \tag{263}$$

$$\frac{d}{d\xi}(1-\xi^2)^{\frac{m}{2}} = \frac{m}{2}(1-\xi^2)^{\frac{m}{2}-1}(-2\xi) = -m\xi(1-\xi^2)^{\frac{m}{2}-1} \tag{264}$$

$$\frac{d^2}{d\xi^2}(1-\xi^2)^{\frac{m}{2}} = -\frac{d}{d\xi}m\xi(1-\xi^2)^{\frac{m}{2}-1} = -m\left[(1-\xi^2)^{\frac{m}{2}-1} + \xi(\frac{m}{2}-1)(1-\xi^2)^{\frac{m}{2}-2}(-2\xi)\right] \tag{265}$$

so Equation (263) becomes

$$-(1-\xi^2)m\upsilon\left[(1-\xi^2)^{\frac{m}{2}-1} - (m-2)\xi^2(1-\xi^2)^{\frac{m}{2}-2}\right] + (1-\xi^2)^{\frac{m}{2}+1}\frac{d^2\upsilon}{d\xi^2} + 2m\xi^2(1-\xi^2)^{\frac{m}{2}-1}\upsilon \tag{266}$$

$$\cdot\left[-2m\xi(1-\xi^2)^{\frac{m}{2}} - 2\xi(1-\xi^2)^{\frac{m}{2}}\right]\frac{d\upsilon}{d\xi} + l(l+1)(1-\xi^2)^{\frac{m}{2}}\upsilon - m^2(1-\xi^2)^{\frac{m}{2}-1}\upsilon = 0$$

or

$$\left[-m(1-\xi^2)^{\frac{m}{2}}+(m^2-2m)\xi^2(1-\xi^2)^{\frac{m}{2}-1}+2m\xi^2(1-\xi^2)^{\frac{m}{2}-1}+\ell(\ell+1)(1-\xi^2)^{\frac{m}{2}}\right.$$

(267)

$$\left.-m^2(1-\xi^2)^{\frac{m}{2}-1}\right]\upsilon-2(m+1)\xi(1-\xi^2)^{\frac{m}{2}}\frac{d\upsilon}{d\xi}+(1-\xi^2)^{\frac{m}{2}+1}\frac{d^2\upsilon}{d\xi^2}=0$$

or

$$\left[-m+m^2\xi^2(1-\xi^2)^{-1}-2m\xi^2(1-\xi^2)^{-1}+2m\xi^2(1-\xi^2)^{-1}+\ell(\ell+1)-m^2(1-\xi^2)^{-1}\right]\upsilon$$

(268)

$$-2(m+1)\xi\frac{d\upsilon}{d\xi}+(1-\xi^2)\frac{d^2\upsilon}{d\xi^2}=0$$

or

(269)

$$\left[-m-m^2(1-\xi^2)^{-1}(1-\xi^2)+\ell(\ell+1)\right]\upsilon-2(m+1)\xi\frac{d\upsilon}{d\xi}+(1-\xi^2)\frac{d^2\upsilon}{d\xi^2}=0$$

or

$$\left\{(1-\xi^2)\frac{d^2}{d\xi^2}-2(m+1)\xi\frac{d}{d\xi}+\left[\ell(\ell+1)-m(m+1)\right]\right\}\upsilon=0 \qquad (270)$$

Now let

$$\upsilon=\frac{d^m p}{d\xi^m} \qquad (271)$$

where p is a function to be determined. Substituting into Equation (270)

$$\left\{(1-\xi^2)\frac{d^2}{d\xi^2} - 2(m+1)\xi\frac{d}{d\xi} + \left[\ell(\ell+1) - m(m+1)\right]\right\}\frac{d^m P}{d\xi^m} = 0 \tag{272}$$

Now it will be shown that

$$\frac{d^m}{d\xi^m}\xi\frac{d}{d\xi} = \left(\xi\frac{d}{d\xi} + m\right)\frac{d^m}{d\xi^m} \tag{273}$$

First let U be any function, then

$$\frac{d}{d\xi}\left(\xi\frac{dU}{d\xi}\right) = \xi\frac{d^2U}{d\xi^2} + \frac{dU}{d\xi} = \left(\xi\frac{d}{d\xi} + 1\right)\frac{dU}{d\xi} \tag{274}$$

$$\frac{d^2}{d\xi^2}\left(\xi\frac{dU}{d\xi}\right) = \frac{d}{d\xi}\left(\xi\frac{d^2U}{d\xi^2} + \frac{dU}{d\xi}\right) = \xi\frac{d^3U}{d\xi^3} + \frac{d^2U}{d\xi^2} + \frac{d^2U}{d\xi^2} = \left(\xi\frac{d}{d\xi} + 2\right)\frac{d^2U}{d\xi^2} \tag{275}$$

$$\frac{d^3}{d\xi^3}\left(\xi\frac{dU}{d\xi}\right) = \frac{d}{d\xi}\left(\xi\frac{d^3U}{d\xi^3} + 2\frac{d^2U}{d\xi^2}\right) = \xi\frac{d^4U}{d\xi^4} + \frac{d^3U}{d\xi^3} + 2\frac{d^3U}{d\xi^3} = \left(\xi\frac{d}{d\xi} + 3\right)\frac{d^3U}{d\xi^3} \tag{276}$$

$$\vdots$$

$$\frac{d^m}{d\xi^m}\left(\xi\frac{dU}{d\xi}\right) = \left(\xi\frac{d}{d\xi} + m\right)\frac{d^m U}{d\xi^m} \tag{277}$$

So Equation (273) is proved. Equation (272) may be written

$$\left[\frac{d^2}{d\xi^2} - \xi^2\frac{d^2}{d\xi^2} - 2m\xi\frac{d}{d\xi} - \xi\frac{d}{d\xi} + \ell(\ell+1) - m^2 - m\right]\frac{d^m P}{d\xi^m} = 0 \tag{278}$$

or

$$\left[\frac{d^2}{d\xi^2} - \left(\xi^2\frac{d^2}{d\xi^2} + 2m\xi\frac{d}{d\xi} + m^2\right) - \left(\xi\frac{d}{d\xi} + m\right) + \ell(\ell+1)\right]\frac{d^m P}{d\xi^m} = 0 \qquad (279)$$

or

$$\left[\frac{d^2}{d\xi^2} - \left(\xi\frac{d}{d\xi} + m\right)\left(\xi\frac{d}{d\xi} + m\right) - \left(\xi\frac{d}{d\xi} + m\right) + \ell(\ell+1)\right]\frac{d^m P}{d\xi^m} = 0 \qquad (280)$$

or

$$\left[\frac{d^{m+2}}{d\xi^{m+2}} - \left(\xi\frac{d}{d\xi} + m\right)\frac{d^m}{d\xi^m}\left(\xi\frac{d}{d\xi}\right) - \frac{d^m}{d\xi^m}\left(\xi\frac{d}{d\xi}\right) + \frac{d^m}{d\xi^m}\ell(\ell+1)\right]P = 0 \qquad (281)$$

or

$$\frac{d^m}{d\xi^m}\left[\frac{d^2}{d\xi^2} - \left(\xi\frac{d}{d\xi}\right)\left(\xi\frac{d}{d\xi}\right) - \xi\frac{d}{d\xi} + \ell(\ell+1)\right]P = 0 \qquad (282)$$

or

$$\frac{d^m}{d\xi^m}\left[\frac{d^2}{d\xi^2} - \xi^2\frac{d^2}{d\xi^2} - \xi\frac{d}{d\xi} - \xi\frac{d}{d\xi} + \ell(\ell+1)\right]P = 0 \qquad (283)$$

or

$$\frac{d^m}{d\xi^m}\left\{\left[(1-\xi^2)\frac{d^2}{d\xi^2} - 2\xi\frac{d}{d\xi} + \ell(\ell+1)\right]P\right\} = 0 \qquad (284)$$

This equation is satisfied for all values of m, including m = 0, if, and only if

$$\left[(1-\xi^2)\frac{d^2}{d\xi^2} - 2\xi\frac{d}{d\xi} + \ell(\ell+1)\right]P = 0 \qquad (285)$$

But this is Legendre's equation, and the solutions to this equation[*] for integral values of ℓ are the Legendre Polynomials, $P_\ell(\xi)$. $P_\ell(\xi)$ is given by

$$P_\ell(\xi) = \frac{(2\ell)!}{2^\ell (\ell!)^2}\left[\xi^\ell - \frac{\ell(\ell-1)}{2(2\ell-1)}\xi^{\ell-2} + \frac{\ell(\ell-1)(\ell-2)(\ell-3)}{2^2 2!\,(2\ell-1)(2\ell-3)}\xi^{\ell-4} - \cdots\right] \qquad (286)$$

Since

$$P = P_\ell(\xi) \qquad (287)$$

and

$$U = \frac{d^m P}{d\xi^m} \qquad (288)$$

we now have

$$U = \frac{d^m P_\ell(\xi)}{d\xi^m} \qquad (289)$$

So from Equation (261) the solution to Equation (243), the Θ equation, is

$$\Theta_\ell^m(\theta) = (1-\cos^2\theta)^{\frac{m}{2}}\frac{d^m P_\ell(\cos\theta)}{d(\cos\theta)^m} \qquad \begin{array}{l} m = \text{any integer} \\ \ell = \text{any integer} \geq |m| \end{array} \qquad (290)$$

These solutions are called the associated Legendre Polynomials, which are usually written as $P_\ell^m(\xi)$. So we have

---

[*] Equation solved in Miller, <u>Partial Differential Equations in Engineering Problems</u>, 2nd. ed., pp. 190-194.

$$\Theta_\ell^m(\theta) = P_\ell^m(\cos\theta) = (1-\cos^2\theta)^{\frac{m}{2}} \frac{d^m P_\ell(\cos\theta)}{d(\cos\theta)^m} \qquad (291)$$

Now one seeks to determine a solution for the remaining Equation (229); which is now

$$\frac{d^2(rR)}{dr^2} + \left(k^2 - \frac{\ell(\ell+1)}{r^2}\right)rR = 0 \qquad (292)$$

Let

$$kr = \rho \qquad (293)$$

and

$$R(r) = \frac{1}{\sqrt{\rho}} Z(\rho) \qquad (294)$$

Also,

$$dr = \frac{1}{k} d\rho \qquad (295)$$

and substitute into Equation (292).

$$k \frac{d^2(\sqrt{\rho}\, Z(\rho))}{d\rho^2} + \left(k^2 - \frac{k^2\ell(\ell+1)}{\rho^2}\right)\frac{\sqrt{\rho}\, Z(\rho)}{k} = 0 \qquad (296)$$

or

$$\frac{d^2(\sqrt{\rho}\, Z(\rho))}{d\rho^2} + \left(1 - \frac{\ell(\ell+1)}{\rho^2}\right)\sqrt{\rho}\, Z(\rho) = 0 \qquad (297)$$

but

$$\frac{d^2(\sqrt{\rho}\,Z)}{d\rho^2} = \frac{d}{d\rho}\left[\frac{d(\sqrt{\rho}\,Z)}{d\rho}\right] = \frac{d}{d\rho}\left[\frac{Z}{2\sqrt{\rho}} + \sqrt{\rho}\,\frac{dZ}{d\rho}\right] \tag{298}$$

$$= -\frac{1}{4}\rho^{-3/2}Z + \frac{1}{2\sqrt{\rho}}\frac{dZ}{d\rho} + \sqrt{\rho}\,\frac{d^2Z}{d\rho^2} + \frac{1}{2\sqrt{\rho}}\frac{dZ}{d\rho} = \sqrt{\rho}\,\frac{d^2Z}{d\rho^2} + \frac{1}{\sqrt{\rho}}\frac{dZ}{d\rho} - \frac{1}{4}\rho^{-3/2}Z$$

so Equation (297) becomes

$$\sqrt{\rho}\,\frac{d^2Z}{d\rho^2} + \frac{1}{\sqrt{\rho}}\frac{dZ}{d\rho} - \frac{Z}{4\rho^{3/2}} + \sqrt{\rho}\,Z - \frac{\ell(\ell+1)}{\rho^{3/2}}Z = 0 \tag{299}$$

or

$$\frac{d^2Z}{d\rho^2} + \frac{1}{\rho}\frac{dZ}{d\rho} + \left[1 - \frac{1+4\ell(\ell+1)}{4\rho^2}\right]Z = 0 \tag{300}$$

but

$$\frac{1+4\ell(\ell+1)}{4\rho^2} = \frac{1+4\ell^2+4\ell}{4\rho^2} = \frac{4\ell^2+4\ell+1}{4\rho^2} = \frac{(2\ell+1)^2}{4\rho^2} = \frac{(\ell+\frac{1}{2})^2}{\rho^2} \tag{301}$$

so

$$\frac{d^2Z}{d\rho^2} + \frac{1}{\rho}\frac{dZ}{d\rho} + \left[1 - \frac{(\ell+\frac{1}{2})^2}{\rho^2}\right]Z = 0 \tag{302}$$

or

$$\rho^2\frac{d^2Z}{d\rho^2} + \rho\frac{dZ}{d\rho} + \left[\rho^2 - (\ell+\frac{1}{2})^2\right]Z = 0 \tag{303}$$

This Equation (303) is Bessel's equation of order $(\ell + \frac{1}{2})$. Two

linearly independent solutions for this equation are $J_{\ell+\frac{1}{2}}(\rho)$, the Bessel function of order $\ell + \frac{1}{2}$, and $N_{\ell+\frac{1}{2}}(\rho)$, the Neumann function of order $\ell + \frac{1}{2}$[*]. The general solution of the second order Equation (303) can then be written

$$Z_\ell(\rho) = A_\ell J_{\ell+\frac{1}{2}}(\rho) + B_\ell N_{\ell+\frac{1}{2}}(\rho) \tag{304}$$

when A_ℓ and B_ℓ are arbitrary constants.

Now,

$$r R = \frac{\rho}{k} \frac{1}{\sqrt{\rho}} Z = \frac{\sqrt{\rho}}{k} Z = \frac{\sqrt{\rho} A_\ell}{k} J_{\ell+\frac{1}{2}}(\rho) + \frac{\sqrt{\rho} B_\ell}{k} N_{\ell+\frac{1}{2}}(\rho) \tag{305}$$

so for convenience, let

$$A_\ell = k \sqrt{\frac{\pi}{2}} \, c_\ell \tag{306}$$

and

$$B_\ell = -k \sqrt{\frac{\pi}{2}} \, d_\ell \tag{307}$$

Then the general solution becomes

$$r R(r) = c_\ell \sqrt{\frac{\pi \rho}{2}} J_{\ell+\frac{1}{2}}(\rho) - d_\ell \sqrt{\frac{\pi \rho}{2}} N_{\ell+\frac{1}{2}}(\rho) \tag{308}$$

---

[*] Watson, A Treatise on the Theory of Bessel Functions, 2nd ed. (1944), p. 56.
Summerfeld, Partial Differential Equations in Physics, p. 113-114.

This is the general solution of Equation (292). The references listed on the bottom of the previous page discuss the $\chi_\ell(\rho)$ and $\Psi_\ell(\rho)$ functions, which are defined by

$$\Psi_\ell(\rho) = \sqrt{\frac{\pi\rho}{2}} \, J_{\ell+\frac{1}{2}}(\rho) \qquad (309) \qquad\qquad \chi_\ell(\rho) = -\sqrt{\frac{\pi\rho}{2}} \, N_{\ell+\frac{1}{2}}(\rho) \qquad (310)$$

The $\Psi_\ell(\rho)$ functions are regular in every finite domain of the ρ plane, including the origin, whereas the $\chi_\ell(\rho)$ functions have singularities at the origin $\rho = 0$, when they become infinite. Thus, the wave inside the sphere may be represented in terms of the $\Psi_\ell(\rho)$ functions but not the $\chi_\ell(\rho)$ functions.

The solution to Equation (292) can now be written as

$$r R(r) = c_\ell \Psi_\ell(kr) + d_\ell \chi_\ell(kr) \qquad (311)$$

For the scattered wave, let $c_\ell = 1$ and $d_\ell = -i$ to get

$$r R(r) = J_\ell^{(1)}(kr) \equiv \Psi_\ell(\rho) - i\chi_\ell(\rho) = \sqrt{\frac{\pi\rho}{2}} \, H_{\ell+\frac{1}{2}}^{(1)}(\rho) \qquad (312)$$

where $H^{(1)}$ is the Hankel function which is given by

$$H_j^{(1)} = J_j + i N_j \qquad (313)$$

The Hankel functions are distinguished from other cylindrical functions by the property that they vanish at infinity in the complex plane. $H^{(1)}$ vanishes in the half plane of the positive imaginary part of ρ and is thus

suitable for the representation of the scattered wave.

Now, Equations (235), (291), and (311) give the solution for Π. Substituting into Equation (217), we now have

$$\Pi = \sum_{\ell=0}^{\infty} \sum_{m=-\ell}^{\ell} \Pi_\ell^m = \sum_{\ell=0}^{\infty} \sum_{m=-\ell}^{\ell} [c_\ell \psi_\ell(kr) + d_\ell \chi_\ell(kr)][P_\ell^m(\cos\theta)][a_m \cos(m\phi) + b_m \sin(m\phi)] \tag{314}$$

where a_m, b_m, c_m, and d_m are arbitrary constants. This is the general solution to the wave equation.

Thus far all that has been done is to solve the wave equation without regard to the boundary conditions. Now the boundary conditions will be applied to determine the values of the constants for this specific problem. To do this, first write the components of the incident wave, given by Equation (57) through Equation (59), in spherical polar coordinates according to Equations (85) through (87).

$$E_r^{(i)}(r,\theta,\phi) = e^{ik^{(I)}r\cos\theta}\sin\theta\cos\phi \tag{315}$$

$$E_\theta^{(i)}(r,\theta,\phi) = e^{ik^{(I)}r\cos\theta}\cos\theta\cos\phi \tag{316}$$

$$E_\phi^{(i)}(r,\theta,\phi) = -e^{ik^{(I)}r\cos\theta}\sin\phi \tag{317}$$

$$H_r^{(i)}(r,\theta,\phi) = \frac{ik^{(I)}}{k_2^{(I)}} e^{ik^{(I)}r\cos\theta}\cos\theta\sin\phi \tag{318}$$

$$H_\theta^{(i)}(r,\theta,\phi) = \frac{ik^{(I)}}{k_2^{(I)}} e^{ik^{(I)}r\cos\theta} \cos\theta \sin\phi \qquad (319)$$

$$H_\phi^{(i)}(r,\theta,\phi) = \frac{ik^{(I)}}{k_2^{(I)}} e^{ik^{(I)}r\cos\theta} \cos\phi \qquad (320)$$

In order to determine the potentials ${}^e\Pi^{(i)}$ and ${}^m\Pi^{(i)}$, substitute Equations (315) through (320) into Equations (209) through (214), respectively, and solve the resulting equations. First, substitute Equation (315) into Equation (209) to get

$$e^{ik^{(I)}r\cos\theta} \sin\theta \cos\phi = \frac{\partial^2 (r\,{}^e\Pi^{(i)})}{\partial r^2} + k^{(I)^2} r\,{}^e\Pi^{(i)} \qquad (321)$$

Now make use of Bauer's formula[*]

$$e^{ik^{(I)}r\cos\theta} = \sum_{\ell=0}^{\infty} i^\ell (2\ell+1) \frac{\psi_\ell(k^{(I)}r)}{k^{(I)}r} P_\ell(\cos\theta) \qquad (322)$$

and the identities

$$e^{ik^{(I)}r\cos\theta} \sin\theta \equiv -\frac{1}{ik^{(I)}r} \frac{\partial}{\partial\theta}\left(e^{ik^{(I)}r\cos\theta}\right) \qquad (323)$$

$$\frac{\partial}{\partial\theta} P_\ell(\cos\theta) \equiv - P_\ell^{(1)}(\cos\theta) \qquad (324)$$

---

[*] Watson, A Treatise on the Theory of Bessel Functions, Cambridge Univ. Press, 2nd ed., (1944), p. 368.

$$P_0^{(1)}(\cos\theta) \equiv 0 \tag{325}$$

so that

$$e^{i k^{(I)} r' \cos\theta} \sin\theta \cos\phi = \frac{1}{(k^{(I)} r)^2} \sum_{\ell=1}^{\infty} i^{\ell-1} (2\ell+1) \psi_\ell(k^{(I)} r) P_\ell^{(1)}(\cos\theta) \cos\phi \tag{326}$$

Equation (321) becomes

$$\frac{\partial^2(r\,^e\Pi^{(i)})}{\partial r^2} + k^{(I)2}\,r\,^e\Pi^{(i)} = \frac{1}{(k^{(I)} r)^2} \sum_{\ell=1}^{\infty} i^{\ell-1} (2\ell+1) \psi_\ell(k^{(I)} r) P_\ell^{(1)}(\cos\theta) \cos\phi \tag{327}$$

Try, as a solution, a series of similar form

$$r\,^e\Pi^{(i)} = \frac{1}{k^{(I)2}} \sum_{\ell=1}^{\infty} \alpha_\ell \psi_\ell(k^{(I)} r) P_\ell^{(1)}(\cos\theta) \cos\phi \tag{328}$$

where α_ℓ is a constant to be determined. Take the second derivative

$$\frac{\partial^2(r\,^e\Pi^{(i)})}{\partial r^2} = \frac{1}{k^{(I)2}} \sum_{\ell=1}^{\infty} \alpha_\ell \frac{\partial^2 \psi_\ell(k^{(I)} r)}{\partial r^2} P_\ell^{(1)}(\cos\theta) \cos\phi \tag{329}$$

and substitute Equations (329) and (328) into Equation (327) to get

$$\frac{1}{k^{(I)2}} \sum_{\ell=1}^{\infty} \left[\alpha_\ell \frac{\partial^2 \psi_\ell(k^{(I)} r)}{\partial r^2} + k^{(I)2} \alpha_\ell \psi_\ell(k^{(I)} r) - \frac{i^{\ell-1}}{r^2}(2\ell+1)\psi_\ell(k^{(I)} r) \right] P_\ell^{(1)}(\cos\theta)\cos\phi = 0 \tag{330}$$

Since this holds for all values of θ and ϕ and since the Lagendre Polynomials are linearly independent,

$$\alpha_\ell \frac{\partial^2 \psi_\ell(k^{(I)}r)}{\partial r^2} + k^{(I)^2} \alpha_\ell \psi_\ell(k^{(I)}r) = \frac{i^{\ell-1}}{r^2}(2\ell+1)\psi_\ell(k^{(I)}r) \tag{331}$$

or

$$\alpha_\ell \left[k^{(I)^2} \psi_\ell(k^{(I)}r) + \frac{\partial^2 \psi_\ell(k^{(I)}r)}{\partial r^2} \right] = i^{\ell-1}(2\ell+1)\frac{\psi_\ell(k^{(I)}r)}{r^2} \tag{332}$$

If one lets $c_\ell = 1$ and $d_\ell = 0$, then from Equation (311) he can see that a solution to Equation (292) is

$$rR = \psi_\ell(k^{(I)}r) \tag{333}$$

so write Equation (292) as

$$\frac{d\psi_\ell}{dr^2} + \left(k^{(I)^2} - \frac{\ell(\ell+1)}{r^2} \right) \psi_\ell = 0 \tag{334}$$

Substitute Equation (334) into Equation (332) to get

$$\alpha_\ell \left[k^{(I)^2} \psi_\ell - k^{(I)^2} \psi_\ell + \frac{\ell(\ell+1)}{r^2} \psi_\ell \right] = i^{\ell-1}(2\ell+1)\frac{\psi_\ell}{r^2} \tag{335}$$

or

$$\alpha_\ell \ell(\ell+1) = i^{\ell-1}(2\ell+1) \tag{336}$$

so

$$\alpha_\ell = i^{\ell-1} \frac{2\ell+1}{\ell(\ell+1)} \tag{337}$$

Thus, using α_ℓ given by Equation (337), Equation (328) becomes a solution of Equation (327). The solution of Equation (327) may be written

$$r\, {}^e\Pi^{(i)} = \frac{1}{k^{(I)^2}} \sum_{\ell=1}^{\infty} i^{\ell-1} \frac{2\ell+1}{\ell(\ell+1)} \psi_\ell(k^{(I)} r) P_\ell^{(1)}(\cos\theta)\cos\phi \tag{338}$$

The Equation (330) for H_r in terms of ${}^m\Pi$ is the same as Equation (209) for E_r in terms of ${}^e\Pi$. The only difference in $H_r^{(i)}$ given by Equation (318) and $E_r^{(i)}$ given by Equation (315) is the constant $\dfrac{ik^{(I)}}{k_2^{(I)}}$, so one may use precisely the same procedure previously used to get ${}^e\Pi^{(i)}$ to determine that

$$r\, {}^m\Pi^{(i)} = \frac{1}{k^{(I)^2}} \sum_{\ell=1}^{\infty} i^\ell \frac{k^{(I)}}{k_2^{(I)}} \frac{2\ell+1}{\ell(\ell+1)} \psi_\ell(k^{(I)} r) P_\ell^{(1)}(\cos\theta)\sin\phi \tag{339}$$

${}^e\Pi^{(i)}$ and ${}^m\Pi^{(i)}$ have now been expressed in the form of the general solution to the wave Equation (314), so the unknown constants have been determined.

Using

$$\Pi = \Pi^{(w)} \qquad \text{inside the sphere} \tag{340}$$

$$\Pi = \Pi^{(i)} + \Pi^{(s)} \qquad \text{outside the sphere} \tag{341}$$

rewrite the boundary conditions Equation (216) as

$$k_1^{(I)}\left[r\left({}^e\Pi^{(i)} + {}^e\Pi^{(s)}\right)\right]_{r=a} = k_1^{(II)}\left[r^{\,e}\Pi^{(w)}\right]_{r=a} \tag{342}$$

$$k_2^{(I)}\left[r\left({}^m\Pi^{(i)} + {}^m\Pi^{(s)}\right)\right]_{r=a} = k_2^{(II)}\left[r^{\,m}\Pi^{(w)}\right]_{r=a} \tag{343}$$

$$\frac{\partial}{\partial r}\left[r\left({}^e\Pi^{(i)} + {}^e\Pi^{(s)}\right)\right]_{r=a} = \frac{\partial}{\partial r}\left[r^{\,e}\Pi^{(w)}\right]_{r=a} \tag{344}$$

$$\frac{\partial}{\partial r}\left[r\left({}^m\Pi^{(i)} + {}^m\Pi^{(s)}\right)\right]_{r=a} = \frac{\partial}{\partial r}\left[r^{\,e}\Pi^{(w)}\right]_{r=a} \tag{345}$$

Looking again at Equations (338) and (339), in order for these boundary conditions to be satisfied for all values of θ and ϕ, only the $m = 1$ terms in Equation (314) may be used. Thus, Equation (314) becomes

$$r\Pi = \sum_{\ell=0}^{\infty}\left\{\left[c_\ell\,\psi_\ell(kr) + d_\ell\,\chi_\ell(kr)\right]P_\ell^{(1)}(\cos\theta)\left[a_1\cos\phi + b_1\sin\phi\right]\right. \tag{346}$$

Also, from Equation (338),

$$b_1 = 0 \tag{347}$$

for the electric potential; and from Equation (339),

$$a_1 = 0 \tag{348}$$

for the magnetic potential

It has previously been recognized that only the Ψ_ℓ functions may be used to represent $\Pi^{(w)}$ because they remain finite; whereas, the χ_ℓ functions go to infinity at $r = 0$. Thus, from Equation (346) and these considerations, write

$$r \, {}^e\Pi^{(w)} = \frac{1}{k^{(\text{II})^2}} \sum_{\ell=1}^{\infty} {}^e A_\ell \, \Psi_\ell(k^{(\text{II})} r) \, P_\ell^{(1)}(\cos\theta) \cos\phi \tag{349}$$

and

$$r \, {}^m\Pi^{(w)} = \frac{i}{k^{(\text{II})} k_2^{(\text{II})}} \sum_{\ell=1}^{\infty} {}^m A_\ell \, \Psi_\ell(k^{(\text{II})} r) \, P_\ell^{(1)}(\cos\theta) \sin\phi \tag{350}$$

It has also been noted that the scattered wave may be represented in terms of the $\varsigma_\ell^{(1)}$ functions, given by Equation (312), where $\varsigma_\ell^{(1)}$ is obtained from the Hankel function $H_\ell^{(1)}$ on multiplication by $\sqrt{\frac{\pi\rho}{2}}$. Thus,

$$r \, {}^e\Pi^{(s)} = \frac{1}{k^{(\text{I})^2}} \sum_{\ell=1}^{\infty} {}^e B_\ell \, \varsigma_\ell^{(1)}(k^{(\text{I})} r) \, P_\ell^{(1)}(\cos\theta) \cos\phi \tag{351}$$

and

$$r \, {}^m\Pi^{(s)} = \frac{i}{k^{(\text{I})} k_2^{(\text{I})}} \sum_{\ell=1}^{m} {}^m B_\ell \, \varsigma_\ell^{(1)}(k^{(\text{I})} r) \, P_\ell^{(1)}(\cos\theta) \sin\phi \tag{352}$$

Now substitute the six expressions for $r\Pi$ into the boundary conditions to obtain linear relations between the coefficients, from which these coefficients may be determined. First substitute Equations (338), (349), and (351) into Equation (344) to get

$$\sum_{\ell=1}^{\infty} P_\ell^{(1)}(\cos\theta)\cos\phi\left[\frac{i^{\ell-1}}{k^{(I)^2}}\frac{2\ell+1}{\ell(\ell+1)}\frac{\partial\psi_\ell(k^{(I)}r)}{\partial r}+\frac{^eB_\ell}{k^{(I)^2}}\frac{\partial\zeta_\ell^{(1)}(k^{(I)}r)}{\partial r}-\frac{^eA_\ell}{k^{(II)^2}}\frac{\partial\psi_\ell(k^{(II)}r)}{\partial r}\right]_{r=a}=0 \tag{353}$$

Since the $P_\ell^{(1)}(\cos\theta)$ are linearly independent for different ℓ, this means that

$$^eB_\ell\frac{1}{k^{(I)^2}}\frac{\partial\zeta_\ell^{(1)}(k^{(I)}a)}{\partial r}+\frac{1}{k^{(I)^2}}i^{\ell-1}\frac{2\ell+1}{\ell(\ell+1)}\frac{\partial\psi_\ell(k^{(I)}a)}{\partial r}=\frac{1}{k^{(II)^2}}{^eA_\ell}\frac{\partial\psi_\ell(k^{(II)}a)}{\partial r} \tag{354}$$

but one can write, for any function

$$y=y(kr) \tag{355}$$

$$\frac{\partial y(kr)}{\partial r}=\frac{\partial(kr)}{\partial r}\frac{\partial y(kr)}{\partial(kr)}=k\frac{\partial y(kr)}{\partial(kr)}=ky'(kr) \tag{356}$$

so write Equation (354) as

$$^eB_\ell\frac{1}{k^{(I)}}\zeta_\ell^{(1)'}(k^{(I)}a)+\frac{1}{k^{(I)}}i^{\ell-1}\frac{2\ell+1}{\ell(\ell+1)}\psi_\ell'(k^{(I)}a)=\frac{1}{k^{(II)}}{^eA_\ell}\psi_\ell'(k^{(II)}a) \tag{357}$$

Now substitute Equations (339), (350), and (352) into Equation (345)

$$\sum_{\ell=1}^{\infty} P_{\ell}^{(1)}(\cos\theta)\sin\phi \left[\frac{1}{k^{(I)}} i^{\ell} \frac{2\ell+1}{\ell(\ell+1)} \psi_{\ell}'(k^{(I)}a) + \frac{i}{k_2^{(I)}}{}^m B_{\ell} \zeta_{\ell}^{(1)'}(k^{(I)}a) - \frac{i}{k_2^{(II)}}{}^m A_{\ell} \psi_{\ell}'(k^{(II)}a) \right] = 0 \tag{358}$$

or

$${}^m B_{\ell} \frac{1}{k_2^{(I)}} \zeta_{\ell}^{(1)'}(k^{(I)}a) + \frac{1}{k_2^{(I)}} i^{\ell-1} \frac{2\ell+1}{\ell(\ell+1)} \psi_{\ell}'(k^{(I)}a) = \frac{1}{k_2^{(II)}}{}^m A_{\ell} \psi_{\ell}'(k^{(II)}a) \tag{359}$$

Similarly, for the other two boundary conditions,

$${}^e B_{\ell} \frac{1}{k_2^{(I)}} \zeta_{\ell}^{(1)}(k^{(I)}a) + \frac{1}{k_2^{(I)}} i^{\ell-1} \frac{2\ell+1}{\ell(\ell+1)} \psi_{\ell}(k^{(I)}a) = \frac{1}{k_2^{(II)}}{}^e A_{\ell} \psi_{\ell}(k^{(II)}a) \tag{360}$$

and

$${}^m B_{\ell} \frac{1}{k^{(I)}} \zeta_{\ell}^{(1)}(k^{(I)}a) + \frac{1}{k^{(I)}} i^{\ell-1} \frac{2\ell+1}{\ell(\ell+1)} \psi_{\ell}(k^{(I)}a) = \frac{1}{k^{(II)}}{}^m A_{\ell} \psi_{\ell}(k^{(II)}a) \tag{361}$$

Equations (357), (359), (360), and (361) are a complete set of equations for the determination of ${}^e A_{\ell}$, ${}^m A_{\ell}$, ${}^e B_{\ell}$, and ${}^m B_{\ell}$.

One is only interested in the coefficients ${}^e B_{\ell}$ and ${}^m B_{\ell}$ which characterize the scattered wave, so he needs only to eliminate ${}^e A_{\ell}$ and ${}^m A_{\ell}$. Write Equations (357) and (359) as

$${}^e A_{\ell} = \frac{k^{(II)}}{\psi_{\ell}'(k^{(II)}a)} \left[{}^e B_{\ell} \frac{1}{k^{(I)}} \zeta_{\ell}^{(1)'}(k^{(I)}a) + \frac{1}{k^{(I)}} i^{\ell-1} \frac{2\ell+1}{\ell(\ell+1)} \psi_{\ell}'(k^{(I)}a) \right] \tag{362}$$

and

$$^{m}A_\ell = \frac{k_2^{(II)}}{\psi_\ell'(k\,\overset{(II)}{a})}\left[^{m}B_\ell \frac{1}{k_2^{(I)}}\zeta_\ell^{(I)}(k\,\overset{(I)}{a}) + \frac{1}{k_2^{(I)}}i^{\ell-1}\frac{2\ell+1}{\ell(\ell+1)}\psi_\ell'(k\,\overset{(I)}{a})\right] \tag{363}$$

and substitute into Equations (360) and (361).

$$^{e}B_\ell\frac{1}{k_2^{(I)}}\zeta_\ell^{(I)}(k\,\overset{(I)}{a}) + \frac{1}{k_2^{(I)}}i^{\ell-1}\frac{2\ell+1}{\ell(\ell+1)}\psi_\ell(k\,\overset{(I)}{a}) = \frac{k\,\psi_\ell^{(II)}(k\,\overset{(II)}{a})}{k_2^{(II)}\psi_\ell'(k\,\overset{(II)}{a})}\left[\frac{^{e}B_\ell}{k^{(I)}}\zeta_\ell''^{(I)}(k\,\overset{(I)}{a}) + \frac{i^{\ell-1}(2\ell+1)}{k^{(I)}\ell(\ell+1)}\psi_\ell'^{(I)}(k\,\overset{(I)}{a})\right] \tag{364}$$

$$^{m}B_\ell\frac{1}{k^{(I)}}\zeta_\ell''^{(I)}(k\,\overset{(I)}{a}) + \frac{i^{\ell-1}}{k^{(I)}}\frac{2\ell+1}{\ell(\ell+1)}\psi_\ell(k\,\overset{(I)}{a}) = \frac{k_2^{(II)}\psi_\ell(k\,\overset{(II)}{a})}{k^{(II)}\psi_\ell'(k\,\overset{(II)}{a})}\left[\frac{^{m}B_\ell}{k_2^{(I)}}\zeta_\ell^{(I)}(k\,\overset{(I)}{a}) + \frac{i^{\ell-1}(2\ell+1)}{k_2^{(I)}\ell(\ell+1)}\psi_\ell'(k\,\overset{(I)}{a})\right] \tag{365}$$

or

$$^{e}B_\ell\left[\frac{1}{k_2^{(I)}}\zeta_\ell^{(I)}(k\,\overset{(I)}{a}) - \frac{k\,\psi_\ell^{(II)}(k\,\overset{(II)}{a})}{k^{(I)}k_2^{(II)}\psi_\ell'(k\,\overset{(II)}{a})}\zeta_\ell^{(I)'}(k\,\overset{(I)}{a})\right] = i^{\ell-1}\frac{2\ell+1}{\ell(\ell+1)}\left[\frac{k_2^{(II)}\psi_\ell^{(II)}(k\,\overset{(II)}{a})\psi_\ell'(k\,\overset{(I)}{a})}{k^{(I)}k^{(I)}\psi_\ell'(k\,\overset{(II)}{a})} - \frac{1}{k_2^{(I)}}\psi_\ell^{(I)}(k\,\overset{(I)}{a})\right] \tag{366}$$

$$^{m}B_\ell\left[\frac{1}{k^{(I)}}\zeta_\ell^{(I)}(k\,\overset{(I)}{a}) - \frac{k_2^{(II)}\psi_\ell^{(II)}(k\,\overset{(II)}{a})}{k_2^{(I)}k^{(II)}\psi_\ell'(k\,\overset{(II)}{a})}\zeta_\ell^{(I)'}(k\,\overset{(I)}{a})\right] = i^{\ell-1}\frac{2\ell+1}{\ell(\ell+1)}\left[\frac{k_2^{(II)}\psi_\ell^{(II)}(k\,\overset{(II)}{a})\psi_\ell'(k\,\overset{(I)}{a})}{k^{(II)}k_2^{(I)}\psi_\ell'(k\,\overset{(II)}{a})} - \frac{1}{k^{(I)}}\psi_\ell^{(I)}(k\,\overset{(I)}{a})\right] \tag{367}$$

or

$$^{e}B_\ell = \frac{i^{\ell-1}(2\ell+1)\left[\frac{k^{(II)}\psi_\ell(k^{(II)}a)\psi_\ell'(k^{(II)}a)}{k^{(I)}k_2^{(I)}\psi_\ell'(k^{(II)}a)} - \frac{1}{k_2^{(I)}}\psi_\ell(k^{(II)}a)\right]}{\ell(\ell+1)\left[\frac{1}{k_2^{(I)}}\zeta_\ell^{(1)}(k^{(I)}a) - \frac{k^{(II)}\psi_\ell(k^{(II)}a)}{k^{(I)}k_2^{(I)}\psi_\ell'(k^{(II)}a)}\zeta_\ell^{(1)'}(k^{(I)}a)\right]} \tag{368}$$

$$^{m}B_\ell = \frac{i^{\ell-1}(2\ell+1)\left[\frac{k_2^{(II)}\psi_\ell(k^{(II)}a)\psi_\ell'(k^{(I)}a)}{k^{(I)}k^{(II)}\psi_\ell'(k^{(II)}a)} - \frac{1}{k^{(I)}}\psi_\ell(k^{(I)}a)\right]}{\ell(\ell+1)\left[\frac{1}{k_2^{(I)}}\zeta_\ell^{(1)}(k^{(I)}a) - \frac{k_2^{(II)}\psi_\ell(k^{(II)}a)}{k^{(I)}k^{(II)}\psi_\ell'(k^{(II)}a)}\zeta_\ell^{(1)}(k^{(I)}a)\right]} \tag{369}$$

or

$$^{e}B_\ell = i^{\ell+1}\frac{2\ell+1}{\ell(\ell+1)}\ \frac{k_2^{(I)}k^{(II)}\psi_\ell'(k^{(I)}a)\psi_\ell(k^{(II)}a) - k_2^{(II)}k^{(I)}\psi_\ell(k^{(II)}a)\psi_\ell(k^{(I)}a)}{k_2^{(I)}k^{(II)}\zeta_\ell^{(1)'}(k^{(I)}a)\psi_\ell(k^{(II)}a) - k_2^{(II)}k^{(I)}\psi_\ell'(k^{(II)}a)\zeta_\ell^{(1)}(k^{(I)}a)} \tag{370}$$

$$^{m}B_\ell = i^{\ell+1}\frac{2\ell+1}{\ell(\ell+1)}\ \frac{k_2^{(I)}k^{(II)}\psi_\ell(k^{(I)}a)\psi_\ell'(k^{(II)}a) - k_2^{(II)}k^{(I)}\psi_\ell(k^{(I)}a)\psi_\ell(k^{(II)}a)}{k_2^{(I)}k^{(II)}\zeta_\ell^{(1)}(k^{(I)}a)\psi_\ell'(k^{(II)}a) - k_2^{(II)}k^{(I)}\zeta_\ell^{(1)'}(k^{(I)}a)\psi_\ell(k^{(II)}a)} \tag{371}$$

The potential functions representing the scattered wave, Equations (351) and (352), for which the constants $^{e}B_\ell$ and $^{m}B_\ell$ have been determined, are now substituted into Equations (209) through (214) to give the components of the scattered field. Substituting Equation (351) into Equation (209) gives

$$E_r^{(s)} = \frac{1}{k^{(I)2}}\sum_{\ell=1}^{\infty} {}^{e}B_\ell P_\ell^{(1)}(\cos\theta)\cos\phi\left[\frac{d^2}{dr^2}+k^{(I)2}\right]\zeta_\ell^{(1)}(k^{(I)}r) \tag{372}$$

Remembering that $rR = \zeta_\ell^{(1)}(kr)$, Equation (312), is a solution of Equation (292)

$$\frac{d^2(rR)}{dr^2} + \left(k^2 - \frac{\ell(\ell+1)}{r^2}\right) rR = 0 \tag{292}$$

write

$$\left[\frac{d^2}{dr^2} + k^{(I)^2}\right]\zeta_\ell^{(1)}(k^{(I)}r) = \frac{\ell(\ell+1)}{r^2}\zeta_\ell^{(1)}(k^{(I)}r) \tag{373}$$

so Equation (372) becomes

$$E_r^{(S)}(r,\theta,\phi) = \frac{1}{k^{(I)^2}}\frac{\cos\phi}{r^2}\sum_{\ell=1}^{\infty}\ell(\ell+1)\,{}^e B_\ell\,\zeta_\ell^{(1)}(k^{(I)}r)\,P_\ell^{(1)}(\cos\theta) \tag{374}$$

Now substitute Equations (351) and (352) into Equation (210).

$$E_\theta^{(S)} = \frac{1}{rk^{(I)}}\sum_{\ell=1}^{\infty}\left[{}^e B_\ell\,\frac{\cos\phi}{k^{(I)}}\,\frac{\partial\zeta_\ell^{(1)}(k^{(I)}r)}{\partial r}\,\frac{\partial P_\ell^{(1)}(\cos\theta)}{\partial\theta} + \frac{i\,{}^m B_\ell}{\sin\theta}\,\zeta_\ell^{(1)}(k^{(I)}r)\,P_\ell^{(1)}(\cos\theta)\cos\phi\right] \tag{375}$$

or

$$E_\theta^{(S)}(r,\theta,\phi) = -\frac{1}{k^{(I)}}\frac{\cos\phi}{r}\sum_{\ell=1}^{\infty}\left[{}^e B_\ell\,\zeta_\ell^{(1)'}(k^{(I)}r)\,P_\ell^{(1)'}(\cos\theta)\sin\theta - i\,{}^m B_\ell\,\zeta_\ell^{(1)}(k^{(I)}r)\,P_\ell^{(1)}(\cos\theta)\frac{1}{\sin\theta}\right] \tag{376}$$

Substitute Equations (351) and (352) into Equation (211).

$$E_{\phi}^{(s)}(r,\theta,\phi) = \frac{1}{r\,k^{(I)}} \sum_{\ell=1}^{\infty} \left[\frac{^{e}B_{\ell}}{\sin\theta} \frac{d\,S_{\ell}^{(1)}(k^{(I)}r)}{dr} \frac{d(\cos\phi)}{d\phi} P_{\ell}^{(1)}(\cos\theta) - i\,^{m}B_{\ell}\,\zeta_{\ell}^{(1)}(k^{(I)}r) \frac{d\,P_{\ell}^{(1)}(\cos\theta)}{d\theta}\sin\phi \right] \tag{377}$$

or

$$E_{\phi}^{(s)}(r,\theta,\phi) = -\frac{\sin\phi}{k^{(I)}r} \sum_{\ell=1}^{\infty} \left[^{e}B_{\ell}\,\zeta_{\ell}^{(1)'}(k^{(I)}r)P_{\ell}^{(1)}(\cos\theta)\frac{1}{\sin\theta} - i\,^{m}B_{\ell}\,\zeta_{\ell}^{(1)}(k^{(I)}r)\,P_{\ell}^{(1)'}(\cos\theta)\sin\theta \right] \tag{378}$$

Substitute Equation (352) into Equation (212).

$$H_{r}^{(s)} = \frac{i}{k^{(I)}k_{2}^{(I)}} \sum_{\ell=1}^{\infty}{}^{m}B_{\ell}\,P_{\ell}^{(1)}(\cos\theta)\sin\phi\left(k^{2}+\frac{d^{2}}{dr^{2}}\right)\zeta_{\ell}^{(1)}(k^{(I)}r) \tag{379}$$

or

$$H_{r}^{(s)}(r,\theta,\phi) = \frac{i}{k^{(I)}k_{2}^{(I)}} \frac{\sin\phi}{r^{2}} \sum_{\ell=1}^{\infty}\ell(\ell+1)\,^{m}B_{\ell}\,\zeta_{\ell}^{(1)}(k^{(I)}r)P_{\ell}^{(1)}(\cos\phi) \tag{380}$$

Substitute Equations (130) and (352) into Equation (213).

$$H_{\theta}^{(s)} = -\frac{1}{k_{2}^{(I)}r} \sum_{\ell=1}^{\infty} \left[\frac{-^{e}B_{\ell}}{\sin\theta}\,\zeta_{\ell}^{(1)}(k^{(I)}r)P_{\ell}^{(1)}(\cos\theta)\frac{d(\cos\phi)}{d\phi} - \frac{i\,^{m}B_{\ell}}{k_{2}^{(I)}} \frac{d\,\zeta_{\ell}^{(1)}(k^{(I)}r)}{dr} \frac{d\,P_{\ell}^{(1)}(\cos\theta)}{d\theta}\sin\phi \right] \tag{381}$$

or

$$H_{\theta}^{(s)}(r,\theta,\phi) = -\frac{\sin\phi}{k_{2}^{(I)}r} \sum_{\ell=1}^{\infty} \left[^{e}B_{\ell}\,\zeta_{\ell}^{(1)}(k^{(I)}r)P_{\ell}^{(1)}(\cos\theta)\frac{1}{\sin\theta} + i\,^{m}B_{\ell}\,\zeta_{\ell}^{(1)'}(k^{(I)}r)P_{\ell}^{(1)'}(\cos\theta)\sin\theta \right] \tag{382}$$

Substitute Equations (351) and (352) into Equation (214).

$$H_\phi^{(s)} = \frac{1}{k^{(I)}r} \sum_{\ell=1}^{\infty} \left[\frac{k_1^{(I)}}{k^{(I)}} {}^eB_\ell \zeta_\ell^{(1)}(k^{(I)}r) \frac{dP_\ell^{(1)}(\cos\theta)}{d\theta} \cos\phi + \frac{i\, {}^mB_\ell}{k_2^{(I)} \sin\theta} \frac{d\zeta_\ell^{(1)}(k^{(I)}r)}{dr} P_\ell^{(1)}(\cos\theta) \frac{d(\sin\phi)}{d\phi} \right] \qquad (383)$$

or

$$H_\phi^{(s)}(r,\theta,\phi) = \frac{1}{k_2^{(I)}} \frac{\cos\phi}{r} \sum_{\ell=1}^{\infty} \left[{}^eB_\ell \zeta_\ell^{(1)}(k^{(I)}r) P_\ell^{(1)}{}'(\cos\theta)\sin\theta + i\, {}^mB_\ell \zeta_\ell^{(1)}{}'(k^{(I)}r) \frac{P_\ell^{(1)}(\cos\theta)}{\sin\theta} \right] \qquad (384)$$

The problem is now solved in that $(\vec{E}^{(s)}, \vec{H}^{(s)})$ has been determined by applying the boundary conditions to Maxwell's equations and $(\vec{E}^{(i)}, \vec{H}^{(i)})$.

What follows is a discussion of this solution. First take a look at the various constants. Since it has been assumed that $\sigma^{(I)} = 0$ (non-conducting medium), one may write $\sigma^{(II)} = \sigma$ for simplicity. Thus, from Equations (39) and (40) one may write

$$k_1^{(I)} = \frac{i\omega}{c} \varepsilon^{(I)} = i \frac{2\pi}{\lambda_o} \varepsilon^{(I)} \qquad (385)$$

$$k_2^{(I)} = \frac{i\omega}{c} = i \frac{2\pi}{\lambda_o} \qquad (386)$$

$$k^{(I)} = \left(-k_1^{(I)} k_2^{(I)} \right)^{\frac{1}{2}} = \frac{\omega}{c} \sqrt{\varepsilon^{(I)}} = \frac{2\pi}{\lambda_o}\sqrt{\varepsilon^{(I)}} = \frac{2\pi}{\lambda^{(I)}} \qquad (387)$$

$$k_1^{(II)} = \frac{i\omega}{c}\left(\varepsilon^{(II)} + i\,\frac{4\pi\sigma}{\omega}\right) = i\,\frac{2\pi}{\lambda_o}\left(\varepsilon^{(II)} + i\,\frac{4\pi\sigma}{\omega}\right) \tag{388}$$

$$k_2^{(II)} = \frac{i\omega}{c} = i\,\frac{2\pi}{\lambda_o} \tag{389}$$

$$k^{(II)} = \left(-k_1^{(II)}k_2^{(II)}\right)^{\frac{1}{2}} = \frac{2\pi}{\lambda_o}\sqrt{\varepsilon^{(II)} + \frac{4\pi\sigma}{\omega}} \tag{390}$$

where λ_o is the wavelength of the light in a vacuum and $\lambda^{(I)}$ is the wavelength in the medium surrounding the sphere.

Sometimes it is convenient to introduce the complex refractive index of the sphere relative to the surrounding medium. Denoting this index by $\hat{n}$,

$$\hat{n}^2 = \frac{n^{(II)^2}}{n^{(I)^2}} = \frac{k^{(II)^2}}{k^{(I)^2}} = \frac{\varepsilon^{(II)}}{\varepsilon^{(I)}} + i\,\frac{4\pi\sigma}{\omega\varepsilon^{(I)}} = \frac{k_1^{(II)}}{k_1^{(I)}} \tag{391}$$

Note that

$$\hat{n} = \left[\frac{k_1^{(II)}}{k_1^{(I)}}\right]^{\frac{1}{2}} = \left[\frac{k^{(II)^2}k_2^{(I)}}{k_2^{(II)}k_1^{(I)^2}} \cdot \frac{k_2^{(I)}}{k_2^{(II)}}\right]^{\frac{1}{2}} = \frac{k^{(II)}k_2^{(I)}}{k_2^{(II)}k^{(I)}} \tag{392}$$

Also, to simplify the equations, introduce the dimensionless parameter q defined by

$$q \equiv \frac{2\pi a}{\lambda^{(I)}} \tag{393}$$

that is, 2π times the ratio of the radius of the sphere to the wavelength of the light in the medium outside the sphere. Now using Equations (392) and (393) write the coefficients given by Equations (370) and (371) as

$$^{e}B_{\ell} = i^{\ell+1} \frac{2\ell+1}{\ell(\ell+1)} \frac{\hat{n}\,\psi'_{\ell}(g)\,\psi_{\ell}(\hat{n}g) - \psi_{\ell}(g)\,\psi'_{\ell}(\hat{n}g)}{\hat{n}\,\zeta''^{(1)}_{\ell}(g)\,\psi_{\ell}(\hat{n}g) - \zeta''^{(1)}_{\ell}(g)\,\psi'_{\ell}(\hat{n}g)} \tag{394}$$

$$^{m}B_{\ell} = i^{\ell+1} \frac{2\ell+1}{\ell(\ell+1)} \frac{\hat{n}\,\psi_{\ell}(g)\,\psi'_{\ell}(\hat{n}g) - \psi'_{\ell}(g)\,\psi_{\ell}(\hat{n}g)}{\hat{n}\,\zeta''^{(1)}_{\ell}(g)\,\psi'_{\ell}(\hat{n}g) - \zeta''^{(1)'}_{\ell}(g)\,\psi_{\ell}(\hat{n}g)} \tag{395}$$

Now examine the intensity of the scattered light. To look at the relative values of the intensity take as a measure of the intensity the square of the real amplitude of the electric vector. Since one here considers only the distant field ($r \gg \lambda$) replace ψ_{ℓ}, ψ'_{ℓ}, $\zeta^{(1)}_{\ell}$, and $\zeta^{(1)'}_{\ell}$ by their asymptotic approximations:

$$\psi_{\ell}(x) = \tfrac{1}{2}\left[i^{\ell+1}e^{-ix} + (-i)^{\ell+1}e^{ix}\right] \tag{396}$$

$$\zeta^{(1)}_{\ell}(x) = (-i)^{\ell+1}e^{ix} \tag{397}$$

$$\psi'_{\ell}(x) = \tfrac{1}{2}\left[i^{\ell}e^{-ix} + (-i)^{\ell}e^{ix}\right] \tag{398}$$

$$\zeta^{(1)'}_{\ell}(x) = (-i)^{\ell}e^{ix} \tag{399}$$

It is seen from Equation (374) that the amplitude of the radial component $E_r^{(s)}$ of the scattered wave falls off as the inverse square of the distance from the scattering center, whereas from Equations (376) and (378) the amplitudes of the transverse components fall off more slowly, as the inverse of the distance. Thus, at sufficiently great distance ($r \gg a$) the radial component may be neglected in comparison with the tangential components, and the wave is considered to be transverse. Thus, for $r \gg a$:

$$E_r^{(s)} = 0 \tag{400}$$

$$E_\theta^{(s)} = -\frac{1}{k^{(I)}} \frac{\cos\phi}{r} \sum_{\ell=1}^{\infty} \left[{}^e B_\ell (-i)^\ell i k^{(I)} r \, P_\ell^{(1)\prime}(\cos\theta) \sin\theta - i \, {}^m B_\ell (-i)^{\ell+1} i k^{(I)} r \frac{P_\ell^{(1)}(\cos\theta)}{\sin\theta} \right] \tag{401}$$

or

$$E_\theta^{(s)} = -\frac{1}{k^{(I)}} \frac{\cos\phi}{r} \sum_{\ell=1}^{\infty} (-i)^\ell e^{i k^{(I)} r} \left[{}^e B_\ell \, P_\ell^{(1)\prime}(\cos\theta) \sin\theta - {}^m B_\ell \frac{P_\ell^{(1)}(\cos\theta)}{\sin\theta} \right] \tag{402}$$

and

$$E_\phi^{(s)} = -\frac{1}{k^{(I)}} \frac{\sin\phi}{r} \sum_{\ell=1}^{\infty} \left[{}^e B_\ell (-i)^\ell e^{-i k^{(I)} r} \frac{P_\ell^{(1)}(\cos\theta)}{\sin\theta} - i \, {}^m B_\ell (-i)^{\ell+1} e^{-i k^{(I)} r} P_\ell^{(1)\prime}(\cos\theta) \sin\theta \right] \tag{403}$$

or

$$E_\phi^{(s)} = -\frac{1}{k^{(I)}} \frac{\sin\phi}{r} \sum_{\ell=1}^{\infty} (-i)^\ell e^{-i k^{(I)} r} \left[{}^e B_\ell \frac{P_\ell^{(1)}(\cos\theta)}{\sin\theta} - {}^m B_\ell \, P_\ell^{(1)\prime}(\cos\theta) \sin\theta \right] \tag{404}$$

Then, letting $I^{(s)}$ represent the intensity of the scattered wave,

$$I_\theta^{(s)} = \frac{1}{k^{(I)^2}} \frac{\cos^2\phi}{r^2} \left| \sum_{\ell=1}^{\infty} (-i)^\ell \left[{}^e B_\ell \, P_\ell^{(1)\prime}(\cos\theta)\sin\theta - {}^m B_\ell \, P_\ell^{(1)}(\cos\theta)\frac{1}{\sin\theta} \right] \right|^2 \tag{405}$$

or, from Equation (387)

$$I_\theta^{(s)} = \frac{\lambda^{(I)^2}}{4\pi^2 r^2} \left| \sum_{\ell=1}^{\infty} (-i)^\ell \left[{}^e B_\ell \, P_\ell^{(1)\prime}(\cos\theta)\sin\theta - {}^m B_\ell \, \frac{P_\ell^{(1)}(\cos\theta)}{\sin\theta} \right] \right|^2 \cos^2\phi \tag{406}$$

Similarly,

$$I_\phi^{(s)} = \frac{\lambda^{(I)^2}}{4\pi^2 r^2} \left| \sum_{\ell=1}^{\infty} (-i)^\ell \left[{}^e B_\ell \, \frac{P_\ell^{(1)}(\cos\theta)}{\sin\theta} - {}^m B_\ell \, P_\ell^{(1)\prime}(\cos\theta)\sin\theta \right] \right|^2 \sin^2\phi \tag{407}$$

Now define the "plane of observation" to be that plane which contains the direction of propagation of the incident light (the z axis) and the direction (θ, ϕ) of observation. ϕ has been defined to be the angle between this plane and the x axis, which is the direction of vibration of the electric vector of the incident wave. Then, if $I_\parallel^{(s)}$ is the intensity of the light parallel to the y direction and $I_\perp^{(s)}$ is the intensity perpendicular, close examination of the relationship between the Cartesian and polar coordinate systems show that

$$E_\theta^{(s)} = E_\parallel^{(s)} \cos\phi \tag{408}$$

$$E_\phi^{(s)} = E_\perp^{(s)} \sin\phi \qquad (409)$$

so write

$$I_\theta^{(s)} = I_{||}^{(s)} \cos^2\phi \qquad (410)$$

$$I_\phi^{(s)} = I_\perp^{(s)} \sin^2\phi \qquad (411)$$

so, comparing these with Equations (405) and (407), one sees that

$$I_{||}^{(s)} = \frac{\lambda^{(I)^2}}{4\pi^2 r^2} \left| \sum_{\ell=1}^{\infty} (-i)^\ell \left[{}^e B_\ell \, P_\ell^{(1)'}(\cos\theta) \sin\theta - {}^m B_\ell \, \frac{P_\ell^{(1)}(\cos\theta)}{\sin\theta} \right] \right|^2 \qquad (412)$$

$$I_\perp^{(s)} = \frac{\lambda^{(I)^2}}{4\pi^2 r^2} \left| \sum_{\ell=1}^{\infty} (-i)^\ell \left[{}^e B_\ell \, \frac{P_\ell^{(1)}(\cos\theta)}{\sin\theta} - {}^m B_\ell \, P_\ell^{(1)'}(\cos\theta) \sin\theta \right] \right|^2 \qquad (413)$$

The total intensity of the scattered light is then given by

$$I^{(s)}(r,\theta,\phi) = I_\theta^{(s)} + I_\phi^{(s)} = I_{||}^{(s)} \cos^2\phi + I_\perp^{(s)} \sin^2\phi \qquad (414)$$

In practice, one is usually concerned with the scattering of unpolarized light, so the appropriate formula may be obtained from the above by averaging over all directions of polarization. Letting a bar denote the average, since

$$\overline{\cos^2\phi} = \overline{\sin^2\phi} = \frac{1}{2} \qquad (415)$$

the equation for unpolarized light is

$$I^{(s)}_{(r,\theta)} = \frac{1}{2} I^{(s)}_{\parallel} + \frac{1}{2} I^{(s)}_{\perp}$$

(416)

or

$$I^{(s)}_{(r,\theta)} = \frac{\lambda^{(I)^2}}{8\pi^2 r^2} \left\{ \left| \sum_{\ell=1}^{\infty} (-i)^{\ell} \left[{}^{e}B_{\ell} P^{(1)\prime}_{\ell}(\cos\theta)\sin\theta - {}^{m}B_{\ell} \frac{P^{(1)}_{\ell}(\cos\theta)}{\sin\theta} \right] \right|^2 \right.$$

(417)

$$\left. + \left| \sum_{\ell=1}^{\infty} (-i)^{\ell} \left[{}^{e}B_{\ell} \frac{P^{(1)\prime}_{\ell}(\cos\theta)}{\sin\theta} - {}^{m}B_{\ell} P^{(1)\prime}_{\ell}(\cos\theta)\sin\theta \right] \right|^2 \right\}$$

(418)

Equations have now been obtained for the amplitude and intensity of the scattered light for a non-polarized beam of incident light. The totality of processes by which energy is removed from the beam is called extinction. The cross section for extinction is the sum of the absorption cross section and the scattering cross section. One may evaluate the extinction cross section for a particle from the amplitude function for $\theta = 0$. The scattering cross section may be evaluated by integration over the entire scattering pattern. The absorption cross section is then the difference between the extinction cross section and the scattering cross section.

Van de Hulst[17] has evaluated the extinction and scattering cross sections using the Mie equations. He gives the Mie coefficients in a form slightly different from Equations (394) and (395) by letting a_n and b_n be called the Mie coefficients, where a_n and b_n are given in terms of ${}^{e}B_n$ and ${}^{m}B_n$ by

$$^e B_n = i^{n+1} \frac{2n+1}{n(n+1)} a_n \tag{418}$$

$$^m B_n = i^{n+1} \frac{2n+1}{n(n+1)} b_n \tag{419}$$

where

$$a_n = \frac{\hat{n}\, \psi_n'(q)\, \psi_n(\hat{n}q) - \psi_n(q)\, \psi_n'(\hat{n}q)}{\hat{n}\, \zeta_n^{(\prime\prime)\prime}(q)\, \psi_n(\hat{n}q) - \zeta_n^{(\prime\prime)}(q)\, \psi_n'(\hat{n}q)} \tag{420}$$

and

$$b_n = \frac{\hat{n}\, \psi_n(q)\, \psi_n'(\hat{n}q) - \psi_n'(q)\, \psi_n(\hat{n}q)}{\hat{n}\, \zeta_\ell^{(\prime\prime)}(q)\, \psi_\ell(\hat{n}q) - \zeta_\ell^{(\prime\prime)\prime}(q)\, \psi_\ell(\hat{n}q)} \tag{421}$$

The components of the scattered wave, Equations (402) and (403) now become

$$E_\theta^{(s)} = -\frac{i e^{-ikr}}{kr} \cos\phi\, S_2(\theta) \tag{422}$$

and

$$E_\phi^{(s)} = \frac{i e^{-ikr}}{kr} \sin\phi\, S_1(\theta) \tag{423}$$

where

$$S_1(\theta) = \sum_{n=1}^{\infty} \frac{2n+1}{n(n+1)} \left[a_n \frac{P_n^{(1)}(\cos\theta)}{\sin\theta} + b_n P_n^{(1)\prime}(\cos\theta)\sin\theta \right] \tag{424}$$

and

$$S_2(\theta) = \sum_{n=1}^{\infty} \frac{2n+1}{n(n+1)} \left[b_n \frac{P_n^{(1)''}(\cos\theta)}{\sin\theta} + a_n P_n^{(1)'}(\cos\theta) \sin\theta \right] \tag{425}$$

These equations represent the outgoing spherical wave for an incident polarized wave. The extinction cross section is found by evaluating the amplitude functions, Equations (424) and (425) for $\theta = 0$. The terms involving the associated Legendre Polynomials can easily be evaluated from the expansion[26]

$$P_n^{(m)}(x) = \frac{1}{2^n m!} \frac{(n+m)!}{(n-m)!} (1-x^2)^{\frac{m}{2}} \left[1 + C_1 \left(\frac{1-x}{2} \right) + C_2 \left(\frac{1-x}{2} \right)^2 + C_3 \left(\frac{1-x}{2} \right)^3 + \cdots \right] \tag{426}$$

where C_1, C_2, . . . depends on n and m only. From Equation (426) and its derivative one finds that

$$\left[\frac{P_\ell^{(1)''}(\cos\theta)}{\sin\theta} \right]_{\theta=0} = \frac{1}{2} \ell(\ell+1) \tag{427}$$

$$\left[P_\ell^{(1)'}(\cos\theta) \sin\theta \right]_{\theta=0} = -\frac{1}{2} \ell(\ell+1) \tag{428}$$

On substituting Equations (427) and (428) into Equations (203) and (204), one finds that

$$S(0) = S_1(0) = S_2(0) = \frac{1}{2} \sum_{n=1}^{\infty} (2n+1)(a_n + b_n) \tag{429}$$

The fact that there is only one $S(0)$ means that the extinction is independent of the state of polarization of the incident light.

The extinction cross section σ_e is defined as the ratio of the rate of dissipation of energy and the rate at which energy is incident on a unit cross sectional area of the particle. Van de Hulst[17] derived for the case of spherical particles the formula

$$\sigma_e = \frac{\lambda^2}{\pi} Re\left\{ S(0) \right\} \tag{430}$$

where Re denotes the real part. Thus,

$$\sigma_e = \frac{\lambda^2}{2\pi} \sum_{n=1}^{\infty} (2n+1) Re\left\{ a_n + b_n \right\} \tag{431}$$

The form of the function defining the intensity of the scattered light may be written

$$F(\theta,\phi) = |S_1(\theta)|^2 \cos^2\phi + |S_2(\theta)|^2 \sin^2\phi \tag{432}$$

Van de Hulst gives[17] for the general case

$$\sigma_s = \frac{\lambda^2}{4\pi^2} \int_0^{2\pi}\int_0^{\pi} F(\theta,\phi) \sin\theta \, d\theta \, d\phi \tag{433}$$

so using Equation (424) one gets

$$\sigma_s = \frac{\lambda^2}{4\pi} \int_0^\pi \left(|S_1(\theta)|^2 + |S_2(\theta)|^2 \right) \sin\theta \, d\theta \qquad (434)$$

The conversion of this result into an expression containing the Mie coefficients is not very simple. Since S_1 and S_2 are in the form of infinite series, their squares are in the form of doubly infinite series. However, when the expression is integrated over θ, most terms in the double series are zero because of the orthogonality relations of the $P_n^{(1)}$. This problem has been investigated by Debye[27]. The result is

$$\sigma_s = \frac{\lambda^2}{2\pi} \sum_{n=1}^{\infty} (2n+1)\left(|a_n|^2 + |b_n|^2 \right) \qquad (435)$$

The absorption cross section is now given by

$$\sigma_a = \sigma_e - \sigma_s \qquad (436)$$

Krascella[12] has used these Mie equations to calculate the effect of particle size, wavelength, and particle temperature on particle opacity in those regions of the ultraviolet, visible, and infrared spectra for which complex index of refraction information was available.

One may write these cross section equations in terms of the non-dimensional size parameter q, defined by

$$q = \frac{2\pi a}{\lambda} \qquad (437)$$

and Equations (431) and (435) become

$$\sigma_e = \frac{2\pi a^2}{g^2} \sum_{n=1}^{\infty} (2n+1) \, Re\{a_n + b_n\} \tag{439}$$

$$\sigma_s = \frac{2\pi a^2}{g^2} \sum_{n=1}^{\infty} (2n+1)\left(|a_n|^2 + |b_n|^2\right) \tag{440}$$

where a_n and b_n are the Mie coefficients given by Equations (420) and (421). These equations are difficult to use in this form, and extensive tables of spherical Bessel functions with complex arguments are not available[12]. Aden[23], however, has developed a transformation called the Logarithmic Derivative Method which can be used to transform Equations (420) and (421) into a more useful form. The transformed equations were used by Krascella to develop a machine program which would allow calculation of σ_e, σ_s, and σ_a in cm^2/particle as a function of material, wavelength, and particle radius. The opacity parameters, or macroscopic cross sections, b_e, b_s, and b_a were also calculated in cm^2/gm from

$$b_e = \frac{\sigma_e}{\rho V} \tag{441}$$

$$b_s = \frac{\sigma_s}{\rho V} \tag{442}$$

$$b_a = \frac{\sigma_a}{\rho V} \tag{443}$$

where ρ is the mass density of the particle and V is the volume of the

spherical particle of radius a. Their results for carbon, which are taken directly from reference 12, are presented in Figures 21 and 22.

One may make use of these results for smaller particles and wavelengths by remembering that if the particle radius a and wavelength λ are both decreased by a factor X, then the macroscopic cross section is increased by X. Since the Mie coefficients are defined in terms of $q = 2\pi \cdot a/\lambda$, they are not affected by multiplying both a and λ by the same factor. Thus, the cross section per particle, given by Equations (438) and (439), would be decreased by X^2. But since the volume of the particle decreases by X^3, the macroscopic cross sections, given by Equations (440), (441), and (442) are increased by X when the particle radius and wavelength are both reduced by X. The graphs given in reference 12 are modified therefore to obtain values more applicable to the nuclear rocket problem.

Figure 23 indicates that for carbon particles of about 0.01 microns radius, scattering is negligible for wavelengths above 1000 Å.
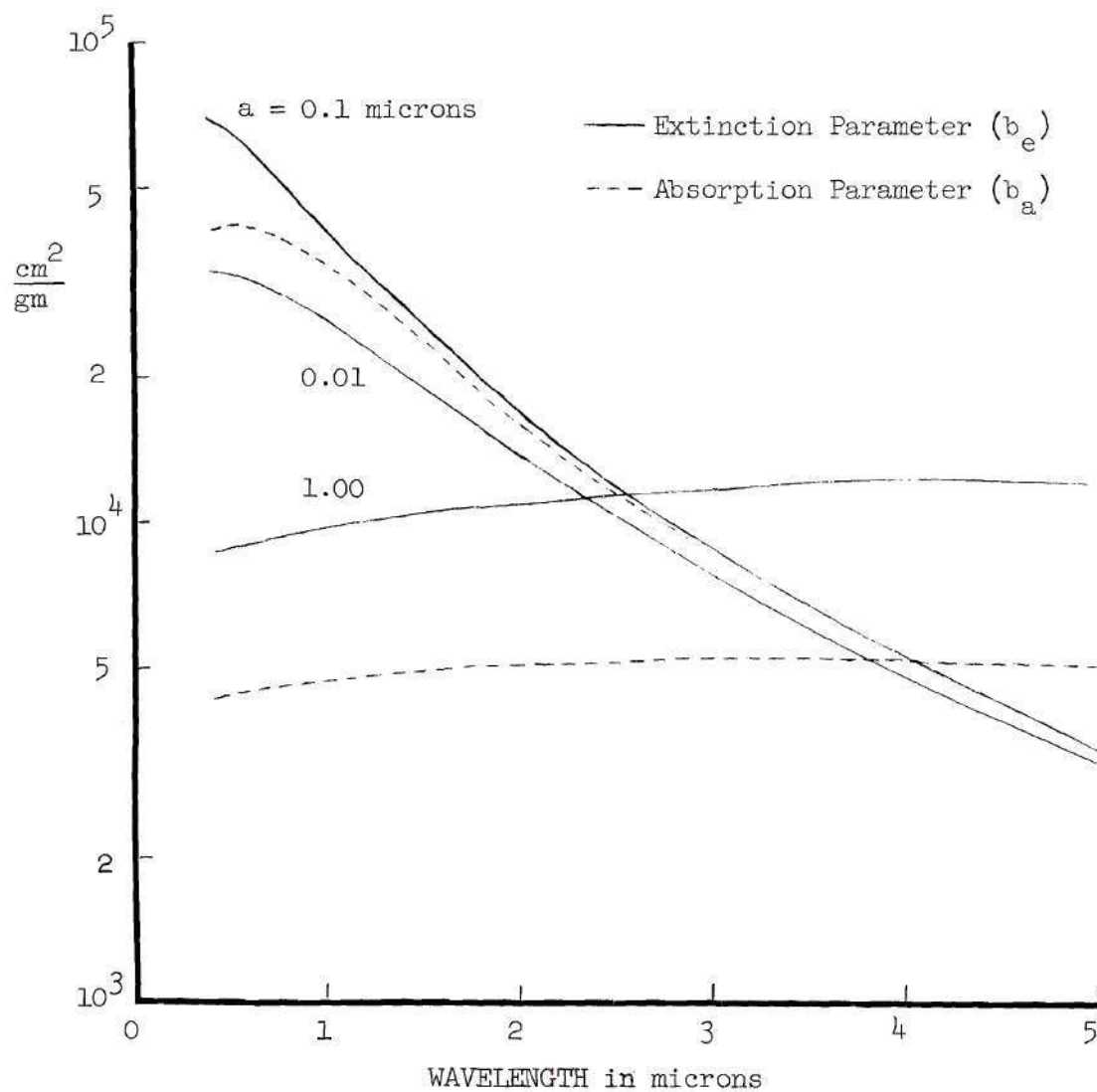
Figure 21. Extinction and Absorption Parameters as a Function of Wavelength-Mie Theory Calculation
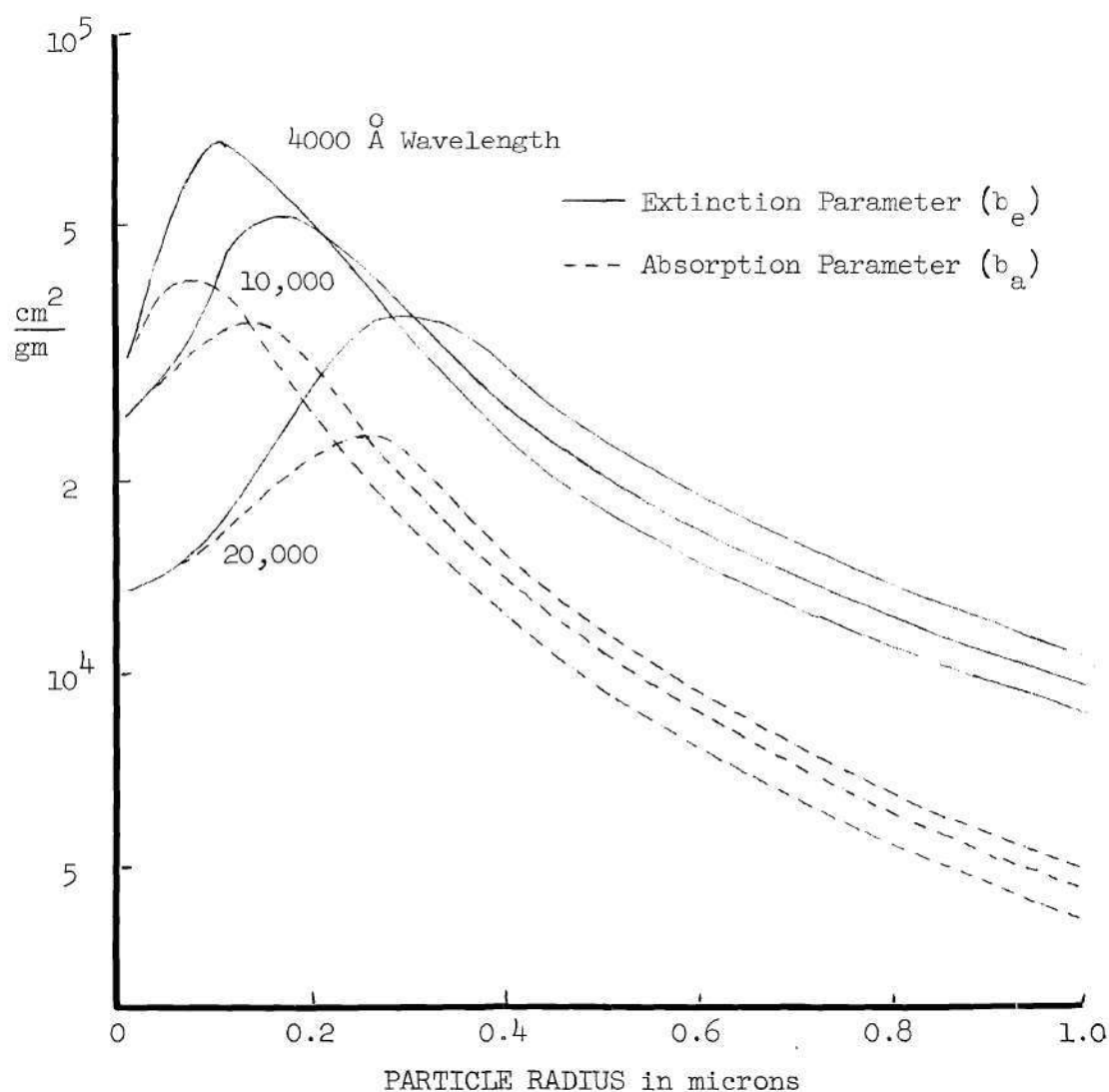
Figure 22. Mass Absorption Coefficient (Absorption Parameter) as a Function of Particle Radius for Spherical Particles - Mie Theory Calculation
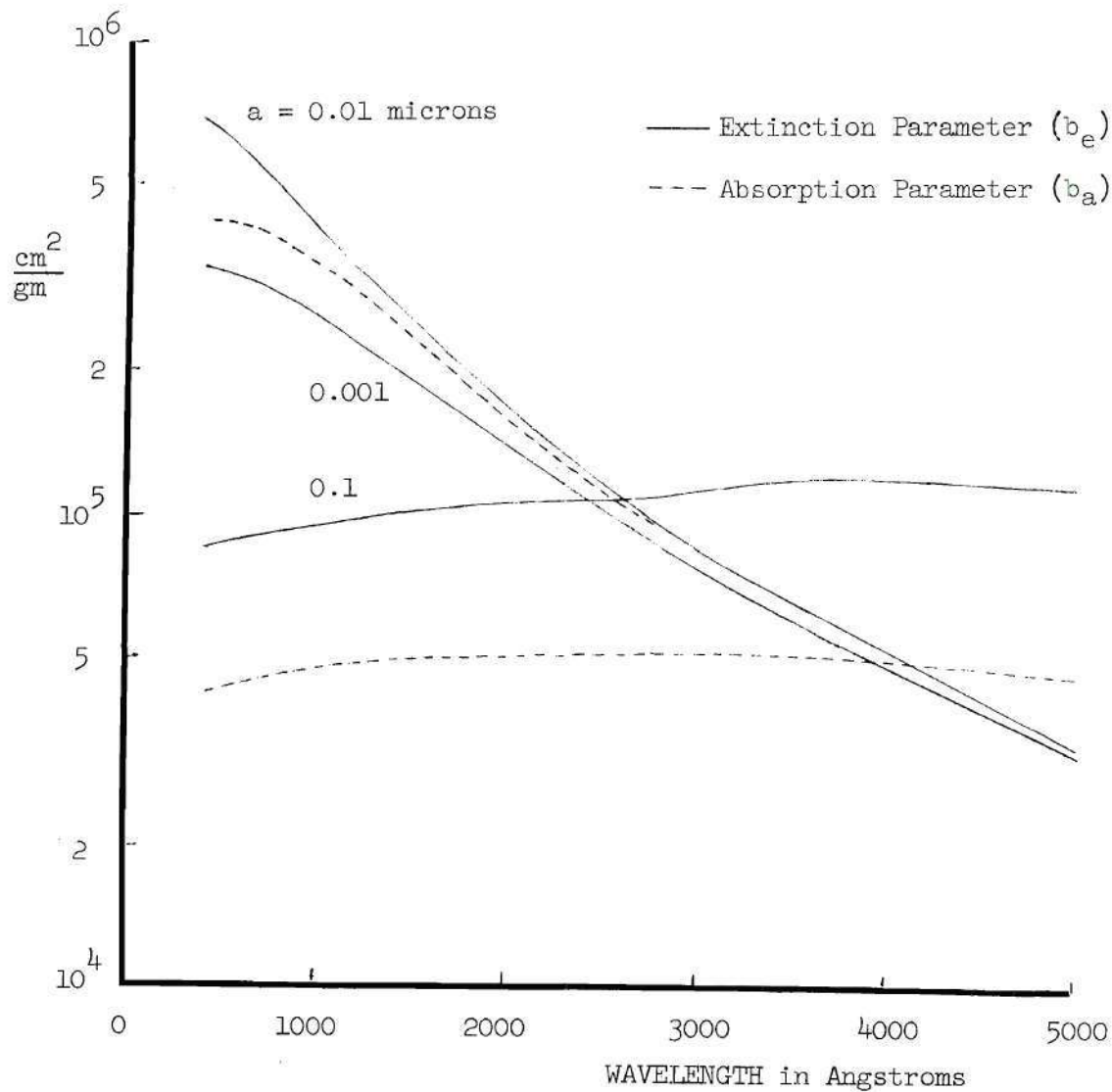
Figure 23. Mass Absorption Coefficient (Absorption Parameter)
as a Function of Wavelength in the Ultraviolet for
Spherical Particles - Mie Theory Calculation

APPENDIX B

EXPERIMENTAL PROCEDURE

The experimental procedure for a single run in which data was taken is outlined below. A "run" involved taking attenuation data at a single temperature for a series of wavelengths. This involved the following operations.

1. Turn on coolant water to capillary discharge light source and inspect the outlet to be sure that the coolant flow is properly established.

2. Turn on coolant water to water jacket.

3. Turn on the cooling fan for the capillary discharge light source.

4. Turn on the spectrometer pressure gauge and set the "current set" on 130.

5. Watch to see that the pressure gauge indicates a pressure in the spectrometer below ten microns of mercury. A higher pressure would indicate a leak.

6. Turn on the gas for the capillary (hydrogen or helium).

7. Increase the gas pressure in the spectrometer to somewhere between 500 and 1000 microns to flush out the spectrometer. Maintain this pressure for about five minutes.

8. Turn on the AC power on the spectrometer power supply. The DC power should not be turned on for a few minutes after the AC is turned on.

9. Turn on the AC power on the photomultiplier power supply.

10. Turn on the Keithley micro-microammeter.

11. Turn on the Keithley millivolt meter.

Note: Operations one through three established the flows necessary
to prevent over-heating of certain components, operations
four through seven flush out the spectrometer, and operations
eight through eleven allow the electronics to warm up before
use.

12. Position the filter intake over the exhaust chimney.

13. Switch the heater power from the other set of equipment to this
equipment.

14. Insert the shorting bar between the copper leads. When the power
is initially turned on, a power surge results which may damage the heating
filament if it is not dissipated by the shorting bar.

15. Reduce the pressure in the spectrometer to the desired level
(usually 200 or 300 microns) by decreasing the gas flow into the capillary.
The gas flow is controlled by a micrometer valve.

16. Turn on the DC power on the spectrometer power supply.

17. Adjust the variac on the spectrometer power supply (i.e., in-
crease the voltage to the capillary) until the discharge tube is ignited.
Then continue to increase the voltage until the current to the capillary
is 300 milliamps.

18. Turn on the DC power to the photomultiplier tube.

19. Raise the DC voltage to 1200 volts.

Note: Operations fifteen through nineteen have started up the
spectrometer and detection systems. Now the spectrum may be
scanned by observing the photomultiplier signal as the wave-
length dial is turned. This is done to locate the peaks in
the spectrum so these wavelengths may be turned to when data
is taken. Thus, the wavelengths observed when taking data
are those wavelengths of greatest intensity. Before this
scan is made, however, the spectrometer and photomultiplier
should warm up.

20. Observe the photomultiplier signal at a representative wave-
length, such as the white point, to be sure that the source and detector

are operating and that nothing is obstructing the light path.

21. Fill the aerosol generating flask with carbon black to several inches below the neck.

22. Connect the aerosol generator tubing to bypass the generator flask.

23. Fill the reservoir jug (jug B, Figure 9) of the sampling apparatus with water to several inches below the neck.

24. Insert stoppers and tubing into the jugs.

25. Insert a filter into the filter holder.

26. Tape the filter holder to insure vacuum tightness.

27. Inspect all the connections of the sampling apparatus to insure vacuum tightness. Apply vacuum grease as needed.

28. Scan the spectrum to determine the desired wavelengths (i.e., scale settings) to take data.

29. Turn on the master switch on the heater power supply control panel.

30. Turn on the filter for the exhaust gas (a vacuum cleaner was used part of the time).

31. Turn on the "window gas" flow.

32. Turn on the nitrogen coolant and adjust to the desired flow rate.

33. Turn on the aerosol generator gas. No aerosol is generated because the generator is in the bypass configuration (operation 22). Adjust the flow rate to the desired value.

34. Place a planchet on the exhaust chimney to decrease the size of the opening at the top. This makes for a smoother flow inside the furnace

and prevents oxygen from diffusing down the exhaust chimney. Without the planchet partially covering the chimney, oxygen diffusion down the chimney prevents data from being taken in the vacuum ultraviolet.

35. Turn on the heater power supply.

36. Turn on the reactor power.

37. Turn on the control panel power.

38. Be sure that the powerstat is set on zero.

39. Pull out the shorting bar.

40. Raise the powerstat to the desired setting.

41. Observe the heating filament through the chimney to see that it is heating.

42. Wait a few minutes until the millivolt meter indicates that temperature equilibrium is about established. During this time record on the data sheet the operating conditions, including the spectrometer gas and pressure, capillary current, photomultiplier voltage, powerstat setting, tank pressures, thermocouple voltage, and the location of the white point and a known spectrum line.

43. Turn the wavelength dial to the pre-established settings and record the micro-microammeter readings. Also, each time a reading is recorded for a particular dial setting, the dial is turned back to a black part of the spectrum and a background reading recorded. This background results from light reaching the photomultiplier from the hot observation chamber. With a thermocouple reading of $1500^{\circ}F$, the observation chamber glows bright red.

44. Set the dial at the chosen reference wavelength. This is a wavelength corresponding to a flat peak in the spectrum which can be turned

back to easily.

45. Again record the thermocouple voltage. It should have changed very little since operation 42.

46. Turn on the chart recorder.

47. Turn off the feeder gas at the tank, not at the pressure regulator, so that when it is turned back on at the tank the flow will be the same.

48. Connect the generating flask so that the aerosol generator now produces an aerosol when the gas is flowing.

49. Turn the gas back on at the tank.

50. Observe the chimney exhaust and the chart recorder to see that the aerosol is produced and recorded properly.

51. If necessary, readjust the "window gas" flow until the chart recorder is properly indicating a steady aerosol. Also the height of the nozzle in the generating flask may need adjustment to produce the desired concentration.

52. Again record data as in operation 43, but in addition, each time a reading is taken at a particular wavelength, the dial is immediately turned to the reference wavelength and the reading recorded. The observation of the reference wavelength allows one to monitor any changes which might occur in the aerosol concentration during a run, and to correct these changes. Also, when about half the data is taken pull a sample of the aerosol in the manner described in Chapter II.

53. Record the thermocouple voltage again.

54. Turn off the aerosol generator gas at the tank,

55. Reconnect the aerosol generator in the bypass configuration.

56. Turn on the aerosol generator gas again.

57. Reset the wavelength dial at the reference line.

58. Observe the chart recorder and exhaust until there is no seed in the exhaust. The signal from the reference line should have the same value it had in operation 43.

59. Turn off the chart recorder.

60. Repeat operation 43.

61. Record the thermocouple voltage. It should not have been changed since operation 43.

62. Record the operating conditions again (operation 42).

63. Turn off the power supply, the control panel power, and the reactor power in that order.

64. Set the powerstat on zero.

65. Reduce the capillary voltage to zero.

66. In the following order, turn off the capillary DC power, the capillary AC power, the photomultiplier DC power, the photomultiplier AC power, the micro-microammeter, the millivolt meter, the coolant gas, the aerosol generator gas, the capillary gas, the "window gas," and the exhaust filter.

67. Measure and record the displaced water in the sampling setup.

68. Remove the filter and put it in a protective container.

69. Check the pressure gauge to be sure it is down to about ten microns again.

70. Turn off the pressure gauge, the fan, the coolant water for the capillary, and the coolant water to the jacket.

71. Weigh the filter on an electronic balance. Also weigh a clean

filter for the next run.

APPENDIX C

DATA

The following data listed in Tables 2 through 16 represent the best runs, and are believed by the author to accurately describe the attenuation of radiant energy in a cloud of carbon particles over a wavelength range from 1100 Å to 8000 Å at room temperature, and over a more limited wavelength range at higher temperatures.

Data taken from runs not listed were discarded for one of the following reasons.

1. The aerosol generator ran out of carbon black or behaved irregularly during the run.

2. The intensity of the light from the capillary discharge tube varied during the run. This occurred occasionally only when the capillary was operated with hydrogen but without an entrance slit. Hence the data from these runs were discarded.

3. The intensity of the signal without particles, I_o, was significantly different at the end of the run from its value at the beginning of the run. This indicated a change in the electronic amplification of the signal or accumulation of carbon on the end of the observation tube around the thermocouple shield.

4. In a few of the early high temperature runs, before the entrance slit was removed, the background signal became great enough to completely obscure the signal from the light beam, and the resulting data had to be

discarded.

Table 2.

Scale	I_o	I	I'	$\dfrac{I_o}{I}$	$\dfrac{I'_o}{I'}$	$\dfrac{k}{k'}$	$\dfrac{k}{\rho_p}$
1630	3.4	.31	4.9	11.0	2.21	3.63	6.06
1590	.70	.04	5.0	16.5	2.16	3.64	7.28
1520	14.0	1.1	5.0	12.7	2.16	3.30	6.60
1443	.27	.12	5.0	2.25	2.16	1.05	2.1
1335	.98	.48	5.2	2.04	2.08	.97	1.94
1180	3.98	2.0	5.2	1.99	2.08	.94	1.88
1130	5.50	2.8	5.3	1.96	2.04	.96	1.92
960	10.8	5.3	5.3	2.04	2.04	1.00	2.0
865	20.1	10.3	5.3	1.95	2.04	.94	1.88
824	21.1	10.9	5.3	1.94	2.04	.93	1.86
780	18.6	9.3	5.3	2.00	2.04	.97	1.94
725	19.4	9.9	5.3	1.96	2.04	.95	1.9
682	19.4	9.3	5.3	2.04	2.04	1.00	2.0
590	16.8	8.0	5.3	2.10	2.04	1.04	2.08
515	46.	21.	5.3	2.19	2.04	1.10	2.2
340	7.3	4.0	5.3	1.83	2.04	.85	1.7
205	9.4	5.0	5.3	1.88	2.04	.89	1.78
20	10.5	5.0	5.3	2.10	2.04	1.04	2.08
9730	14.9	7.9	5.3	1.89	2.04	.89	1.78

Run No. 2   Temperature 63°F

Table 3.

| Run No. 6 | | | | | | Temperature 63°F. | |
Scale	I_o	I	I'	$\dfrac{I_o}{I}$	$\dfrac{I'_o}{I'}$	$\dfrac{k}{k'}$	$\dfrac{k}{\rho_p}$
1735	1.02	.16	.62	6.38	2.50	2.025	4.05
1725	1.83	.17	.64	10.76	2.42	2.69	5.38
1713	3.3	.22	.68	15.0	2.28	3.37	6.74
1700	4.7	.21	.64	22.4	2.42	3.52	7.04
1675	2.7	.085	.62	31.8	2.50	3.77	8.74
1662	1.7	.075	.65	22.7	2.38	3.51	7.02
1650	1.7	.076	.68	22.4	2.28	3.77	8.74
1615	2.65	.080	.72	33.1	2.15	4.57	9.14
1590	17.8	.079	.72	225.	2.15	7.09	14.18
1583	18.2	.080	.74	228.	2.09	7.37	14.74
1550	1.68	.125	.84	13.4	1.85	4.22	8.44
1450	1.42	.74	.80	1.92	1.94	.985	1.97
1400	1.55	.80	.80	1.94	1.94	1.00	2.00
1350	1.3	.61	.78	2.13	1.99	1.10	2.2
1250	3.25	1.35	.73	2.41	2.12	1.17	2.34
1150	13.7	6.2	.73	2.21	2.12	1.055	2.11
1050	42.0	17.	.70	2.47	2.22	1.13	2.26
1000	45.5	17.5	.70	2.60	2.22	1.19	2.38
900	47.2	19.	.68	2.48	2.28	1.10	2.20
800	41.0	17.	.66	2.41	2.35	1.03	2.06
700	32.5	14.	.68	2.32	2.28	1.02	2.04
400	8.1	3.9	.72	2.08	2.15	.957	1.94
200	16.2	7.5	.74	2.16	2.09	1.045	2.09
0	33.0	15.0	.75	2.2	2.07	1.08	2.16
9600	30.8	17.0	.85	1.81	1.83	.98	1.96

Table 4.

Run No. 7   Temperature 63°F

Scale	I_o	I	I'	$\dfrac{I_o}{I}$	$\dfrac{I'_o}{I'}$	$\dfrac{k}{\bar{k}}$	$\dfrac{k}{\rho_p}$
1735	1.02	.145	.74	7.04	2.09	2.65	5.30
1725	1.83	.15	.68	12.2	2.28	3.05	6.10
1713	3.3	.18	.74	18.3	2.09	3.94	7.88
1700	4.7	.17	.76	27.6	2.04	4.65	9.30
1675	2.7	.105	.76	25.7	2.04	4.56	9.12
1662	1.7	.084	.76	20.2	2.04	4.22	8.44
1650	1.7	.077	.77	22.1	2.01	4.44	8.88
1615	2.65	.079	.74	33.6	2.09	4.77	9.54
1590	17.8	.082	.68	217.	2.28	6.54	13.08
1583	18.2	.075	.68	243.	2.28	6.67	13.34
1550	1.68	.088	.68	19.1	2.28	3.59	7.18
1450	1.42	.63	.70	2.25	2.22	1.015	2.03
1400	1.55	.70	.70	2.22	2.22	1.00	2.00
1250	3.25	1.5	.78	2.16	1.99	1.12	2.24
1200	5.1	2.6	.80	1.96	1.94	1.01	2.02
1150	13.7	6.6	.82	2.08	1.89	1.15	2.3

Table 5.

Scale	I_o	I	I'	$\dfrac{I_o}{I}$	$\dfrac{I'_o}{I'}$	$\dfrac{k}{k'}$	$\dfrac{k}{\rho_p}$
Run No. 8						Temperature $63^{\circ}F$	
1750	1.00	.50	2.0	2.00	1.9	1.121	2.242
1727	3.30	1.7	2.0	1.94	1.9	1.031	2.062
1711	6.25	3.25	2.0	1.92	1.9	1.150	2.300
1660	3.6	1.95	2.05	1.85	1.89	.969	1.938
1625	3.3	2.05	2.2	1.64	1.72	.914	1.828
1590	35.0	22.	2.25	1.59	1.68	.896	1.792
1540	2.0	1.2	2.4	1.66	1.58	1.109	2.218
1490	1.8	1.25	2.45	1.45	1.55	.849	1.698
1450	3.1	2.1	2.5	1.47	1.52	.919	1.838
1400	3.7	2.5	2.55	1.48	1.49	.986	1.972
1350	2.8	2.05	2.6	1.39	1.48	.840	1.680
1300	4.2	1.5	1.4	2.80	2.71	.959	1.918
1250	8.0	2.6	1.35	3.08	2.81	1.070	2.140
1200	12.1	3.5	1.2	3.46	3.16	1.090	2.180
1150	20.	6.1	1.25	3.28	3.02	1.060	2.120
1105	47.	17.	1.3	2.76	2.92	.996	1.992
1095	64.	23.	1.3	2.78	2.92	.995	1.990
1030	36.	11.	1.3	3.28	2.92	1.110	2.220
935	52.	15.	1.3	3.46	2.92	1.180	2.360
900	52.	17.	1.3	3.06	2.92	1.070	2.140
700	38.	13.5	1.6	2.81	2.38	1.157	2.314
500	15.5	7.1	1.7	1.9	2.219	.986	1.972
200	21.5	111.	1.9	2.362	2.000	1.236	2.472
0	30.	14.	2.0	2.141	1.908	1.185	2.370
9800	38.	17.	1.95	2.239	1.952	1.195	1.390
9600	34.	15.	1.9	2.262	2.00	1.176	2.352

Table 6.

Run No. 9						Temperature 63°F	
Scale	I_o	I	I'	$\dfrac{I_o}{I}$	$\dfrac{I'_o}{I'}$	$\dfrac{k}{k'}$	$\dfrac{k}{\rho_p}$
1750	1.00	.54	1.9	1.851	2.0	.8902	1.7804
1727	3.30	1.5	1.9	2.195	2.0	1.131	2.262
1720	4.15	2.0	1.9	2.075	2.0	1.052	2.104
1711	6.25	2.9	2.0	2.155	1.9	1.199	2.298
1700	7.4	3.9	2.1	1.890	1.81	1.072	2.144
1690	6.5	4.1	2.2	1.565	1.725	.8840	1.7680
1680	4.9	2.6	2.0	1.865	1.9	.9740	1.9480
1660	3.6	1.9	2.0	1.885	1.725	.9880	1.9760
1625	3.3	1.9	2.8	1.770	1.585	1.048	2.096
1590	35.	21.	2.4	1.665	1.502	1.1025	2.2050
1540	2.0	1.4	2.5	1.430	1.460	.8825	1.7650
1450	3.1	2.2	2.6	1.409	1.490	.895	1.790
1400	3.7	2.4	2.55	1.540	1.502	1.104	2.208
1350	2.8	1.9	2.5	1.475	1.502	.962	1.924
1300	4.2	2.9	2.5	1.446	1.502	.900	1.800
1250	8.0	5.5	2.5	1.451	1.502	.9105	1.8210
1200	12.1	8.3	2.5	1.460	1.502	.0139	1.8278
1150	20.	13.	2.4	1.538	1.583	.9425	1.8850
1095	64.	45.	2.5	1.4400	1.520	.8720	1.7440
1030	36.	25.	2.6	1.440	1.460	.9640	1.9280
935	52.	39.	2.9	1.332	1.332	1.055	2.110
900	52.	4q.	2.8	1.300	1.355	.8625	1.7230
600	35.	25.	2.7	1.400	1.405	1.150	2.200
500	15.5	11.6	2.8	1.335	1.355	1.000	2.000
400	15.	11.	2.9	1.365	1.310	1.086	2.172
200	21.5	17.	3.0	1.265	1.265	1.052	2.104
9800	38.	31.	3.1	1.226	1.260	.8660	1.7320
9700	34.	29.	3.1	1.172	1.260	.8660	1.7320

Table 7.

| Run No. 26 | | | | | | Temperature 63°F | |
Scale	I_o	I	I'	$\dfrac{I_o}{I}$	$\dfrac{I'_o}{I'}$	$\dfrac{k}{k'}$	$\dfrac{k}{\rho_p}$
1083	9.7	.14	.63	69.25	73.0	.986	1.97
956	5.25	.09	.63	58.3	73.0	.948	1.9
867	230.0	3.3	.68	67.7	67.6	1.045	2.09
826	36.5	.53	.78	68.9	59.1	1.039	2.08
791	11.	.22	.73	50.0	63.0	.945	1.89
685	130.	1.8	.63	72.25	73.0	.990	1.98
607	46.	.63	.63	73.0	73.0	1.000	2.00
544	53.	.68	.63	56.9	73.0	.9425	1.89
514	73.	.88	.63	83.0	73.0	1.029	2.06
250	54.	.48	.63	112.0	73.0	1.105	2.21
91	11.5	.11	.63	104.5	73.0	1.095	2.2

Table 8.

Run No. 10						Temperature $500^{\circ}F$	
Scale	I_o	I	I'	$\dfrac{I_o}{I}$	$\dfrac{I'_o}{I'}$	$\dfrac{k}{k'}$	$\dfrac{k}{\rho_p}$
1400	.49	0.24	.24	2.210	2.04	1.045	2.08
1260	1.10	0.42	.20	2.620	2.45	1.072	2.14
1090	9.0	1.4	.20	6.420	2.450	----	----
1035	6.0	1.9	.19	3.145	2.578	1.189	2.38
945	8.5	2.9	.19	2.925	2.578	1.162	2.32
700	6.25	2.3	.19	2.715	2.450	1.125	2.25
400	2.25	.77	.20	2.970	2.450	1.215	2.43
200	3.45	1.15	.20	3.000	2.450	1.222	2.44
0	4.75	1.55	.20	3.070	2.450	1.251	2.50
9800	5.95	2.0	.20	2.980	2.450	1.219	2.44

Table 9.

Run No. 27							Temperature 500°F
Scale	I_o	I	I'	$\dfrac{I_o}{I}$	$\dfrac{I'_o}{I'}$	$\dfrac{k}{k'}$	$\dfrac{k}{\rho_p}$
867	180.	73.	15.5	2.465	2.385	1.056	2.1
826	29.	14.5	17.	2.00	2.18	.892	1.78
791	9.7	4.7	16.	2.06	2.31	.864	1.73
607	37.	16.	16.	2.31	2.31	1.	2.0
544	43.	22.	16.	2.28	2.31	.984	1.97
250	43.5	20.	16.	2.175	2.31	.927	1.86
9980	1.21	.48	15.	2.52	2.462	.9002	1.022

Table 10.

Run No. 11						Temperature 700°F	
Scale	I_o	$\bar{I}$	$\bar{I}'$	$\dfrac{I_o}{\bar{I}}$	$\dfrac{I_o'}{\bar{I}'}$	$\dfrac{k}{k'}$	$\dfrac{k}{\rho_p}$
1350	.345	---	---	---	---	---	---
1200	1.23	.102	1.7	1.205	7.117	.920	1.84
1100	10.4	1.3	1.7	8.01	7.117	1.061	2.12
1000	12.1	1.7	1.7	7.12	7.117	1.00	2.0
900	11.6	2.6	1.7	6.83	7.117	.981	1.96
800	10.4	2.4	1.7	4.34	7.117	.749	1.5
700	8.0	2.0	1.7	4.00	7.117	.706	1.41
600	5.5	1.05	1.7	5.23	7.117	.845	1.69
500	2.7	.62	1.7	4.345	7.117	.750	1.5
400	1.7	.42	1.7	4.055	7.117	.713	1.43
200	4.1	.68	1.7	6.025	7.117	.916	1.83
0	7.3	1.35	1.7	5.405	7.117	.860	1.72

Table 11.

| Run No. 12 | | | | | | Temperature 750°F | |
Scale	I_o	I	I'	$\dfrac{I_o}{I}$	$\dfrac{I'_o}{I'}$	$\dfrac{k}{k_r}$	$\dfrac{k}{\rho_p}$
1650	.045	.015	.3?	2.81	5.64	.771	1.542
1585	.41	.10	.35	4.1	6.29	.77	1.54
1275	.077	.017	.38	4.03	5.79	.794	1.588
1200	.13	.030	.47	4.34	4.68	.950	1.900
1100	1.7	.39	.49	4.36	4.48	.984	1.969
900	3.45	.81	.51	4.26	4.315	1.20	2.40
800	3.3	.76	.51	4.34	4.315	1.05	2.10
700	.27	.063	.52	4.29	4.23	1.01	2.02
600	.15	.035	.52	4.28	4.23	1.03	2.18
500	.79	.17	.52	4.64	4.23	1.06	2.12
400	.51	.13	.52	3.92	4.23	.9625	1.924
300	.525	.14	.55	3.75	4.00	.940	1.880
200	.77	.21	.55	3.67	4.00	.940	1.880
0	1.45	.35	.55	3.86	4.00	.960	1.920

Table 12.

Run No. 15   Temperature 900°F

Scale	I_o	I	I'	$\dfrac{I_o}{I}$	$\dfrac{I'_o}{I}$	$\dfrac{k'}{k}$	$\dfrac{k}{\rho_p}$
1450	.070	.026	1.3	2.695	3.145	1.145	2.290
1200	.245	.084	1.4	2.92	2.9245	1.000	2.000
1150	.91	.29	1.45	3.12	2.822	1.093	2.186
1000	4.1	1.6	1.65	2.561	2.481	1.036	2.072
950	4.6	1.7	1.65	2.71	2.481	1.099	2.198
900	4.2	1.7	1.7	2.47	2.41	1.026	2.052
850	3.7	1.5	1.7	2.465	2.41	1.024	2.048
800	3.85	1.5	1.7	2.565	2.41	1.071	2.142
750	3.15	1.5	1.8	2.1	2.275	.901	1.802
700	3.3	1.4	1.8	2.348	2.275	1.036	2.072
650	2.75	1.3	1.8	2.115	2.275	.910	1.820
600	1.60	.75	1.8	2.126	2.275	.915	1.882
579	5.95	3.1	2.0	1.920	2.0045	.941	1.992
550	1.7	1.0	.21	1.7	1.900	.855	1.710
200	1.16	.57	.18	2.019	2.275	.851	1.702
0	2.67	1.2	1.8	2.222	2.275	.970	1.940
9800	2.65	1.1	1.8	2.41	2.275	1.071	2.210

Table 13.

Run No. 31						Temperature	$1400°F$
Scale	I_o	I	I'	$\dfrac{I_o}{I}$	$\dfrac{I'_o}{I'}$	$\dfrac{k}{k'}$	$\dfrac{k}{\rho_p}$
1160	.28	.04	6.3	7.00	8.73	.896	1.792
1088	11.	1.5	6.7	7.34	8.21	.945	1.890
1030	1.6	.25	6.9	6.40	7.96	.896	1.792
961	5.8	1.09	8.4	5.32	6.55	.911	1.822
870	310.	39.	8.0	7.95	6.88	1.041	2.082
795	14.	3.5	13.8	4.00	3.98	1.02	2.04
688	175.	48.	16.	3.64	3.44	1.045	2.090
611	55.	17.	16.	3.24	3.44	.954	1.908
543	68.	19.5	16.5	3.49	3.38	1.027	2.054
517	91.	25.4	15.4	3.58	3.57	1.001	2.002
95	16.	3.8	13.3	4.21	4.14	1.09	2.18
9985	1.8	.35	12.6	5.15	4.37	1.12	2.24
9835	5.2	1.0	11.	5.20	5.00	1.102	2.204
9770	3.1	.05	10.5	6.20	5.25	1.105	2.210

Table 14.

Run No. 32   Temperature 1500°F

Scale	I_o	I	I'	$\dfrac{I_o}{I}$	$\dfrac{I'_o}{I'}$	$\dfrac{k}{k'}$	$\dfrac{k}{\rho_p}$
1088	6.5	2.5	12.	2.6	2.75	.944	1.888
961	3.4	1.1	11.	3.09	3.00	1.026	2.052
795	9.	3.	11.	3.00	3.00	.999	1.998
688	111.	33.	11.	3.36	3.00	1.105	2.210
611	33.	11.	11.	3.00	3.00	.999	1.998
543	41.	12.	11.	3.42	3.00	1.12	2.24
517	52.	16.	10.	3.25	3.3	.986	1.972
252	40.	11.7	10.	3.419	3.3	1.065	2.130
9935	2.5	.9	12.	2.78	2.75	1.1	2.2

Table 15.

| Run No. 33 | | | | | | Temperature 1500°F | |
Scale	I_o	I	I'	$\dfrac{I_o}{I}$	$\dfrac{I'_o}{I'}$	$\dfrac{k}{k'}$	$\dfrac{k}{\rho_p}$
960	3.9	1.4	13.	2.789	2.69	1.035	2.070
868	190.	56.	12.	3.399	2.91	1.15	2.30
830	29.	11.5	14.	2.52	2.49	1.013	2.026
794	8.4	3.5	15.	2.40	2.33	1.034	2.068
685	120.	46.	15.	2.61	2.33	1.130	2.260
611	35.	15.7	15.	2.22	2.33	.942	1.884
544	45.	19.	15.	2.37	2.33	.972	1.944
518	58.	26.	15.	2.23	2.33	.948	1.896
9985	1.05	.5	15.	2.1	2.33	.876	1.752
9836	3.02	1.3	15.	2.31	2.33	.989	1.978
9770	1.7	.7	15.	2.43	2.33	1.048	2.096

Table No. 16

Run No. 35						Temperature 1525 $^{\circ}$F	
Scale	I_o	I	I'	$\dfrac{I_o}{I}$	$\dfrac{I_o'}{I'}$	$\dfrac{k}{k'}$	k
1084	21	3.6	14.5	5.84	6.28	0.973	1.95
958	12.2	1.7	12	7.19	7.58	0.973	1.95
834	77	13	16	5.91	5.69	1.021	2.04
792	23	4.5	17	5.56	5.35	1.024	2.05
686	305	48	17	6.35	5.35	1.100	2.2
611	91	16	16	5.69	5.69	1.000	2.0
545	115	21	16	5.49	5.69	0.983	1.97
519	150	28	17	5.36	5.35	1.005	2.0
9842	8.7	3	25	2.89	3.64	0.882	1.76

APPENDIX D

EQUIPMENT DRAWINGS AND PHOTOGRAPHS
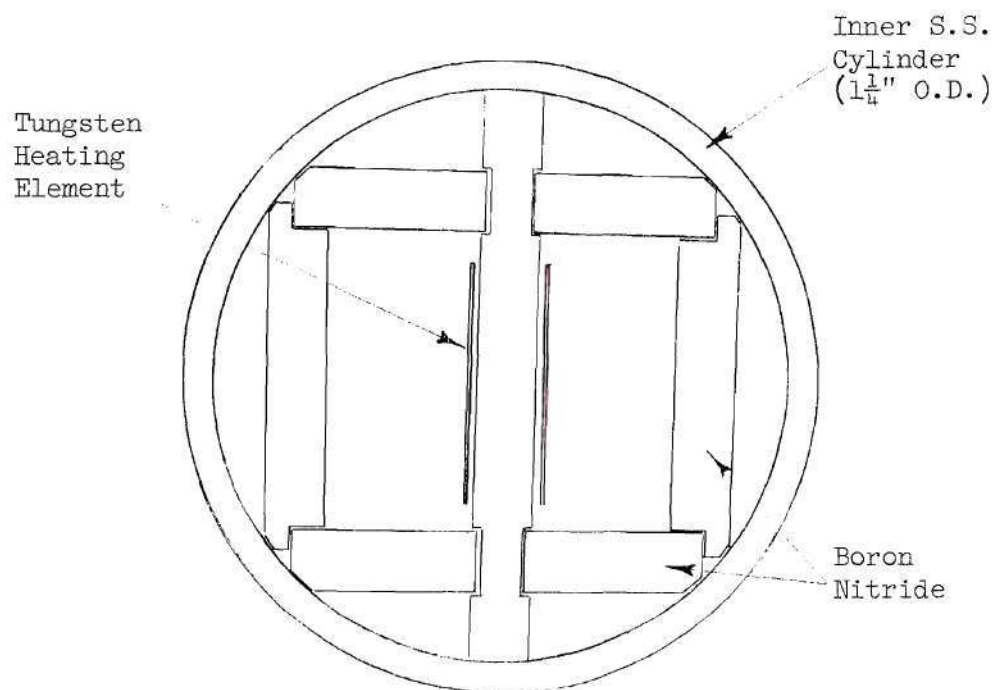
Figure 24. Heating Chamber Cross Section
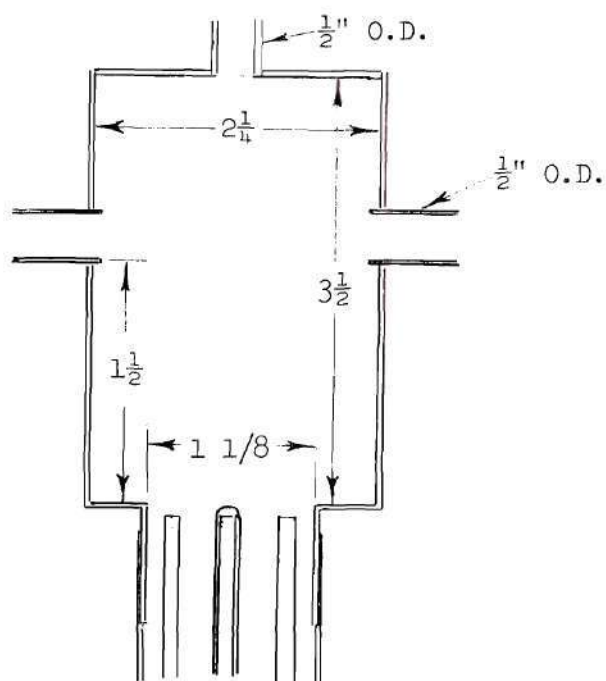
Figure 25. Observation Chamber ($\frac{1}{2}$ scale)
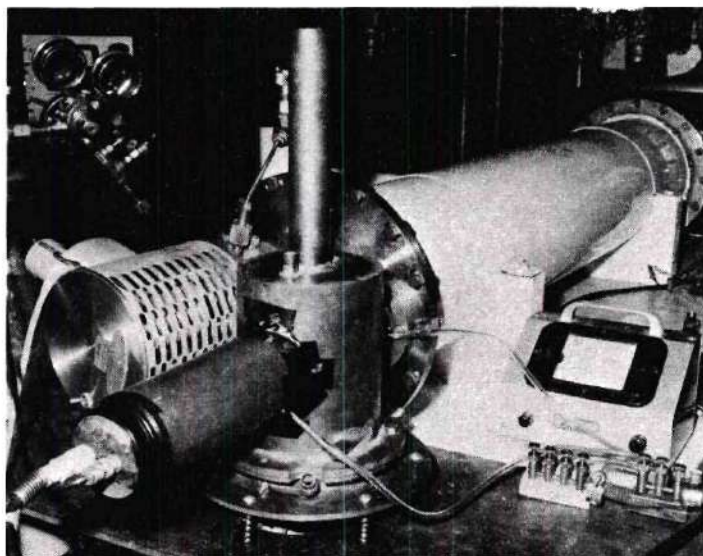
Figure 27. Spectrometer with Furnace
and Photomultiplier Attached

Figure 28.   Micromicroammeter,
Millivoltmeter and
Wavelength Dial

Figure 26.
Furnace Components
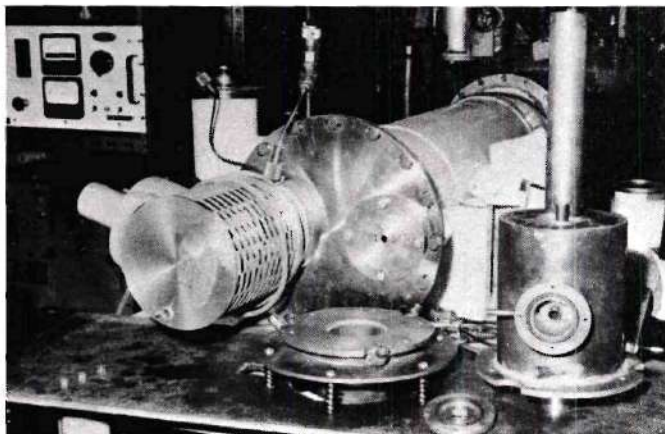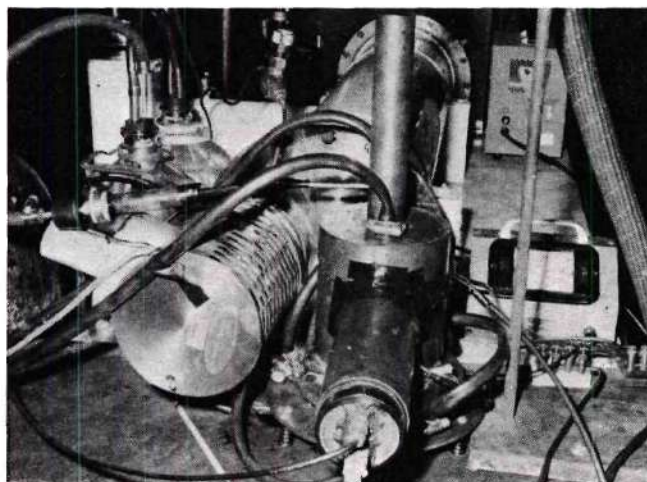
Figure 29.
Furnace Prior
to Assembly
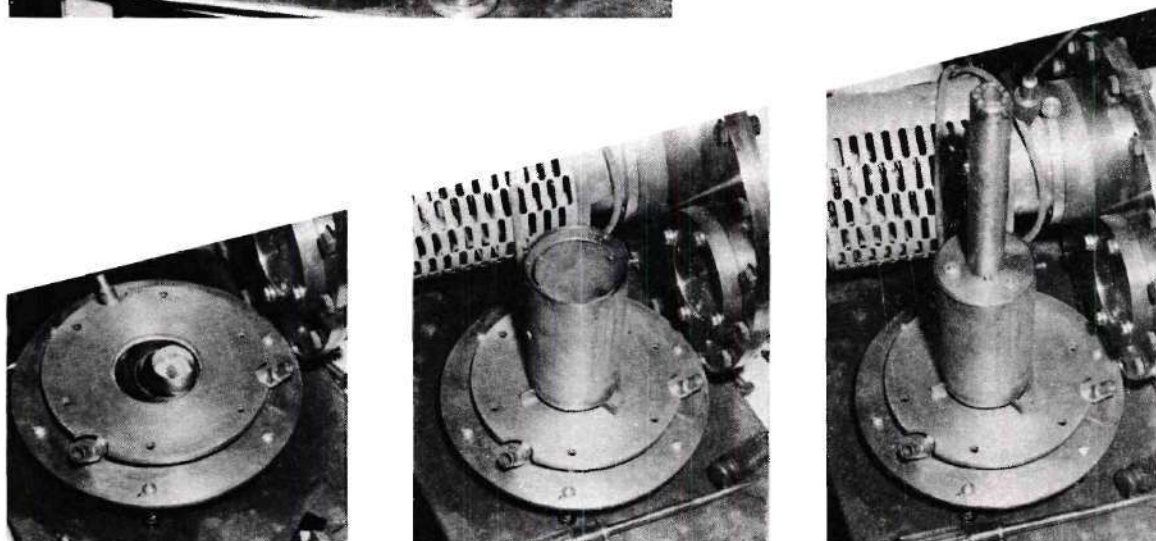
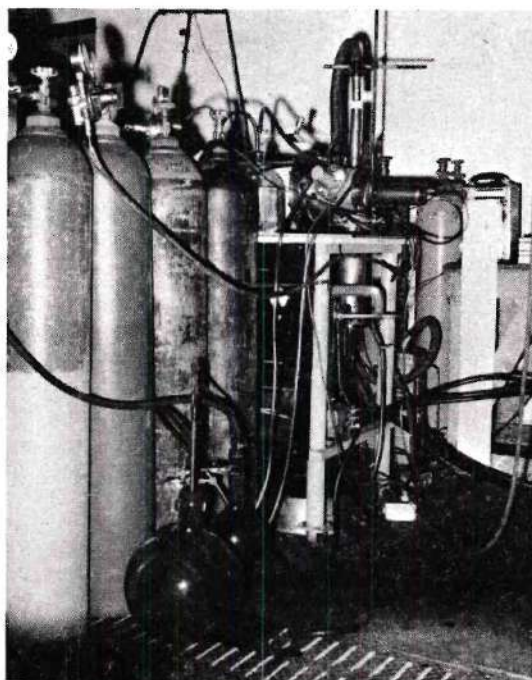Figure 30. Furnace Assembly Procedure

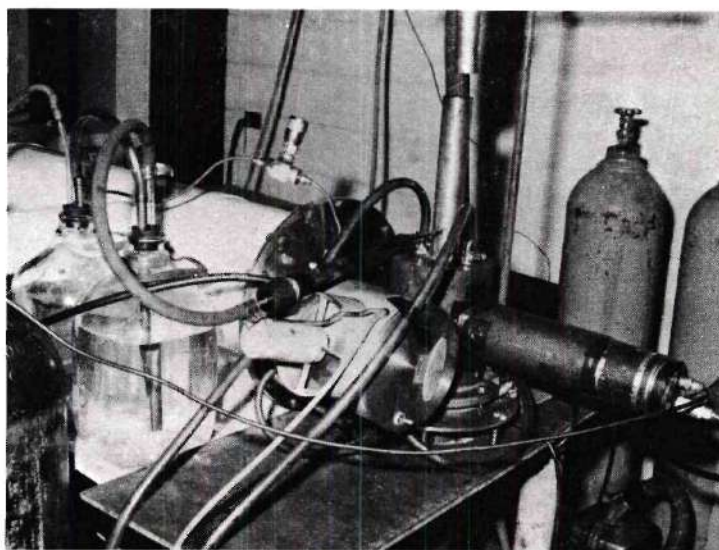Figure 31.
Furnace After
Assembly

Figure 32. Aerosol Generator

Figure 33. Sampling Apparatus

APPENDIX E

SOURCE SPECTRA

The following graphs show the spectra that were used as a source of light through the aerosol. Figures 34 and 35 present the hydrogen spectra when the entrance slit is in place. Figures 36 and 37 represent the hydrogen and helium spectra without the entrance slit.
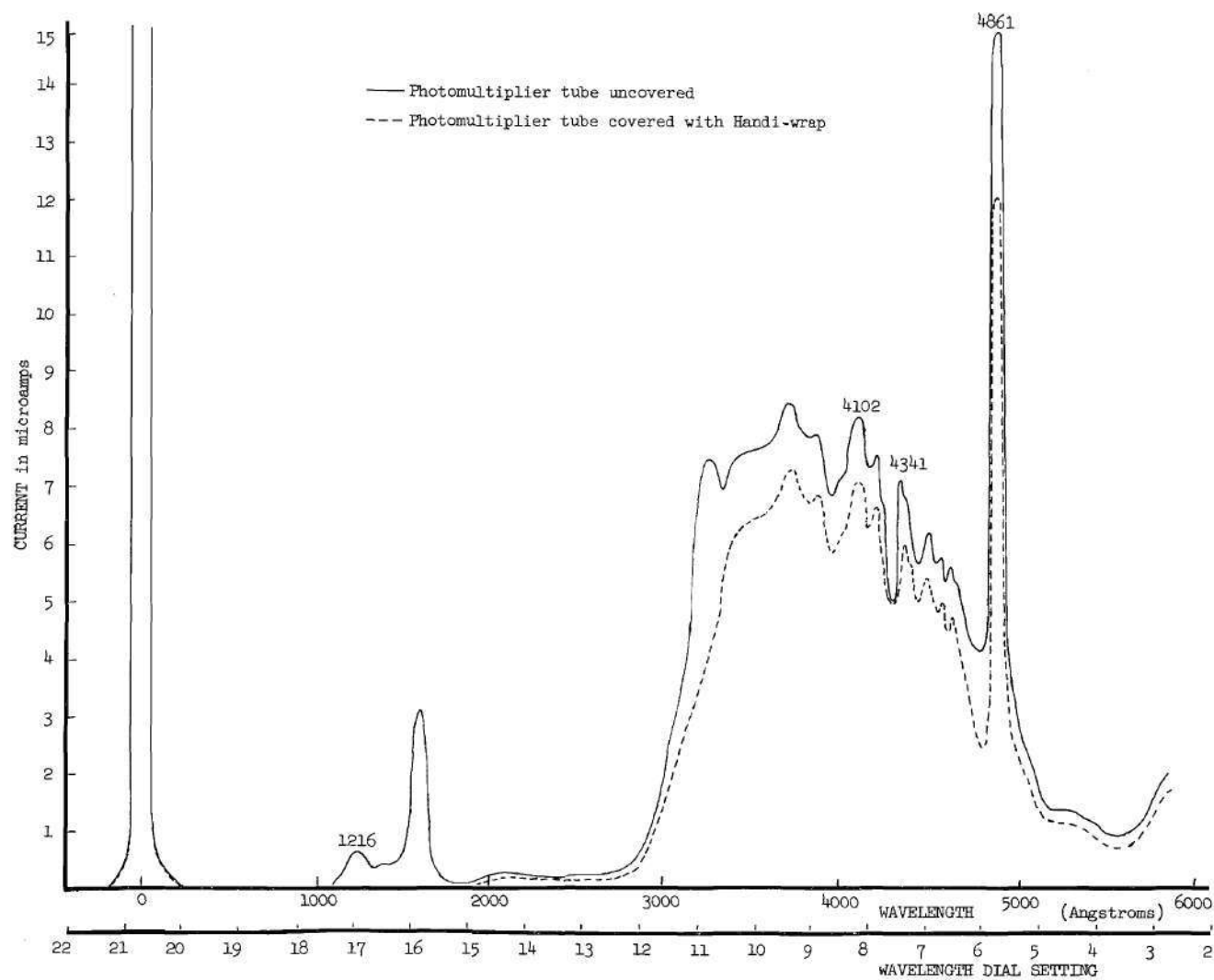
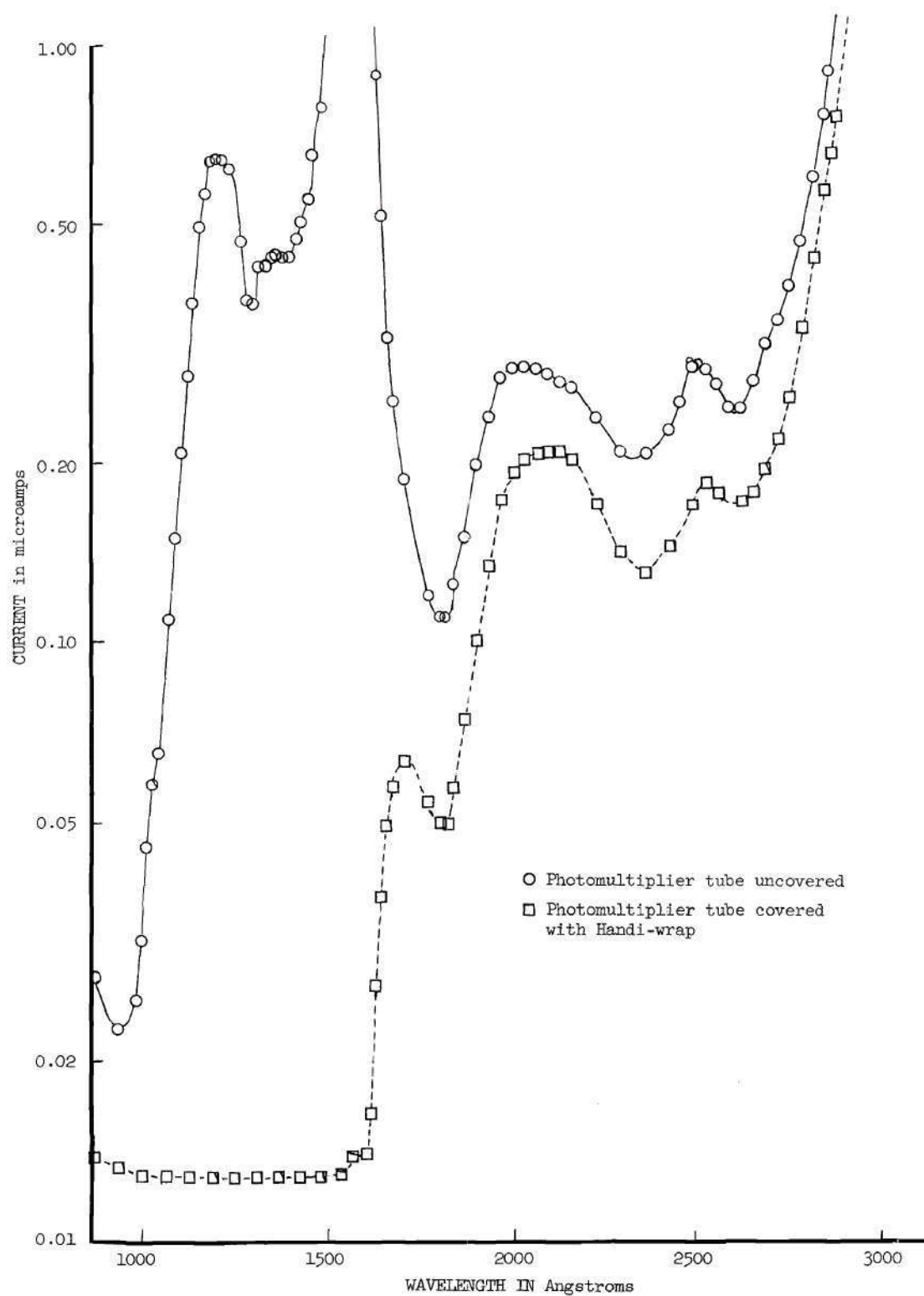Figure 34.   Source Spectrum of Hydrogen With Entrance Slit

Figure 35. Source Spectrum of Hydrogen with Entrance Slit in the Ultraviolet Region
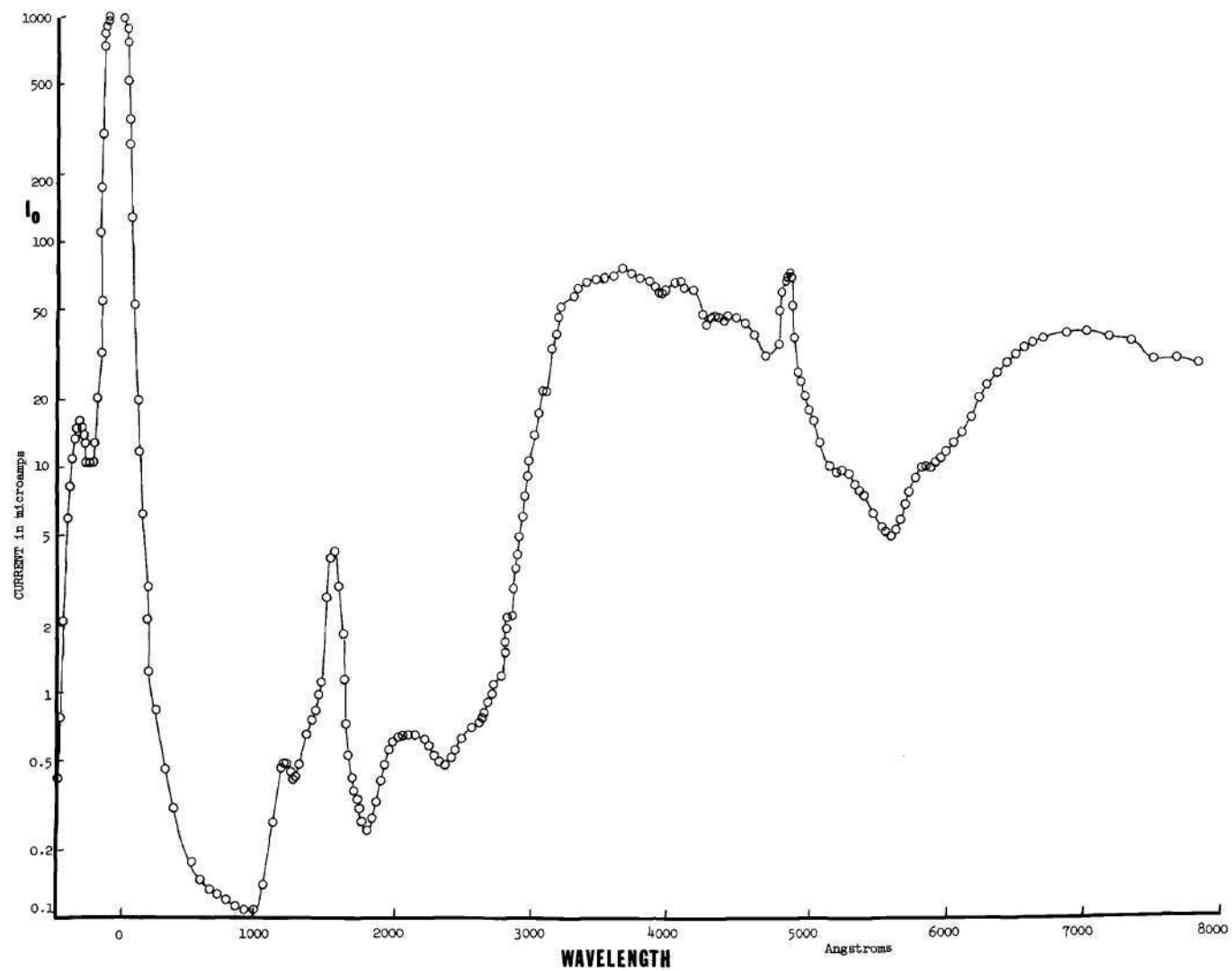
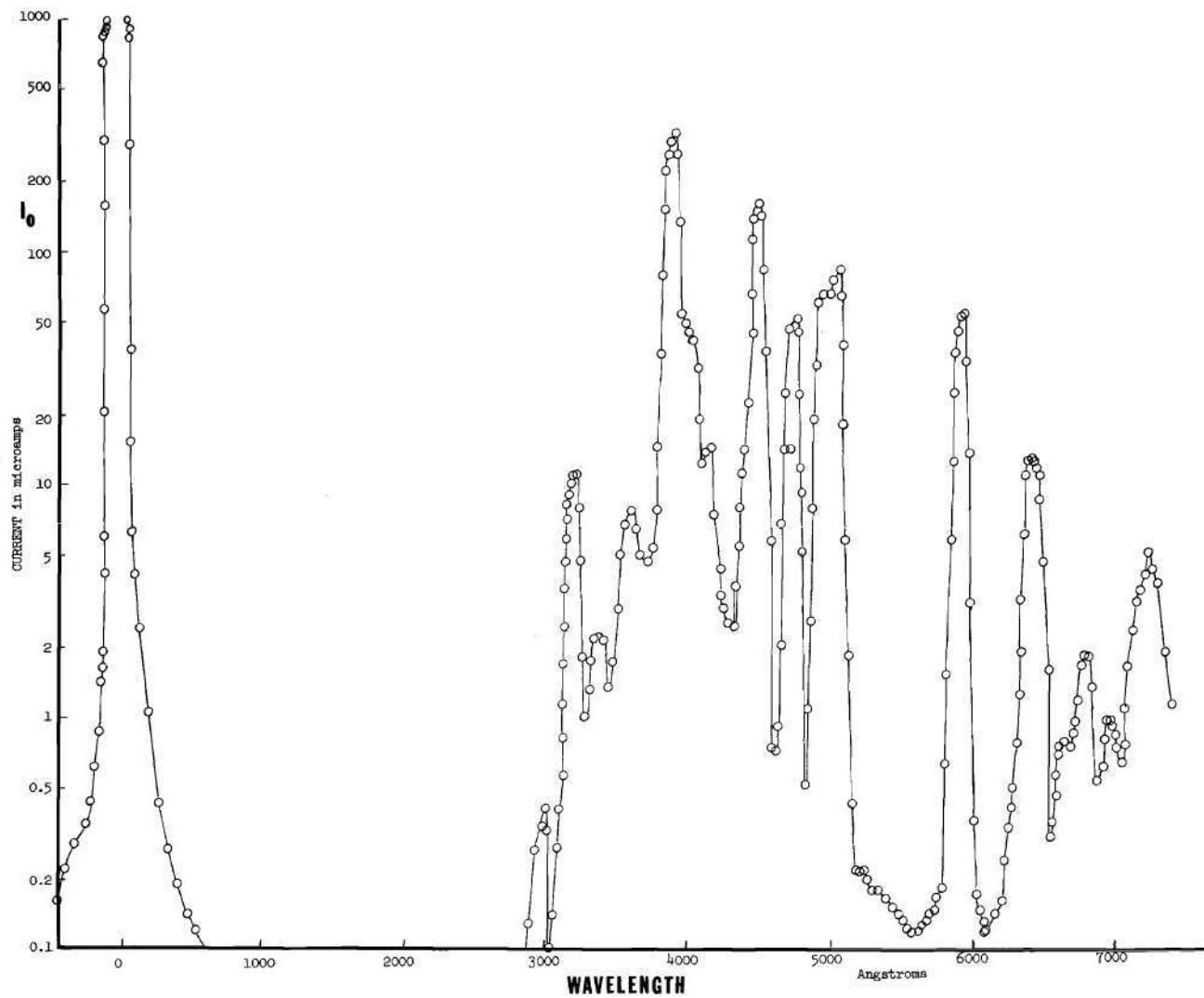Figure 36. Source Spectrum of Hydrogen Without Entrance Slit

Figure 37.   Source Spectrum of Helium Without Entrance Slit

APPENDIX F

SCALE CALIBRATION

The wavelength dial reading has been referred to in Tables 2 through 16 as the scale reading. This dial reading was related to the wavelength by recording the signal intensity for the various dial settings and finding which dial settings correspond to known lines in the spectrum (Figure 34). The correspondence between wavelength and dial reading is linear (Equation (14)), and this relationship is represented by Figure 38. Table 17 presents the information used to produce the calibration curve of Figure 38.

Table 17. Wavelength Dial Calibration

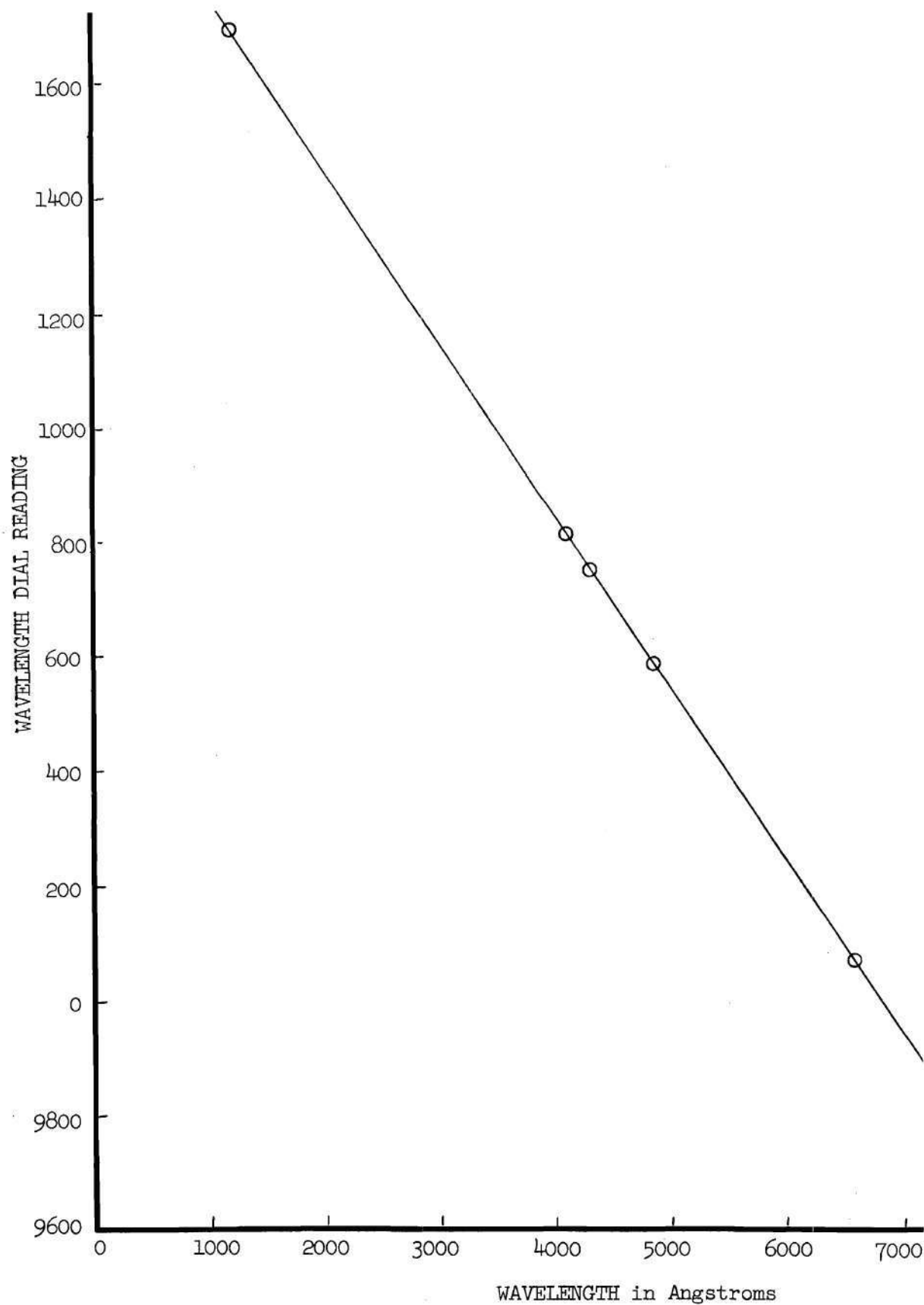| Scale Reading	Series	Line	Wavelength
2070	"White Point"		0
1695	Lyman	Alpha	1216 Å
815	Balmer	Delta	4102 Å
745	Balmer	Gamma	4341 Å
575	Balmer	Beta	4861 Å
55	Balmer	Alpha	6563 Å

Figure 38.   Wavelength Dial Calibration

BIBLIOGRAPHY

1. M. W. Hunter, Jr., "Single Stage Spaceships Should Be Our Goal," Nucleonics Handbook of Nuclear Research and Technology, 74-77 (1966).

2. H. B. Finger, "The Case for Nuclear Energy," Nucleonics 19, No. 4, 64 (1961).

3. Frank E. Rom, "Coaxial Flow Gaseous Nuclear Reactor Concept," Proceedings of an Advanced Nuclear Propulsion Symposium, Los Alamos, LA-3229, p. 177-179 (January 1965).

4. Stanley Ulam, "Nuclear Rocketry: The Orion Project," Nuclear News 8, Vol. 1, pp. 25-26 (January 1965).

5. G. H. McLafferty, "Work on the Nuclear Light Bulb at UAC Research Laboratories," Proceedings of an Advanced Nuclear Propulsion Symposium, Los Alamos, LA-3229, pp. 137-147 (January 1965).

6. C. D. Lanzo and R. G. Ragsdale, NASA TND-1405, (September 1962).

7. C. D. Lanzo and R. G. Ragsdale, Proceedings of the 1964 Heat Transfer and Fluid Mechanics Institute, H. Hiedt and Solomon Levy, Editors. (Standard University Press, 1964).

8. C. C. Masser, NASA Report TND-3197,(January 1965).

9. J. A. McAlister, David Kocsis, and Clyde Orr, Jr., "Heat Transfer to a Gas Containing a Cloud of Particles," Semi-annual Status Report No. 8 of Project A-635-002, Georgia Institute of Technology, E.E.S. (June 25, 1966).

10. J. A. McAlister, Edward Keng, and Clyde Orr, Jr., Semi-annual Status Report No. 6 of Project A-635-002, Georgia Institute of Technology, E.E.S. (July 30, 1965).

11. P. J. Marteney, "Experimental Investigation of the Opacity of Small Particles," UAC Research Laboratories Report C-910092-2, (September 1964).

12. N. L. Krascella, "Theoretical Investigation of the Absorption and Scattering Characteristics of Small Particles," UAC Research Laboratories Report C-910092-1, (September 1964).

13. Valerie C. Burkig, "Thermal Absorption in Seeded Gases," Douglas Report DAC-59985, Nasw-1310 (January 1967).

14. F. A. Jenkins and H. E. White, Fundamentals of Optics, (McGraw-Hill Book Company, New York, 1957), p. 424.

15. R. G. Ragsdale, "Coaxial Flow Research Studies," Proceedings of an Advanced Nuclear Propulsion Symposium, Los Alamos, LA-3299-MS, 200 (1965).

16. N. L. Krascella, "Tables of the Composition, Opacity, and Thermodynamic Properties of Hydrogen at High Temperatures," NASA-AP-3005 (September 1963).

17. H. D. Van de Hulst, Light Scattering by Small Particles, (John Wiley and Sons, Inc., 1957).

18. C. N. Davis, "Survey of Scattering and Absorption of Light by Particles," Brit. J. Appl. Physics, Suppl. No. 3, 564-565 (1954).

19. Max Born and Emil Wolf, Principles of Optics, (McMillan Company, 2nd edition, 1964).

20. E. G. Schneider, Physical Review 49, 341 (1936).

21. G. Mie, Ann. d. Physik (4), 25, 277 (1908).

22. Peter Debye, Ann. d. Physik 30, 57 (1909).

23. A. L. Aden, "Electromagnetic Scattering from Spheres with Sizes Comparable to the Wavelength," J. Appl. Phys. 22, 5 (May 1951).

24. John David Jackson, Classical Electrodynamics, John Wiley and Sons, Inc. (1962).

25. J. A. Stratton, Electromagnetic Theory (McGraw-Hill Book Company, Inc. New York, 1941).

26. W. Magnus, F. Oberbettinger, Formulas and Theorems for the Functions of Mathematical Physics, (Chelsea Publishing Company, New York, 1954) p. 54.

27. Peter Debye, Ann. d. Physik 30, 59 (1909).

VITA

Richard Williams was born in Millen, Georgia on July 7, 1941 and has lived in Georgia since birth. Mr. Williams graduated from the La Grange High School, La Grange, Georgia, in June 1959, and entered the Georgia Institute of Technology in September 1959. As a senior and first year graduate student in physics (September 1961 through June 1963), he was a physics lab instructor in charge of three sophomore physics lab sessions each week. While working on his M.S. in physics (June 1962 to June 1964), he worked for the Space Sciences Branch of the Georgia Tech Engineering Experiment Station developing computerized techniques to analyze data from ionized clouds produced by rockets in the upper atmosphere. After receiving his M.S. in physics, Mr. Williams transferred to nuclear engineering and began work toward a Ph.D. degree. He worked for one year (June 1964 to June 1965) for the Nuclear Sciences Division of the Georgia Tech Engineering Experiment Station on a project to develop a method to determine the concentrations and species of fission product radioisotopes in natural water supplies. From September 1964 to June 1966, he was a graduate teaching assistant developing experiments for graduate nuclear engineering laboratory courses which utilized the reactor, subcritical assembly, neutron generator, and a wide range of nuclear instrumentation.

Mr. Williams received two fellowships as an undergraduate, and in 1965 he was awarded a NDEA fellowship. He is a member of Tau Beta Pi and Sigma Xi. He has been active in a number of campus organizations and

organized the Georgia Tech Student Branch of the American Nuclear Society. He is a member of the Lambda Chi Alpha Social Fraternity.

On September 21, 1963, Mr. Williams married Barbara Ann Buckelew of La Grange, Georgia, and they have two daughters, Stephanie Jane and Laura Noël.